

KICK-OFF TRAINING

TUM - Garching-bei-München
2018 Jan 8-12

Mistuning and damping devices

Christian Maria Firrone, Teresa Berruti
Politecnico di Torino

Introduction and mathematical models

- The effect of asymmetries in bladed disks
- Symptoms of mistuning and causes
- Lumped parameters model
- Numerical techniques to take into account mistuning:
a literature overview
- Numerical techniques to take into account mistuning in the
presence of friction contacts

The effect of asymmetries in bladed disks

Test rig design to study the dynamics of bladed disks

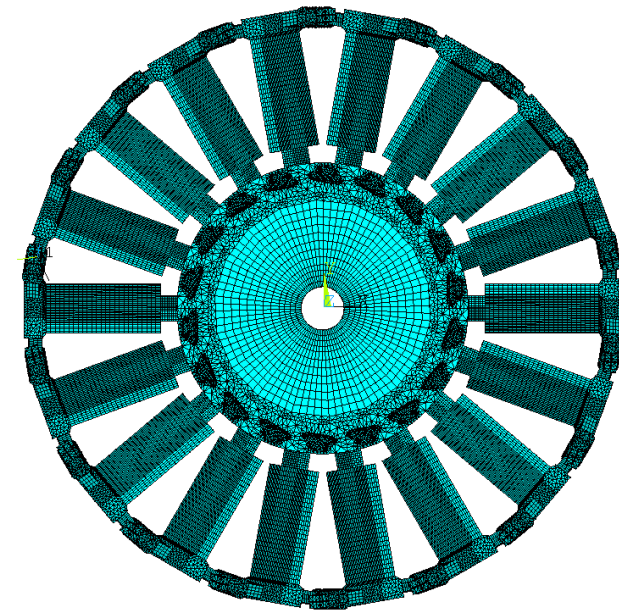
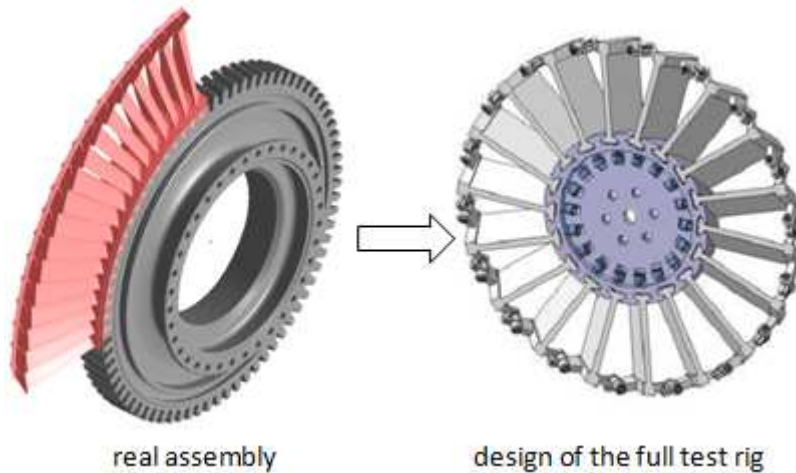
Requirement:

- Presence of joints: shroud and blade root joints
- Out-of-plane displacements
- LPT configuration & machining costs

Proposal:

- Non-integral bladed disk
- 45° stagger angle
- Blade vibration at 1F resonances

The final solution comes as an iterative process based on FEM

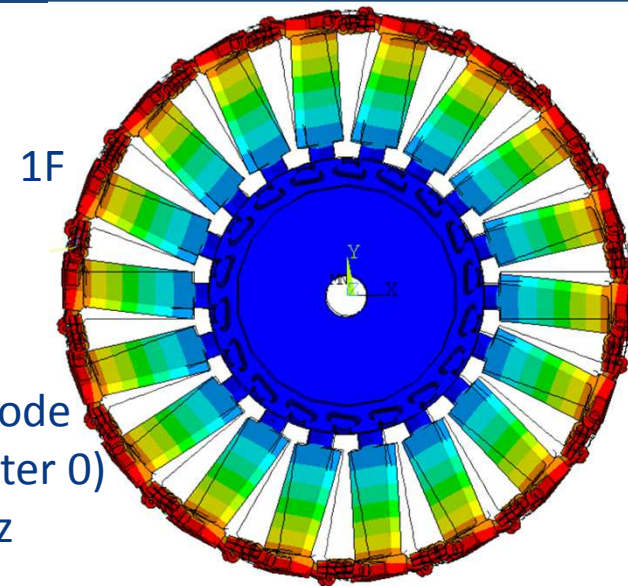
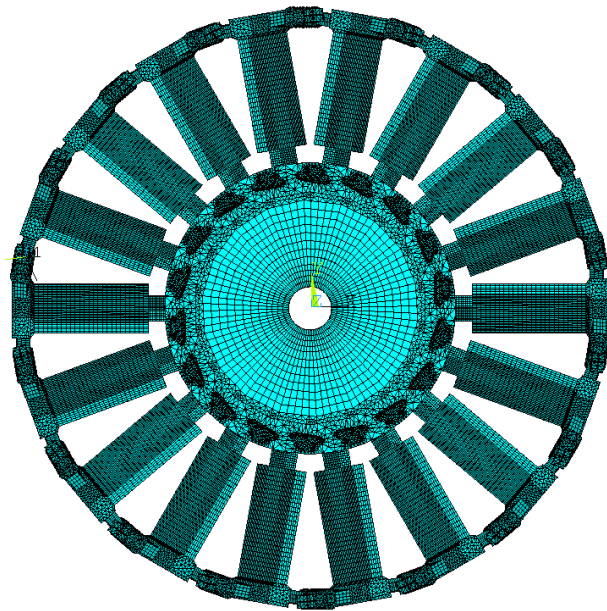


N=18 Blades

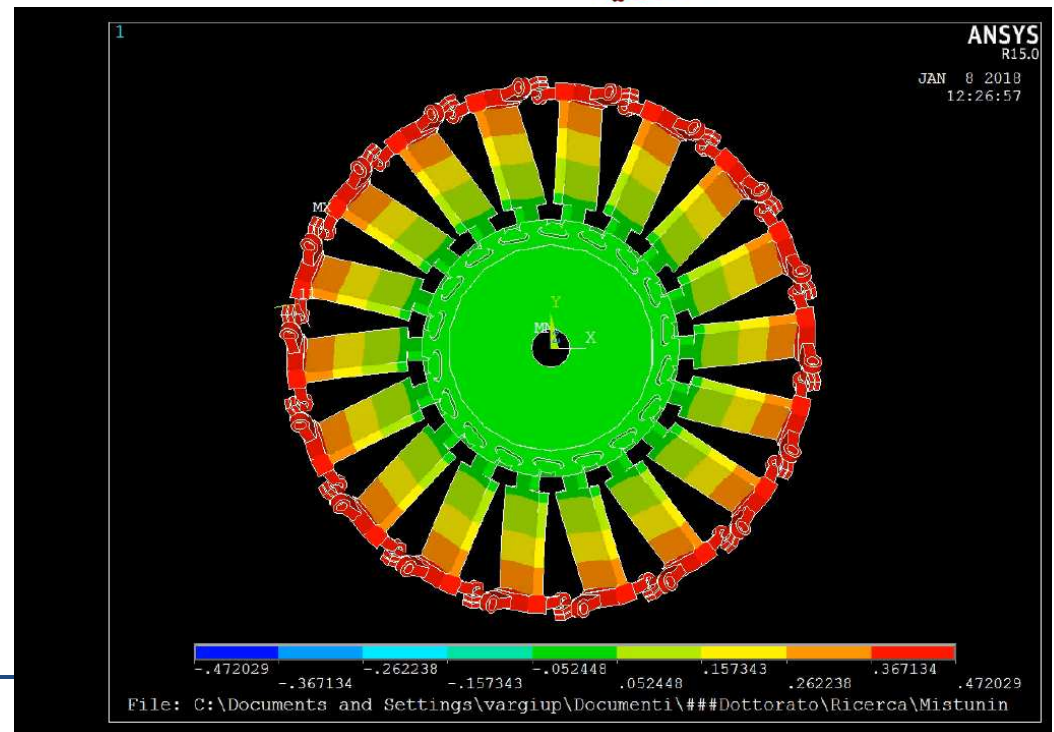
The effect of asymmetries in bladed disks

FEM modelling - Modal analysis

The final solution comes as an iterative process based on FEM



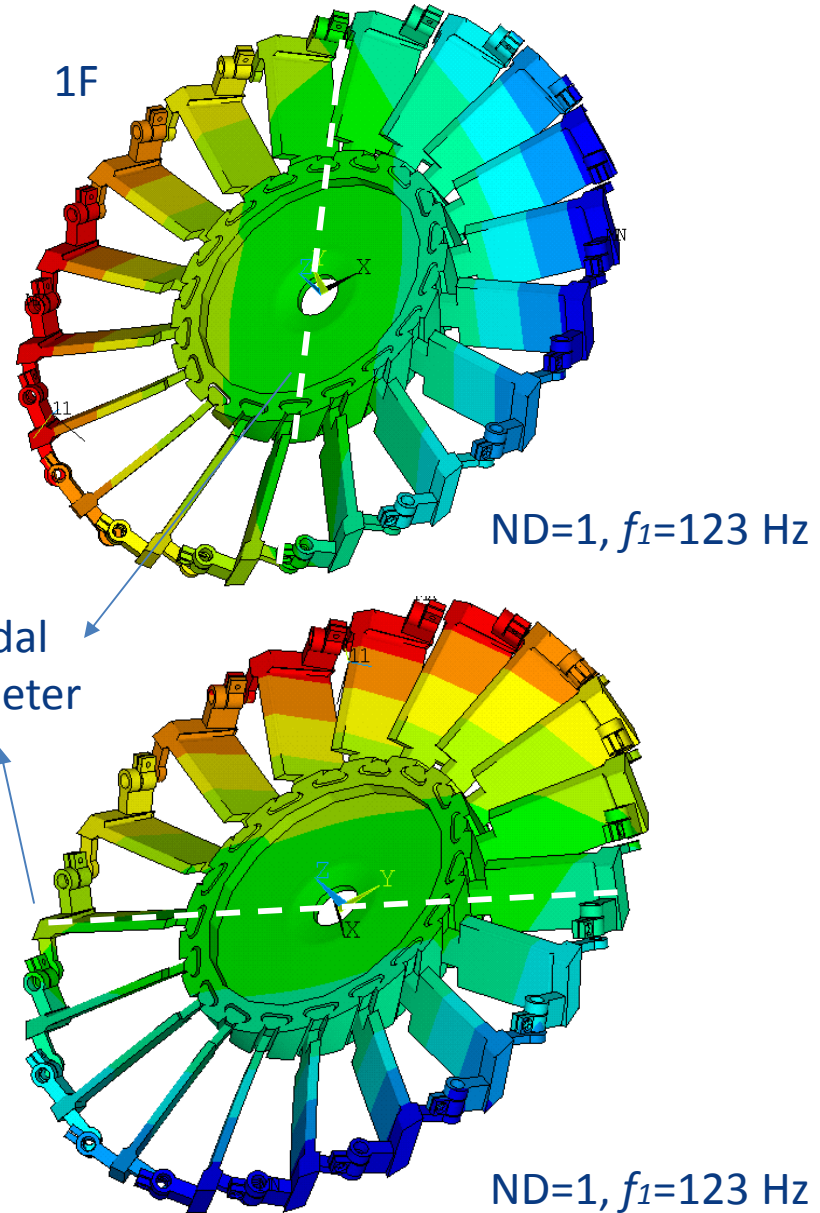
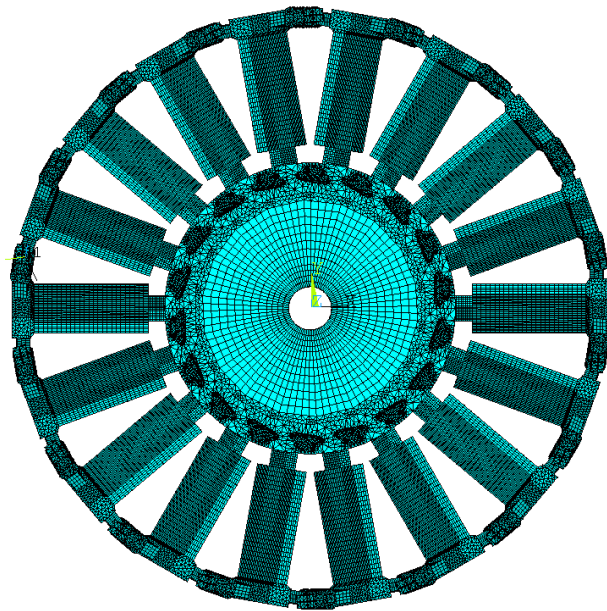
Umbrella mode
(Nodal Diameter 0)
 $f_0=147$ Hz



The effect of asymmetries in bladed disks

FEM modelling - Modal analysis

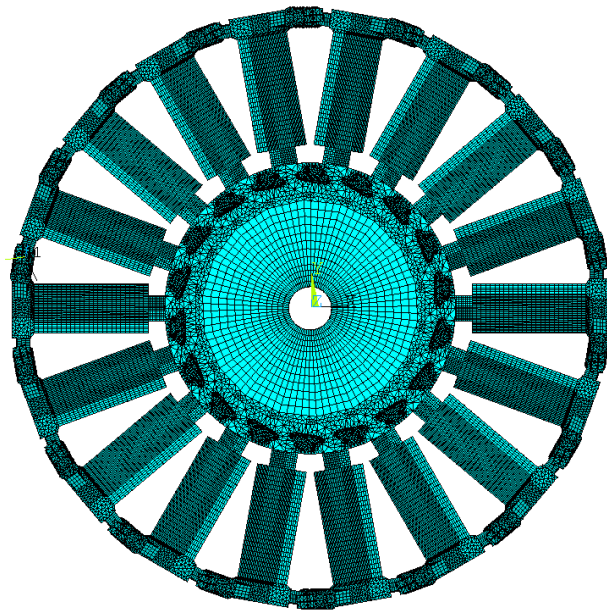
The final solution comes as an iterative process based on FEM



The effect of asymmetries in bladed disks

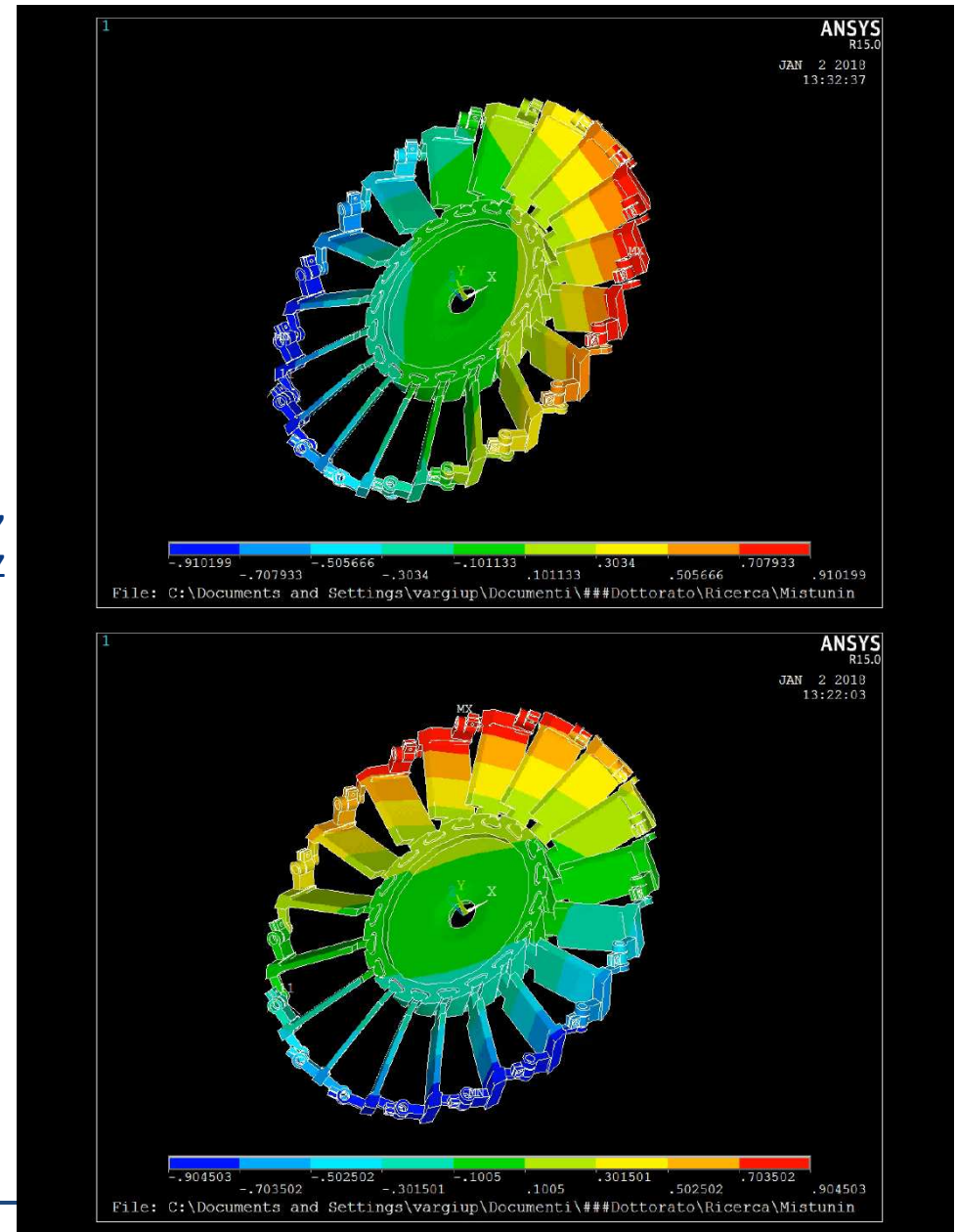
FEM modelling - Modal analysis

The final solution comes as an iterative process based on FEM



ND=1,
 $f_1=123$ Hz

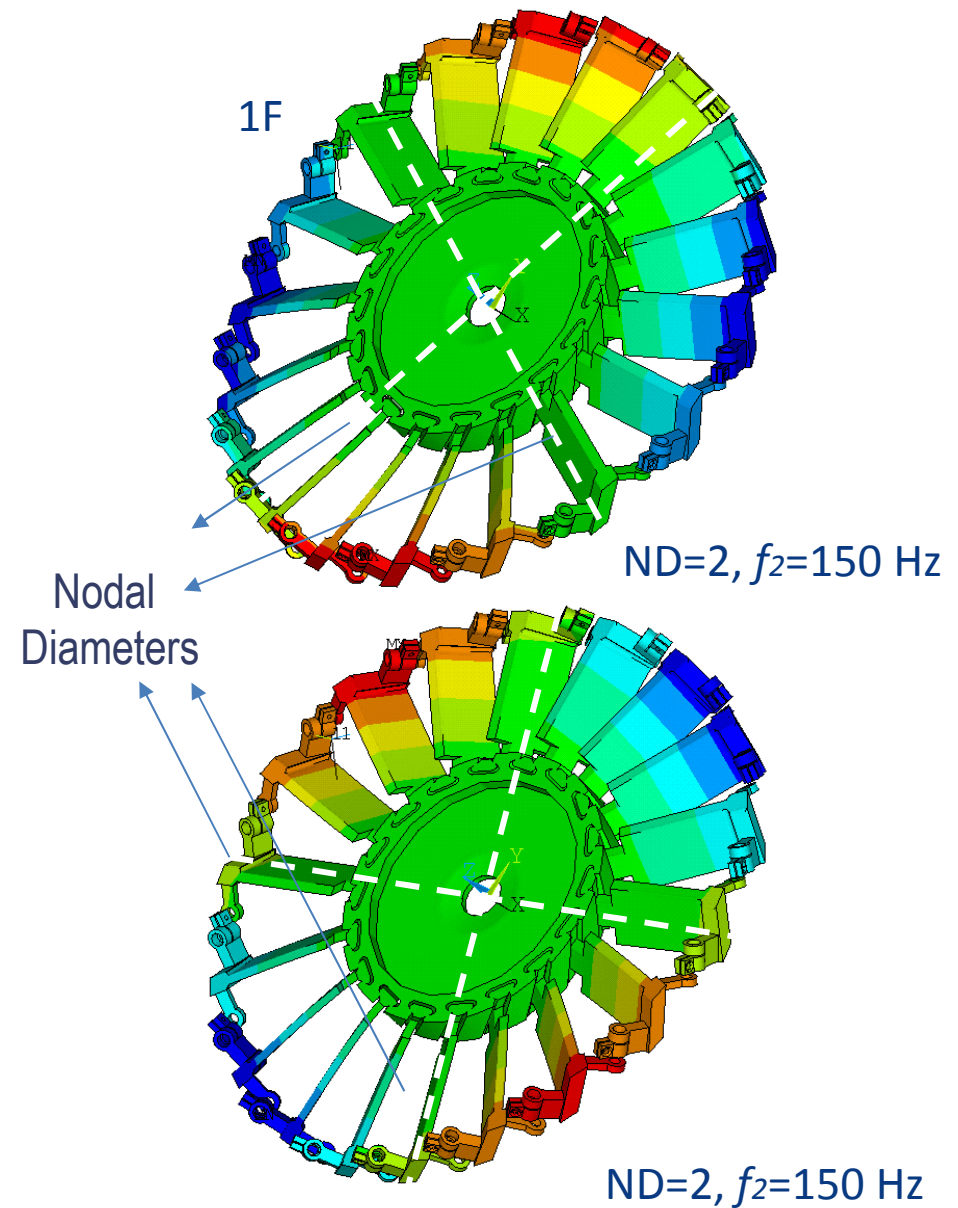
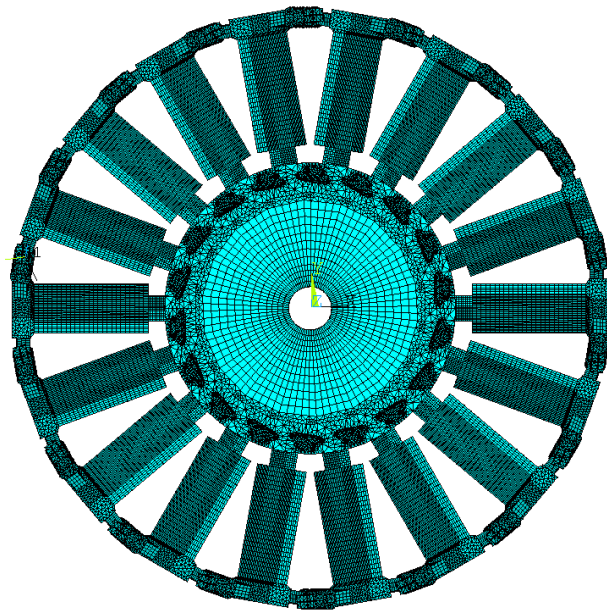
ND=1,
 $f_1=123$ Hz



The effect of asymmetries in bladed disks

FEM modelling - Modal analysis

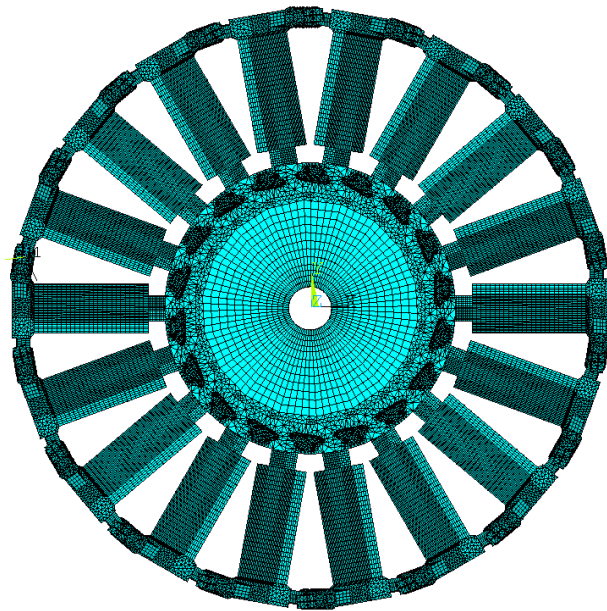
The final solution comes as an iterative process based on FEM



The effect of asymmetries in bladed disks

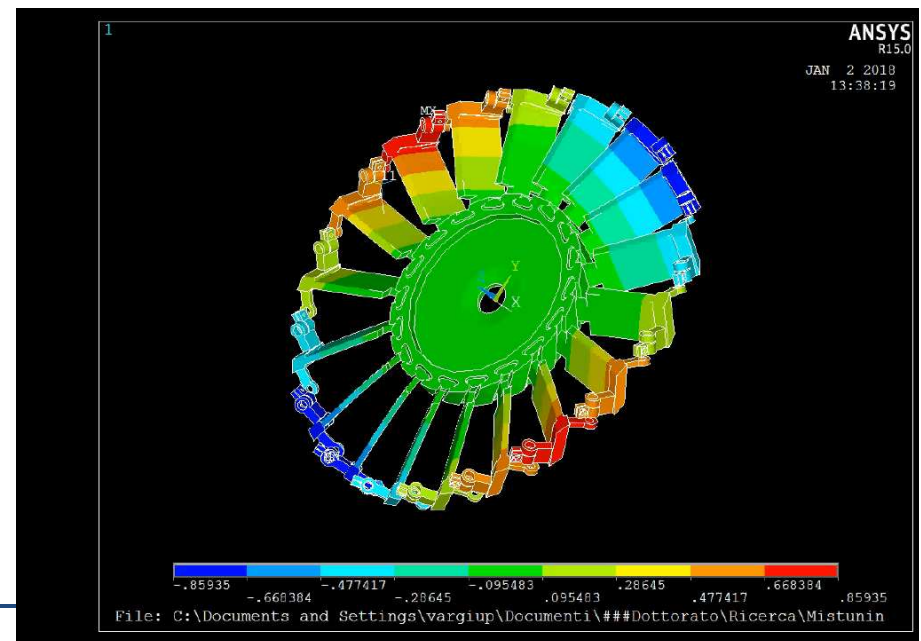
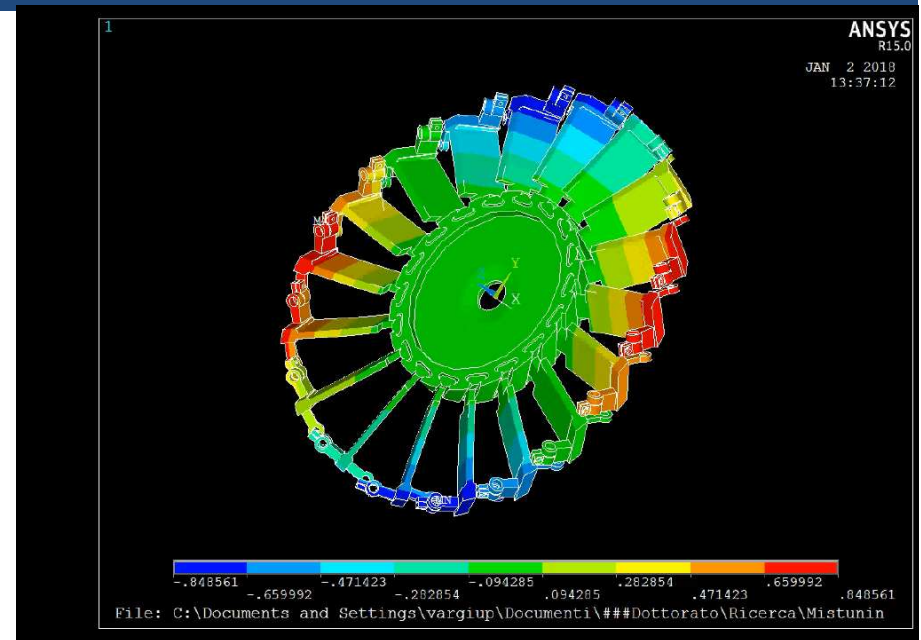
FEM modelling - Modal analysis

The final solution comes as an iterative process based on FEM



ND=2,
 $f_2=150$ Hz

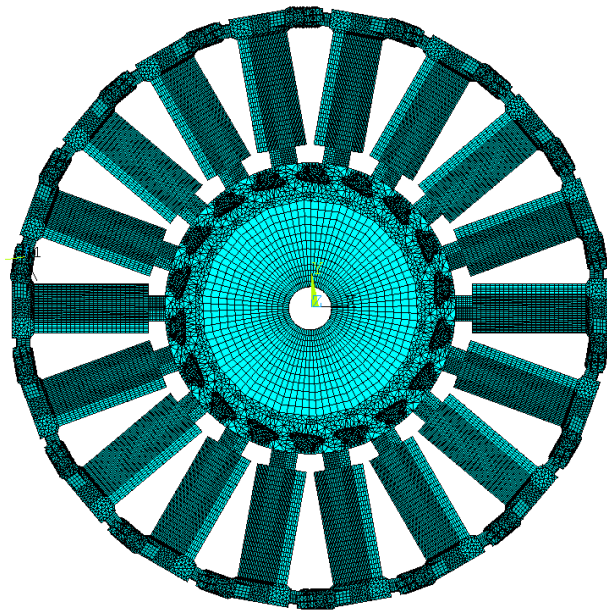
ND=2,
 $f_2=150$ Hz



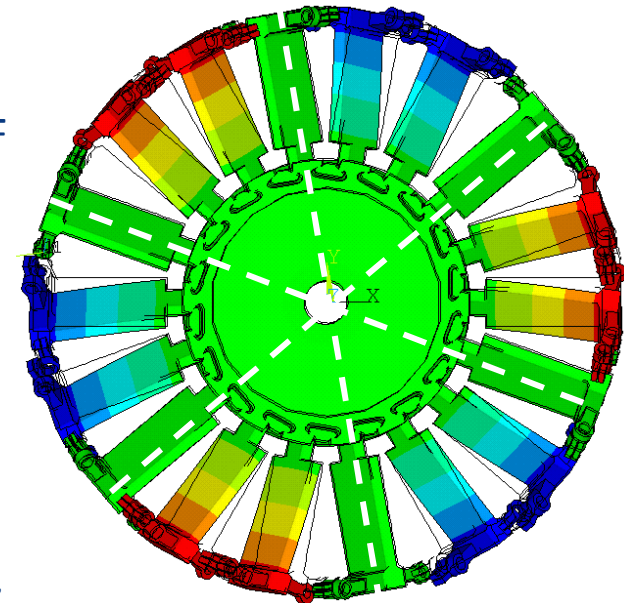
The effect of asymmetries in bladed disks

FEM modelling - Modal analysis

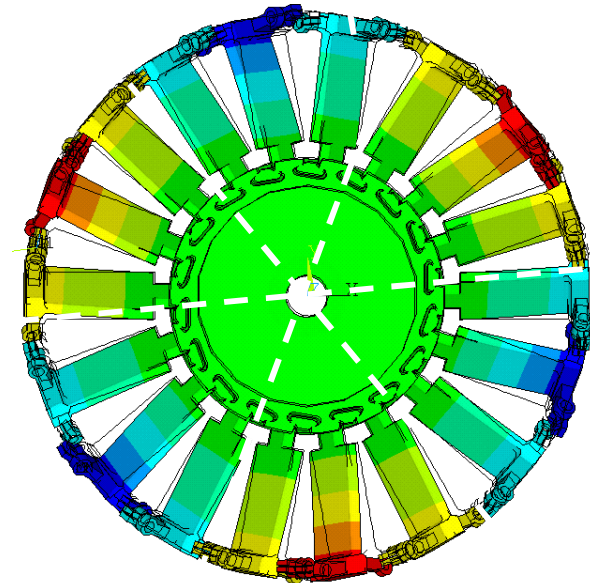
The final solution comes as an iterative process based on FEM



1F



ND=3, $f_3=155$ Hz

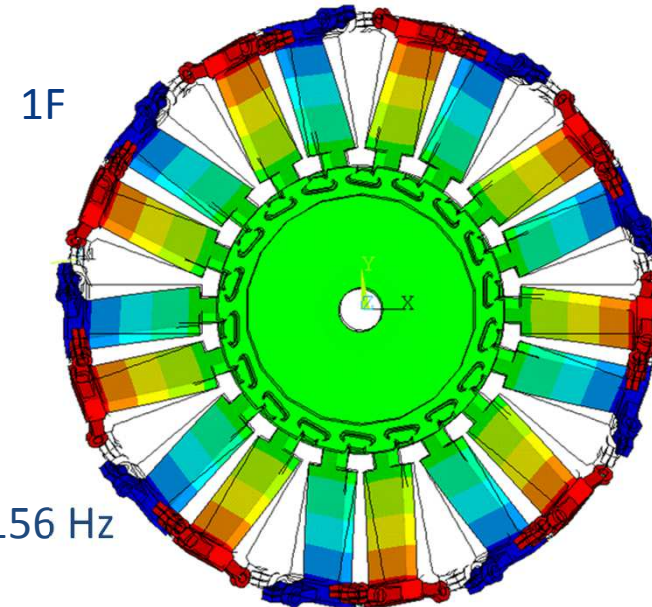
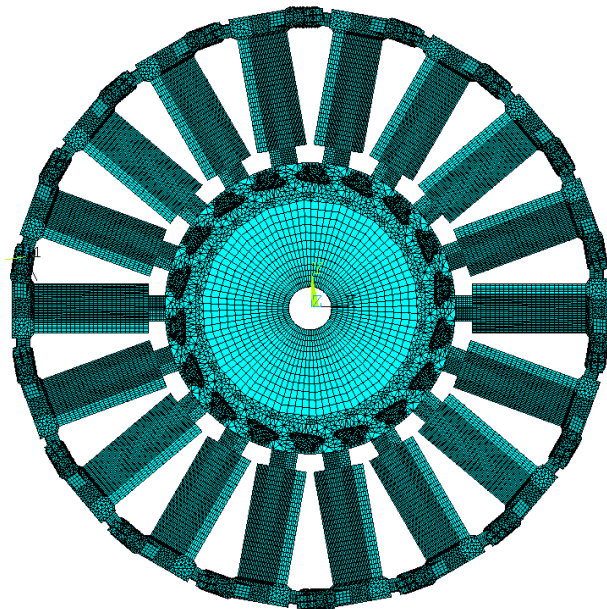


ND=3, $f_3=155$ Hz

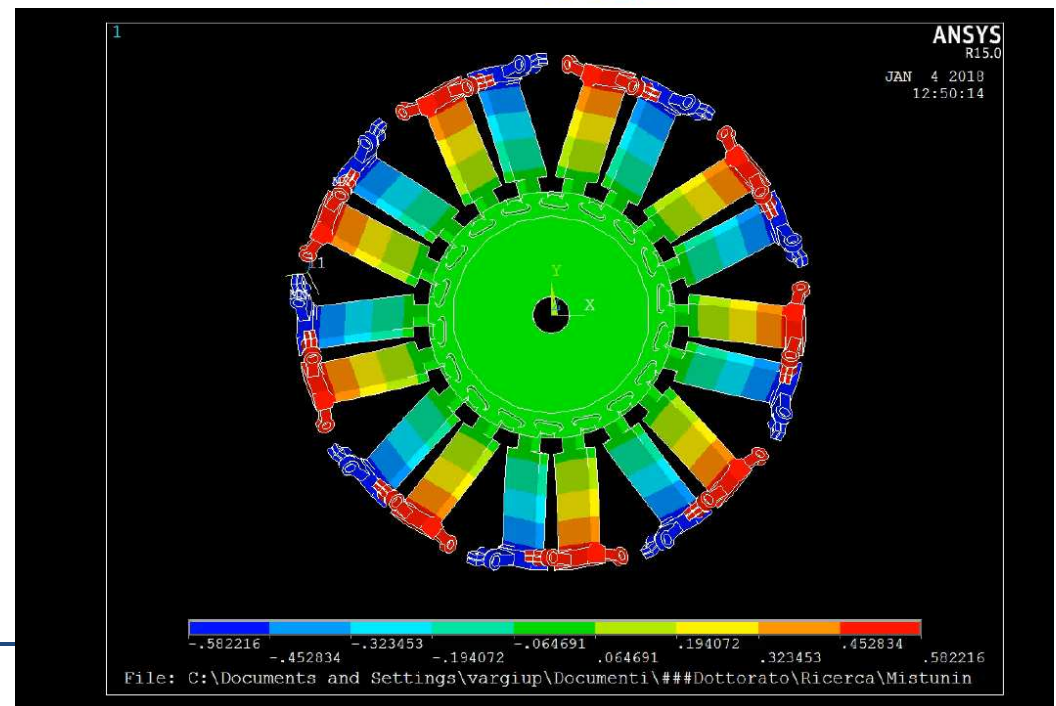
The effect of asymmetries in bladed disks

FEM modelling - Modal analysis

The final solution comes as an iterative process based on FEM



...ND=9, $f_9=156$ Hz

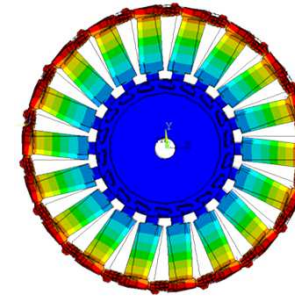


The effect of asymmetries in bladed disks

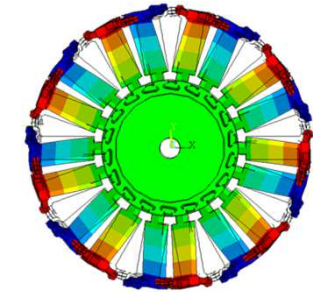
FEM modelling - Modal analysis

To resume: a modal family is obtained

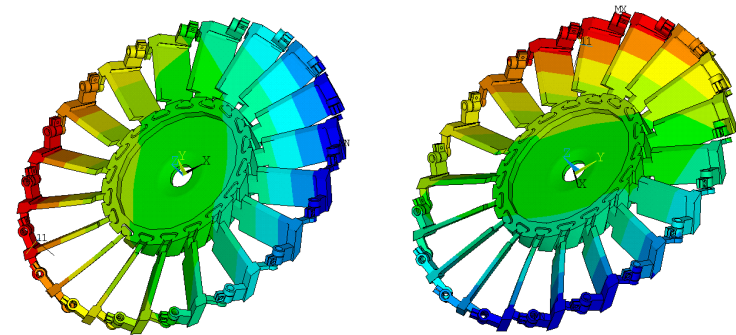
- $ND_{min}=0$ and $ND_{max}=\text{int}(N/2)$ are single modes and are stationary (real eigenvectors)
- The other ND mode shapes are repeated (stationary, real eigenvectors) and, if properly excited, give rotating mode shapes (complex eigenvectors)
 - Each sector behaves like the other with a given phase lag
 - I can use one basic sector to calculate the whole mode shape (*Cyclic symmetry constraint*)



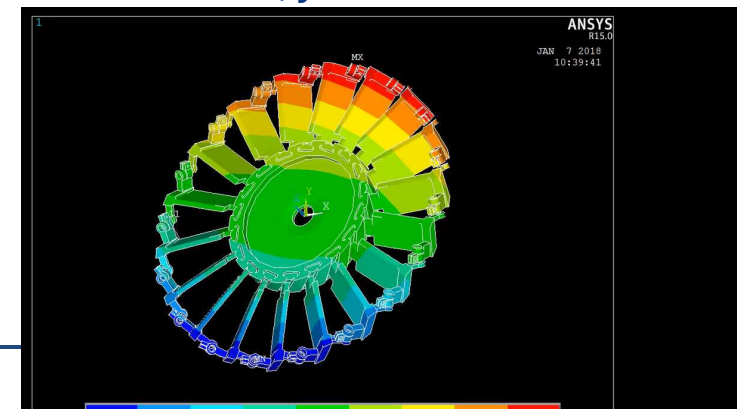
Umbrella mode
($ND=0$)
 $f_0=147$ Hz



$ND=9$
 $f_9=156$ Hz

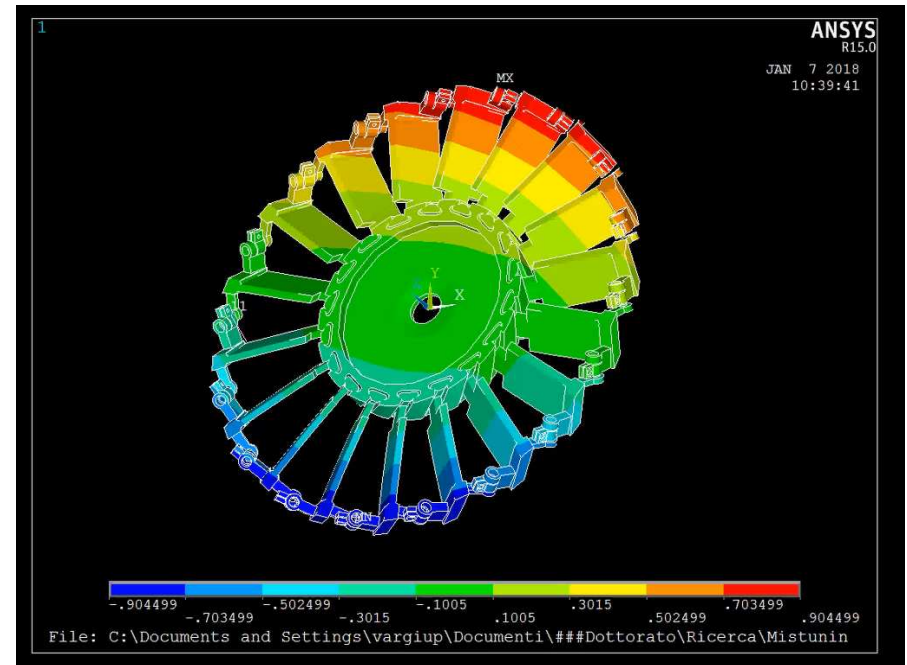
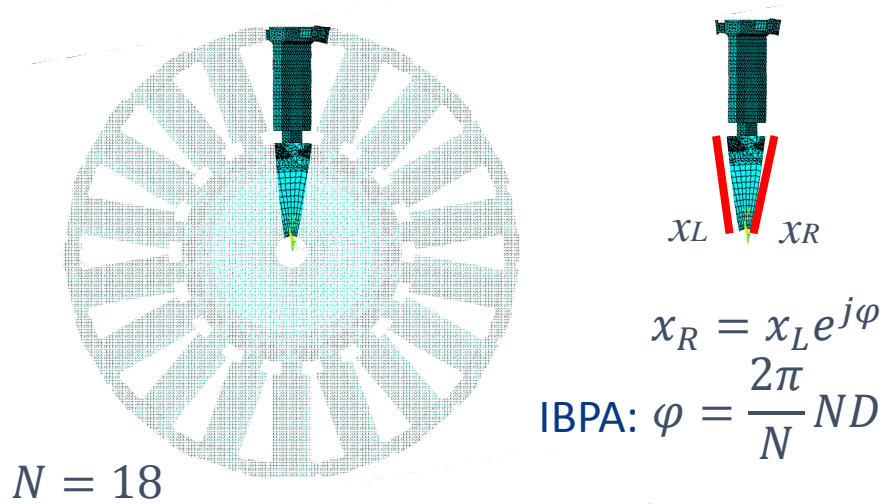


$ND=1, f_1=123$ Hz

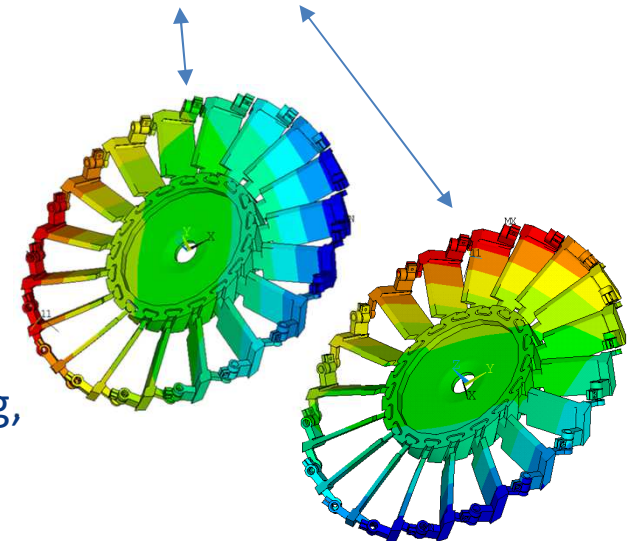


The effect of asymmetries in bladed disks

FEM modelling - cyclic symmetry



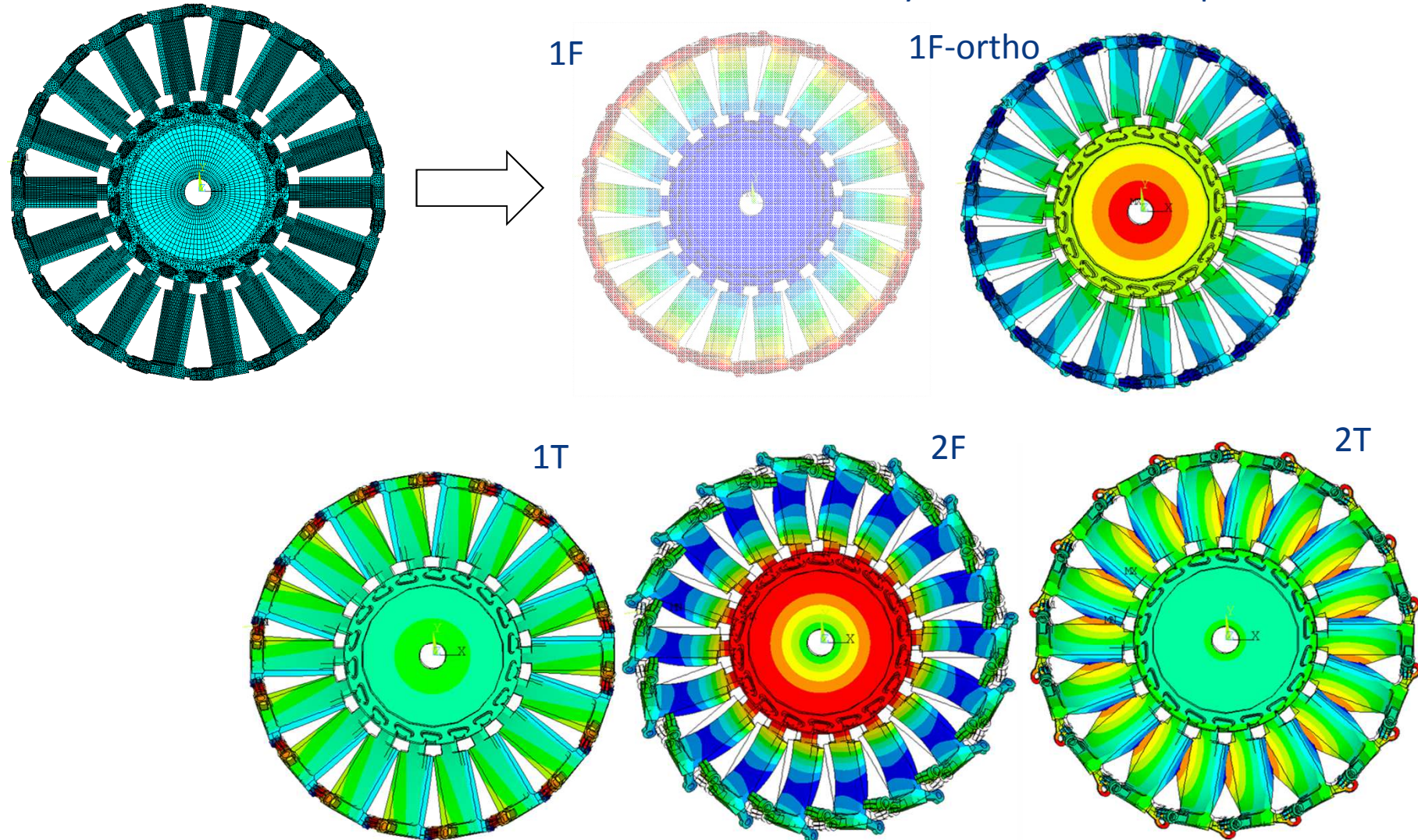
- If $\varphi = 0 \rightarrow x_R = x_L \rightarrow ND=0$ stationary mode
- If $\varphi = \pi \rightarrow x_R = -x_L \rightarrow ND=9$ stationary mode
- If $0 < \varphi < \pi \rightarrow 0 < ND < 9$ rotating, complex modes
note: the two stationary, repeated modes can be associated to the real and imaginary part of the rotating, complex mode



The effect of asymmetries in bladed disks

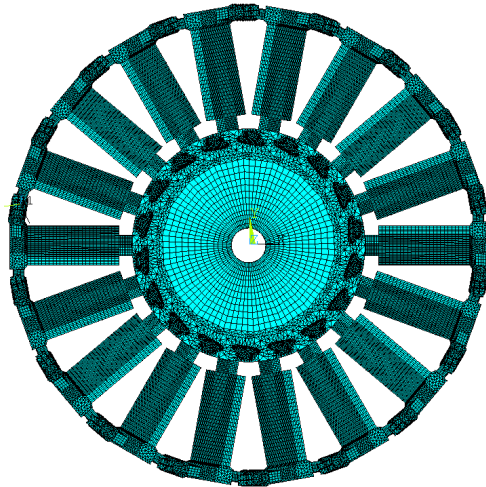
FEM modelling – modal families

Different modal families exist, all of them characterized by the $0 \dots N/2$ ND sequence

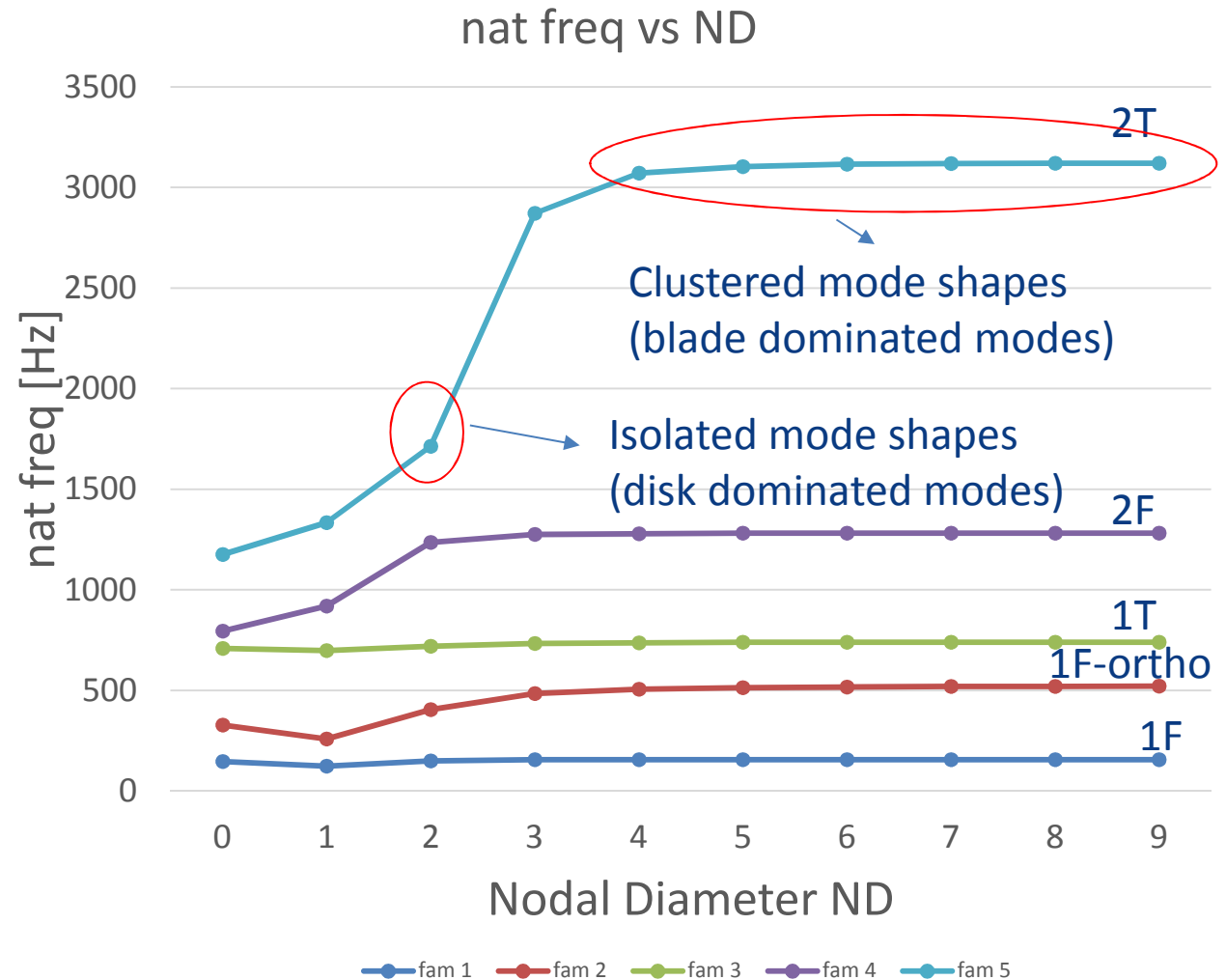


The effect of asymmetries in bladed disks

FEM modelling – modal families



Different modal families exist, all of them characterized by the $0 \dots N/2$ ND sequence

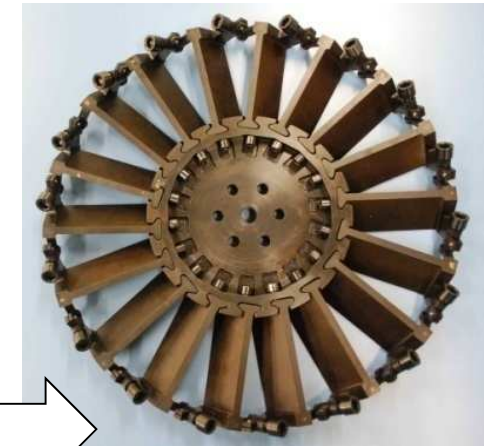
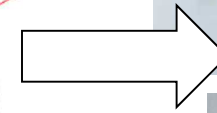
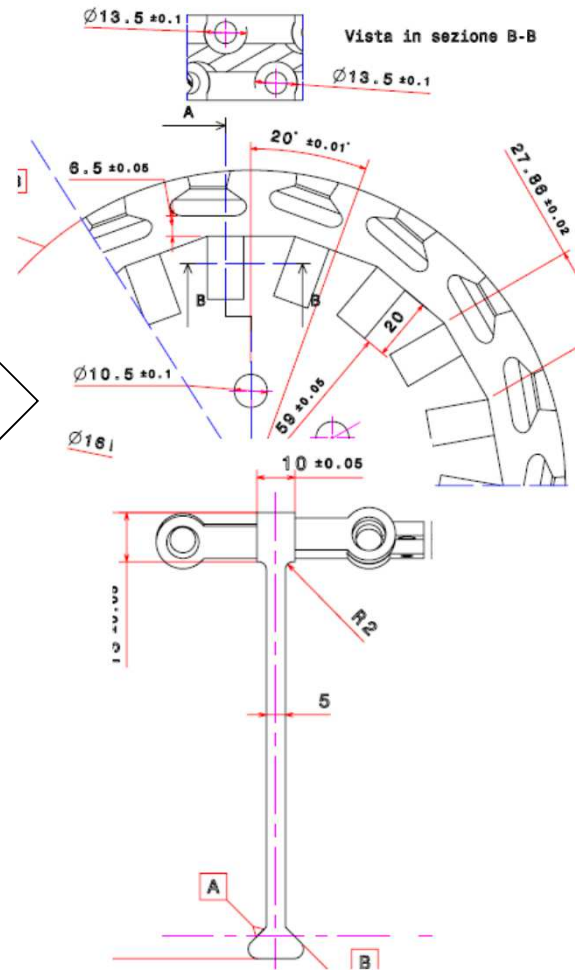
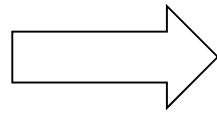
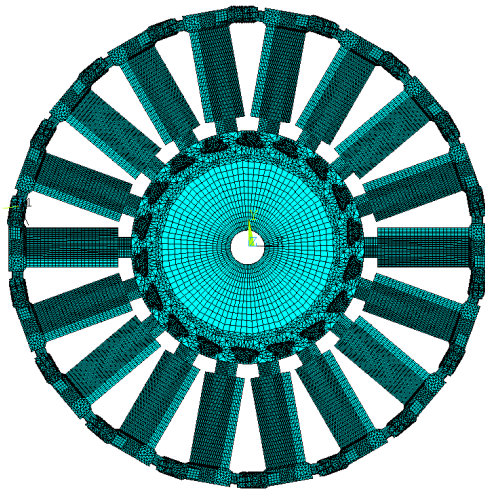


The effect of asymmetries in bladed disks

From FEM to reality

Technical Drawings

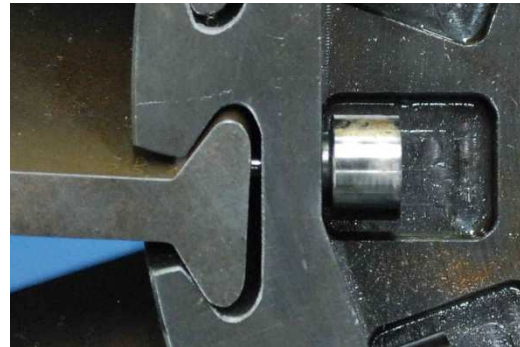
Manufacturing



The effect of asymmetries in bladed disks

Experimental campaign

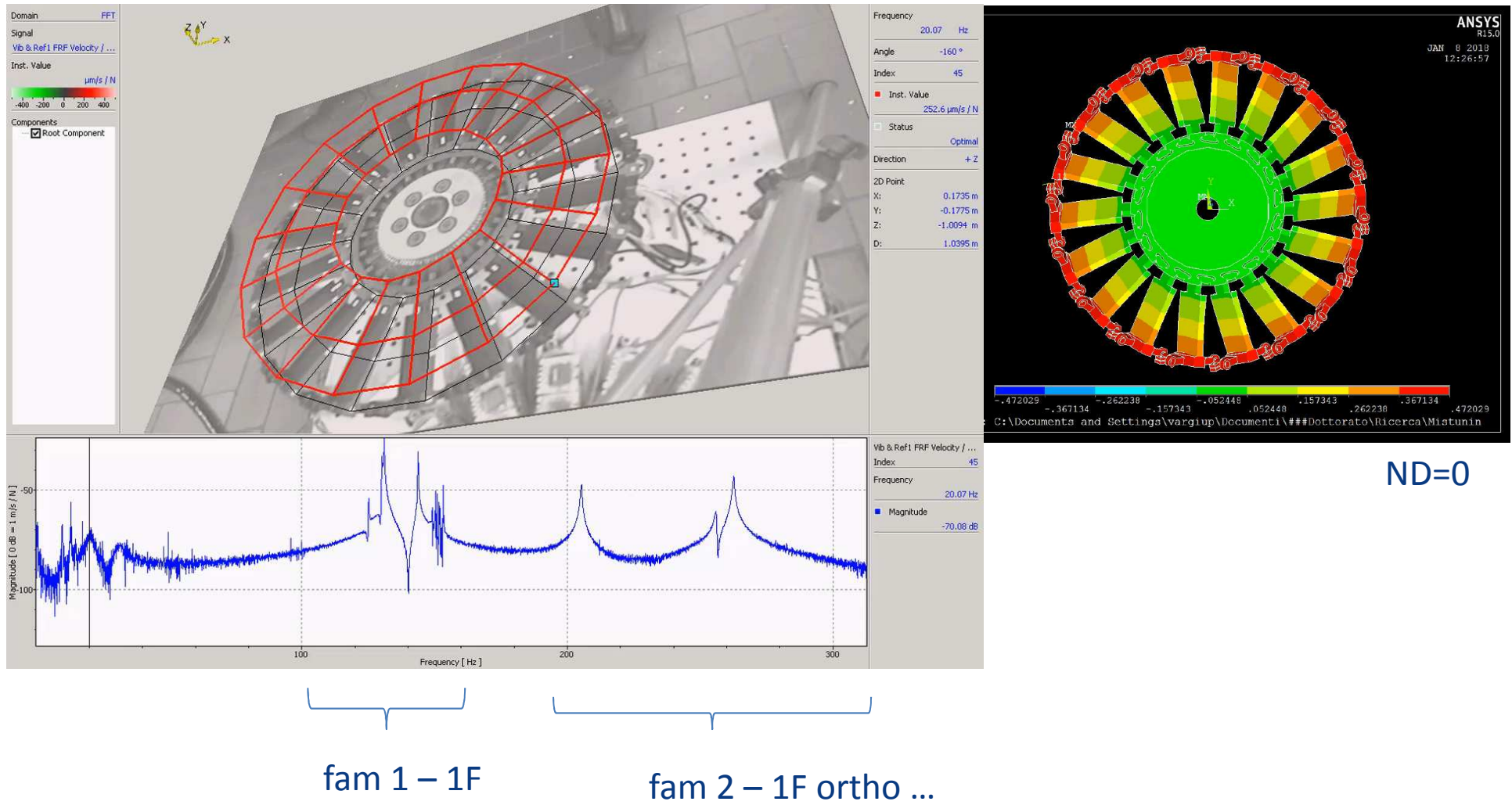
Testing: hammer test



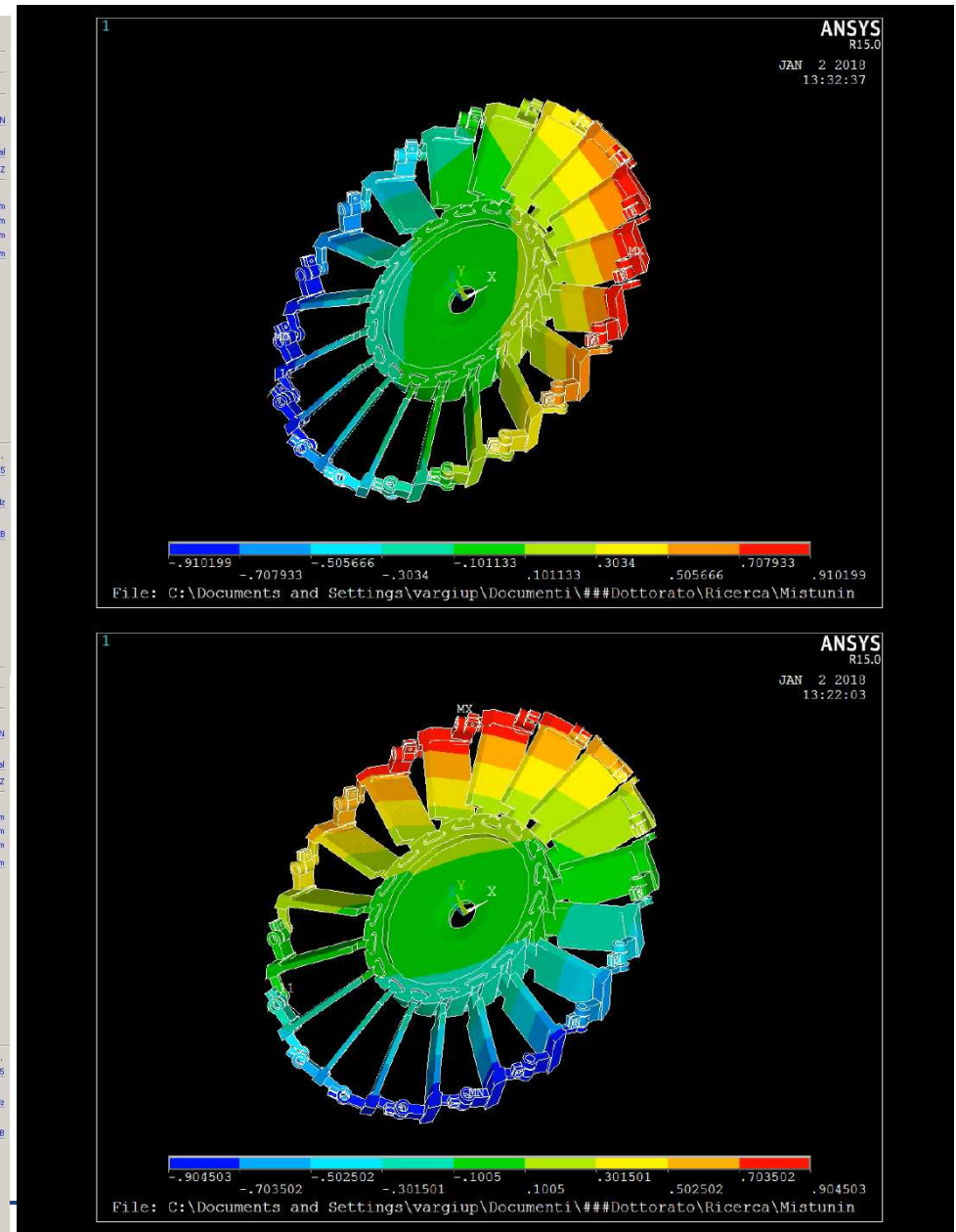
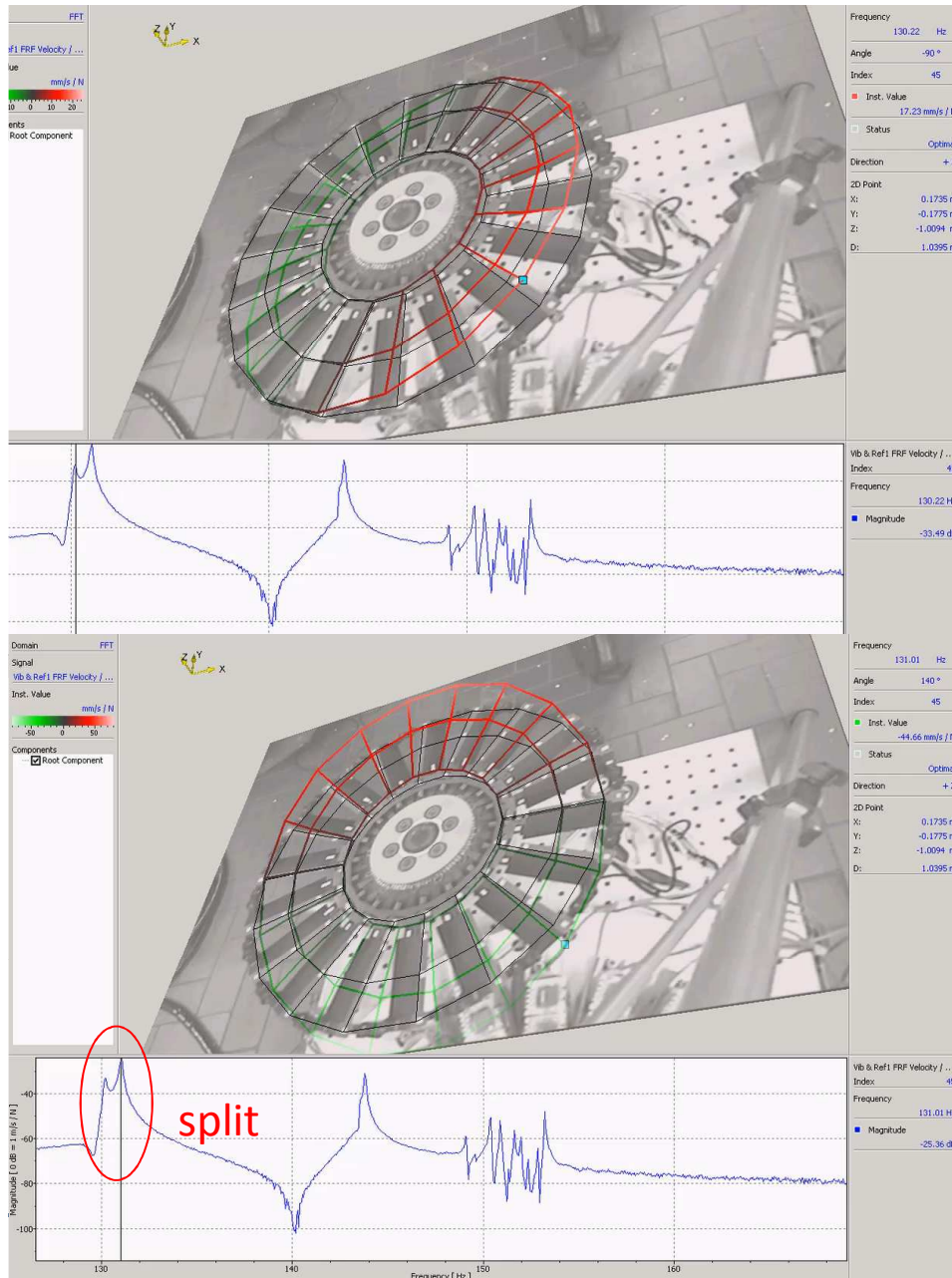
The effect of asymmetries in bladed disks

Experimental campaign

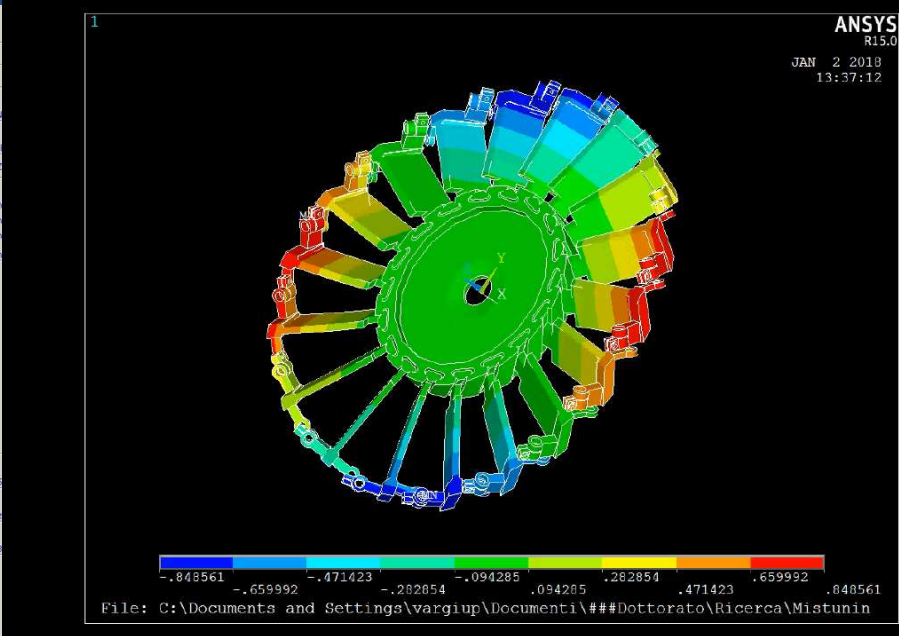
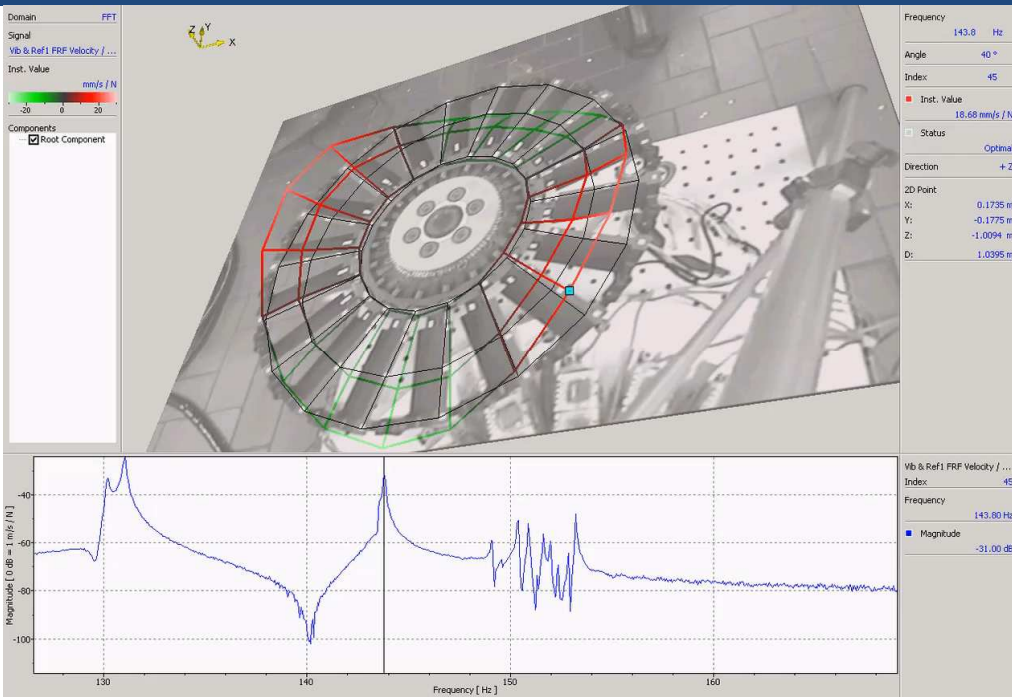
Results and comparison with simulations



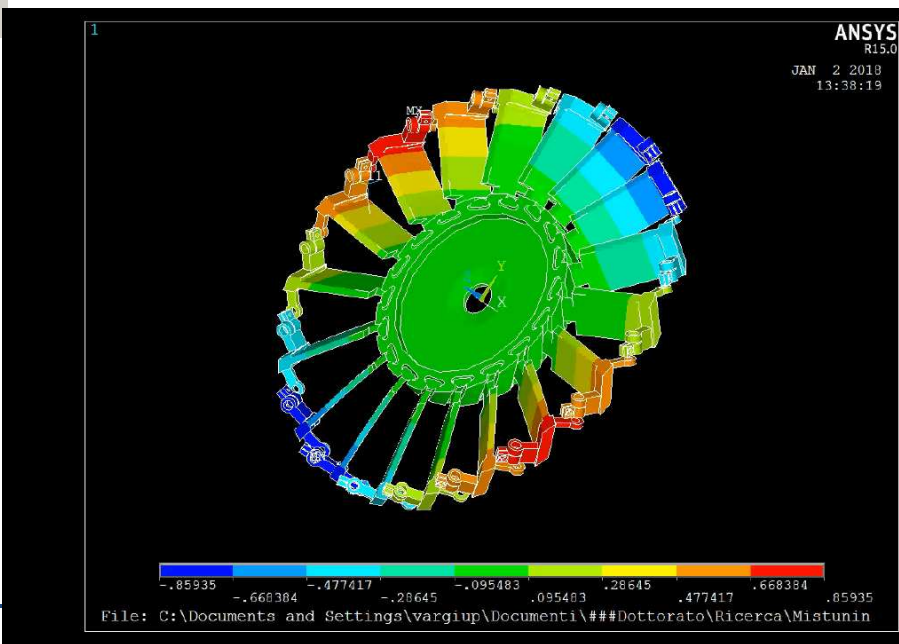
The effect of asymmetries in bladed disks



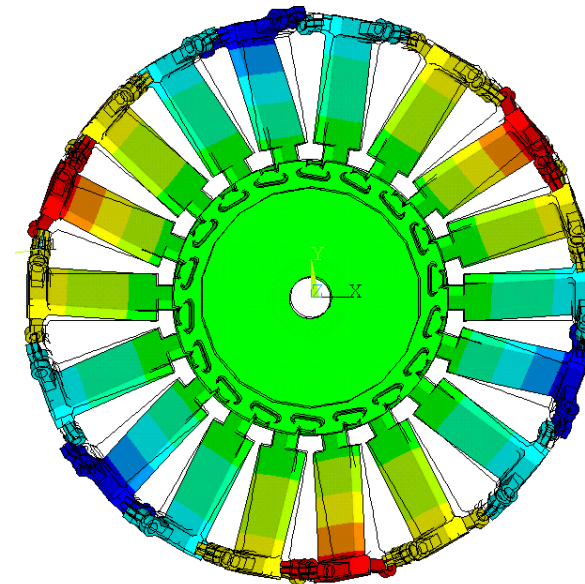
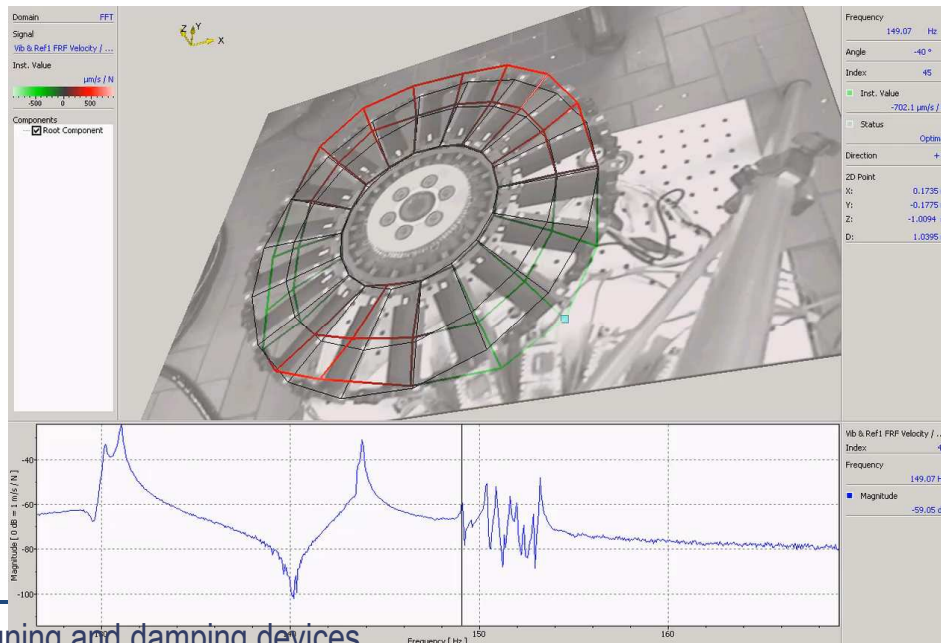
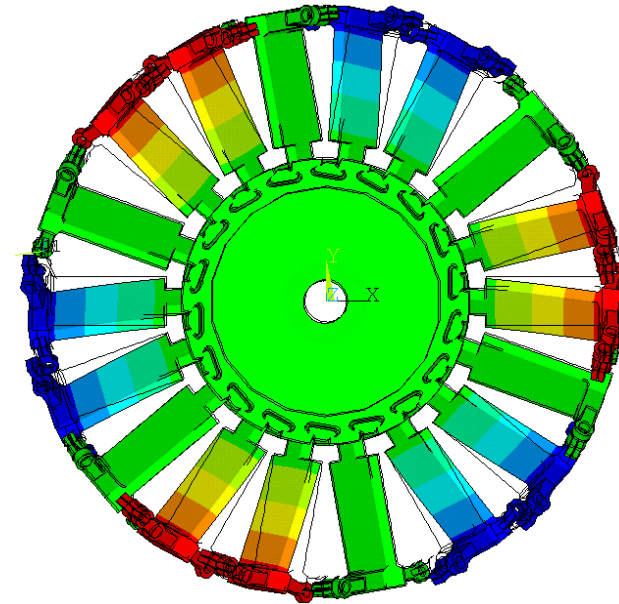
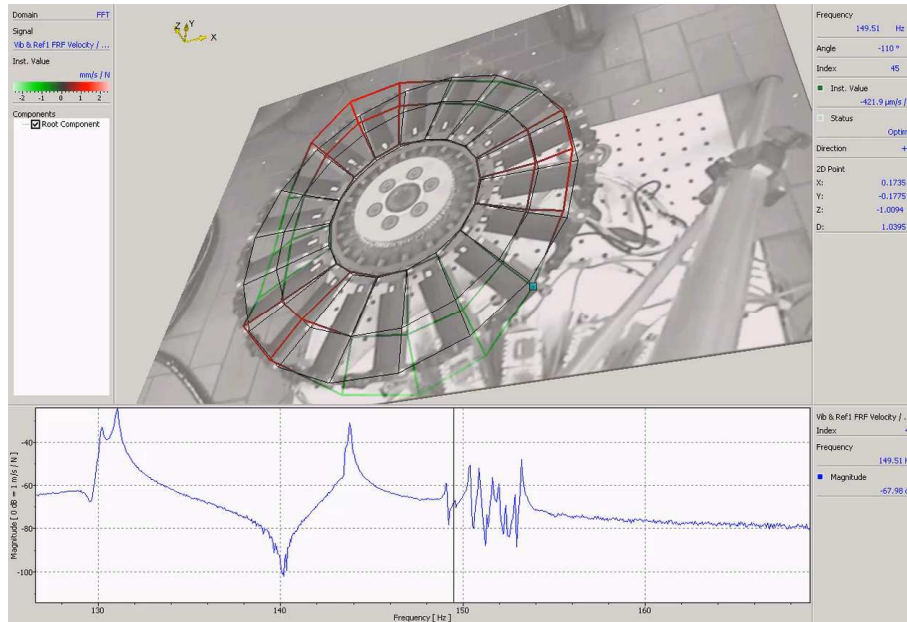
The effect of asymmetries in bladed disks



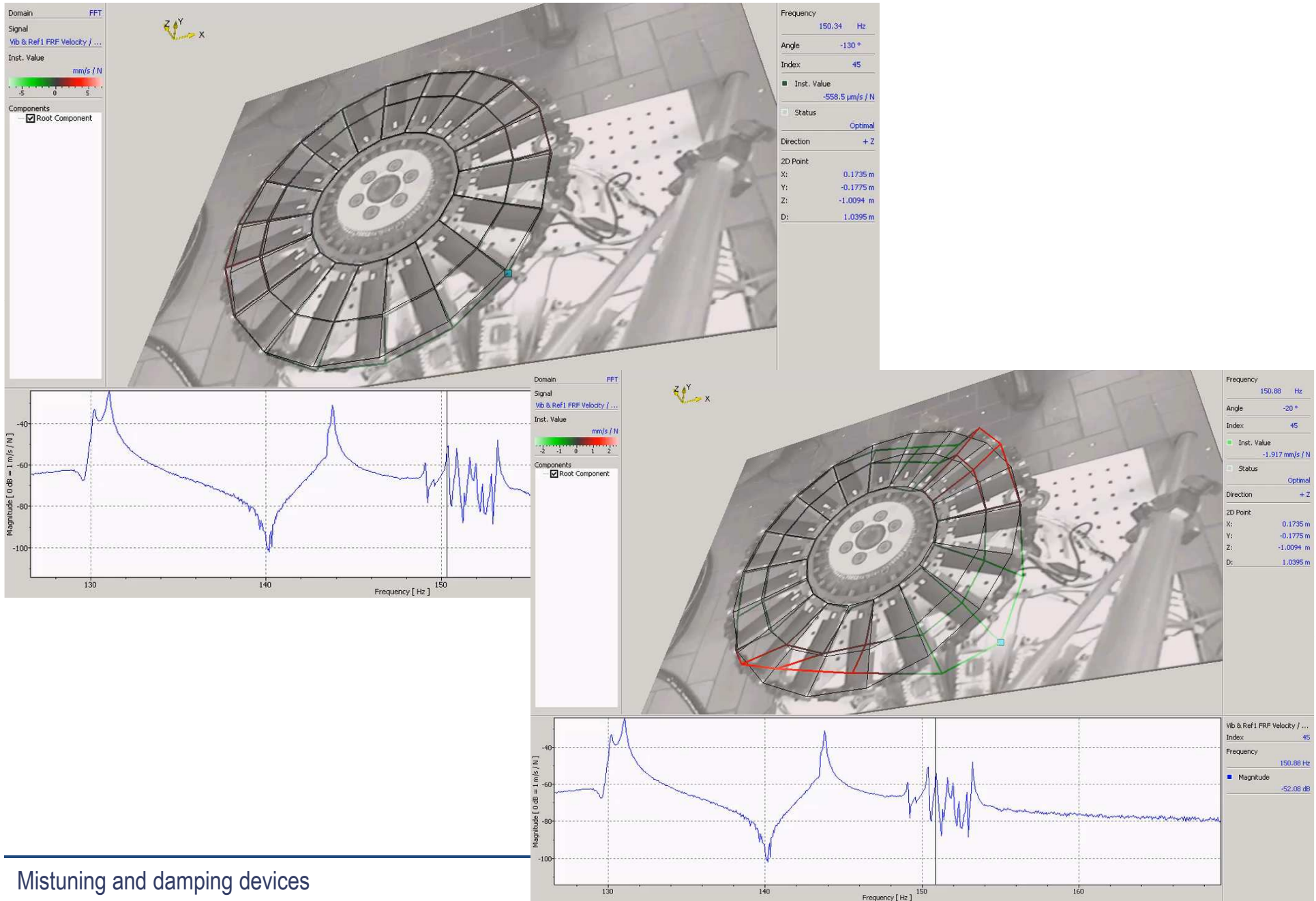
No show!



The effect of asymmetries in bladed disks

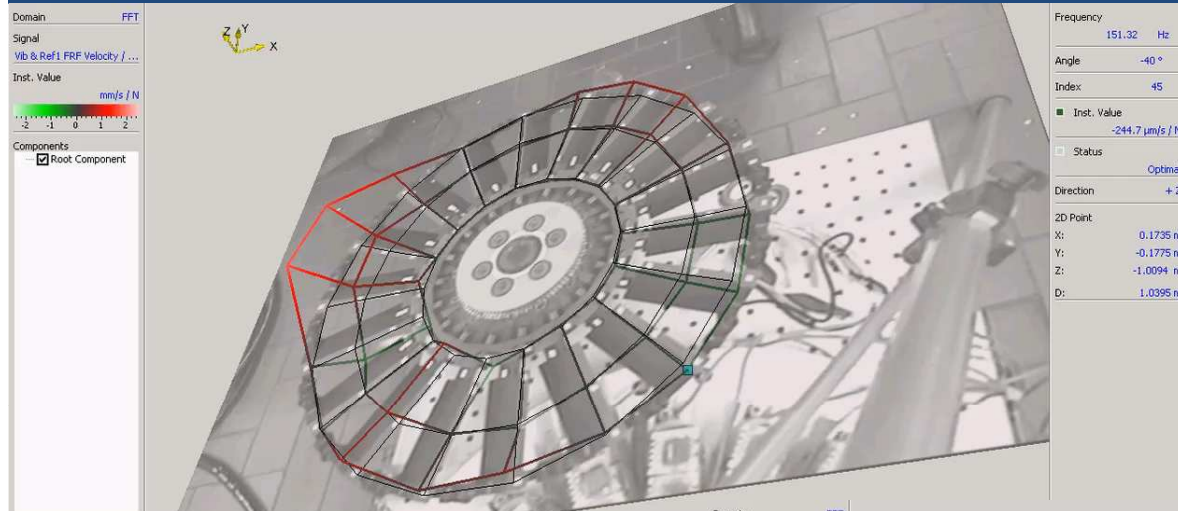


The effect of asymmetries in bladed disks

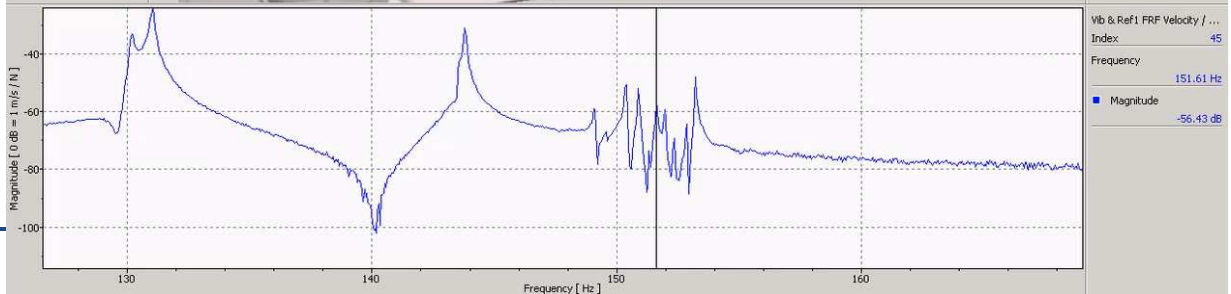
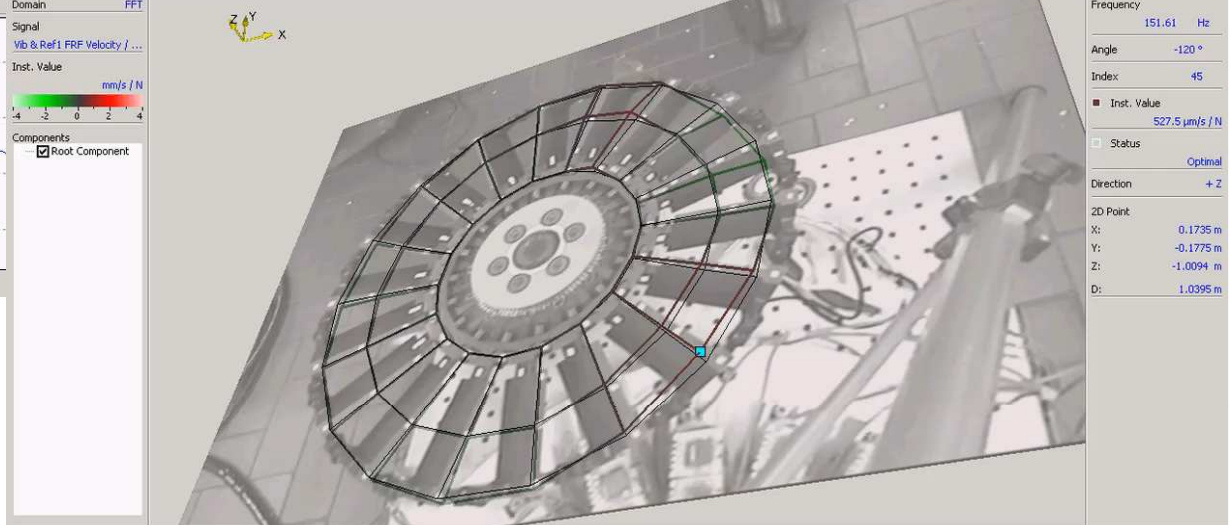
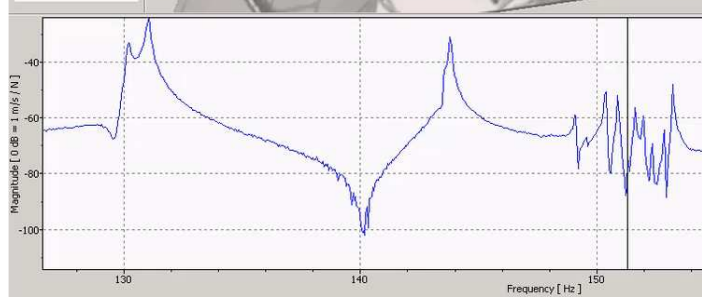


Mistuning and damping devices

The effect of asymmetries in bladed disks

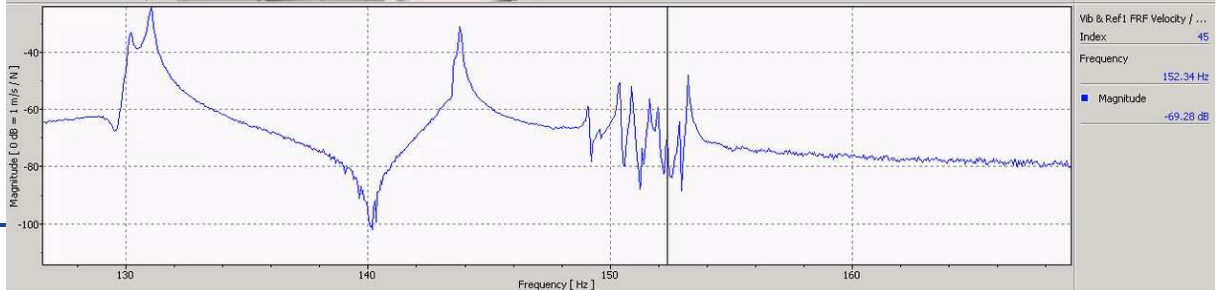
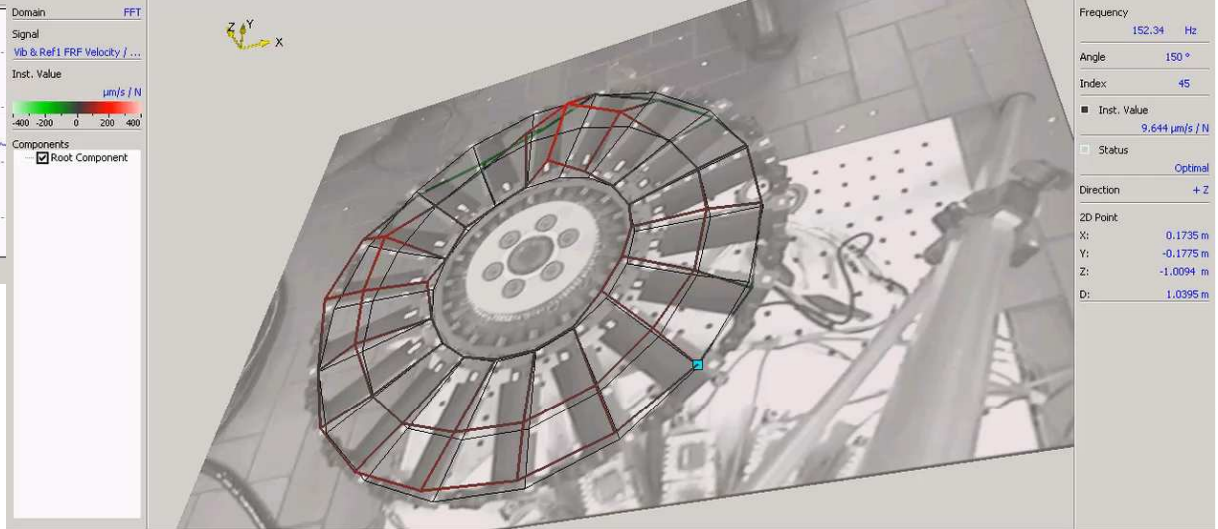
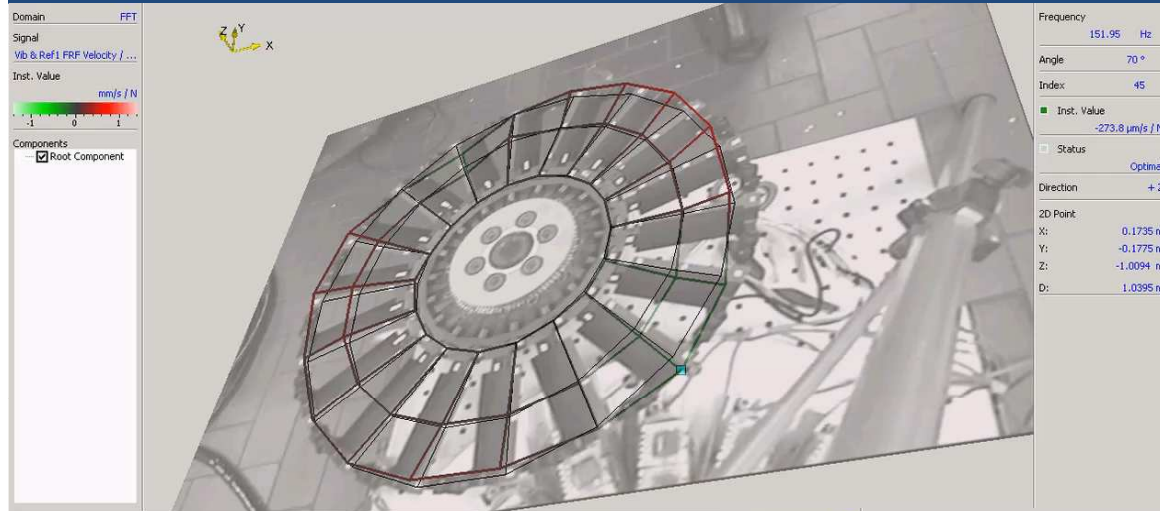


Response amplification for some blades



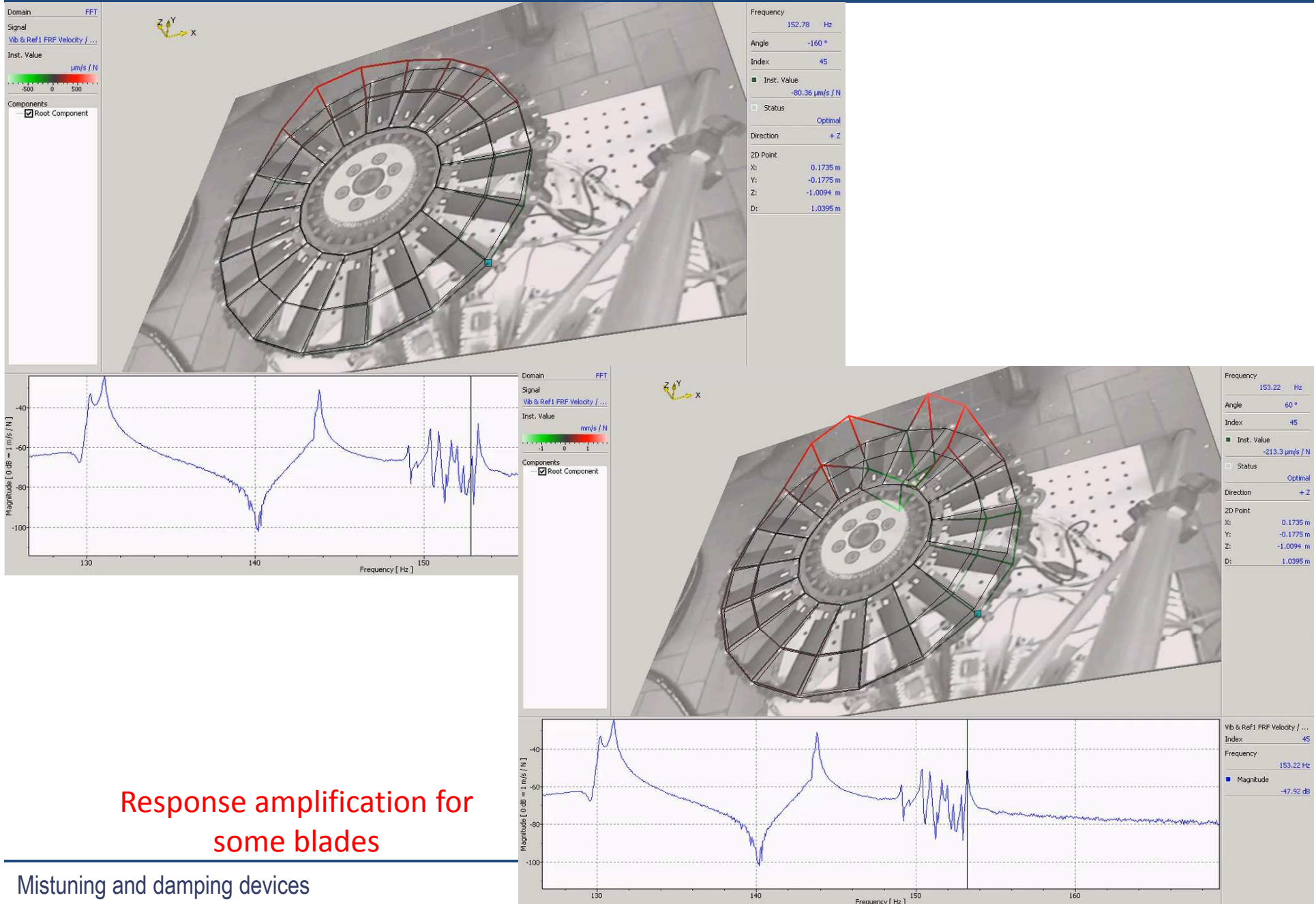
Mistuning and damping devices

The effect of asymmetries in bladed disks



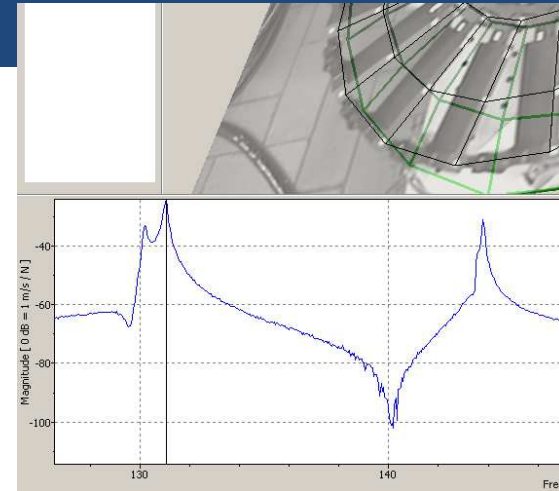
Mistuning and damping devices

The effect of asymmetries in bladed disks

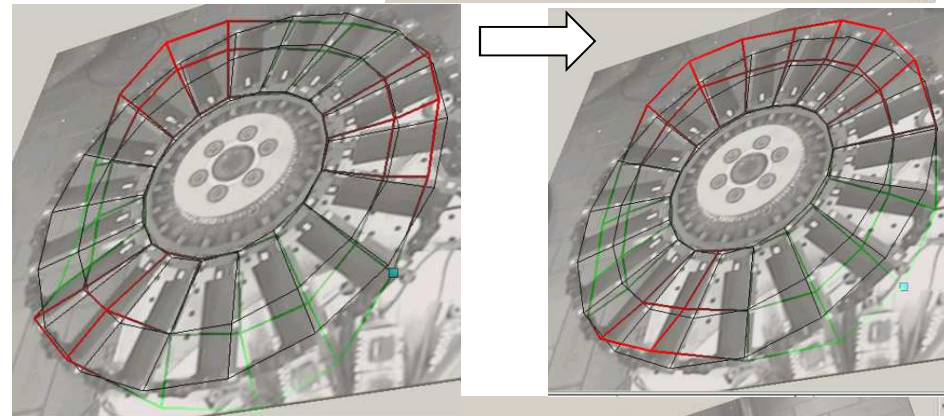


Symptoms of mistuning and causes

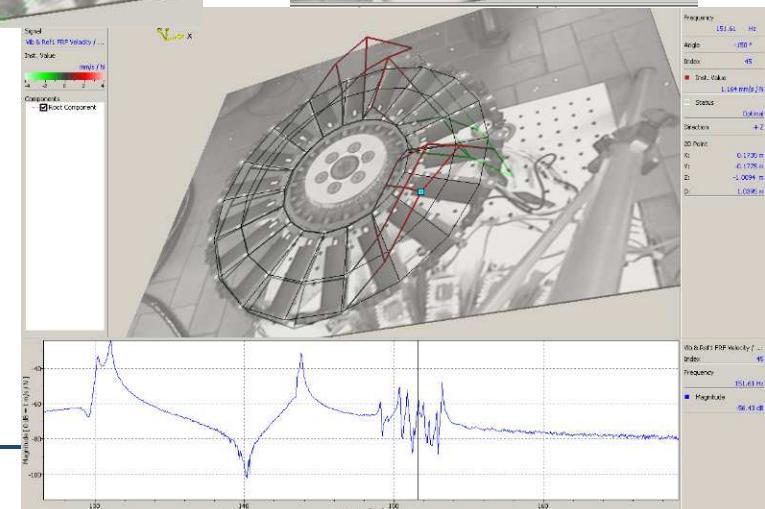
Split of the repeated frequency



Nodal Diameter distortion
(isolated mode shapes)

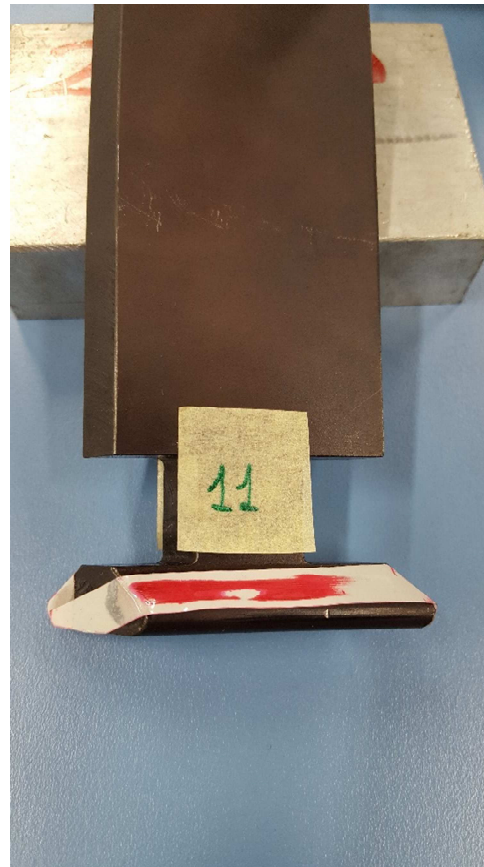
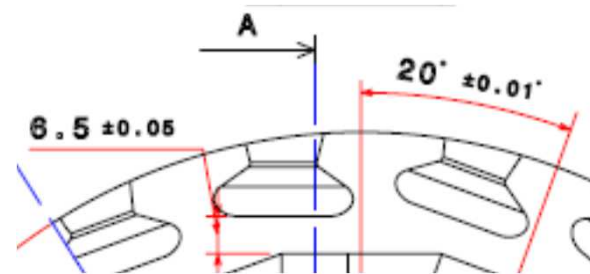


Amplification factor (high modal density regions)



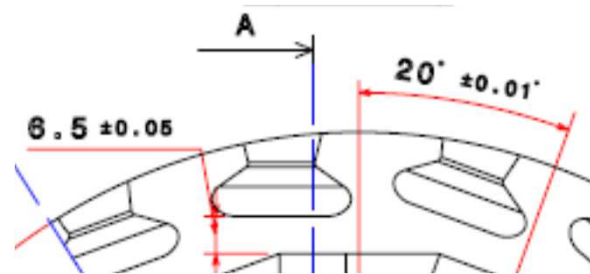
Symptoms of mistuning and causes

Manufacturing tolerances



Symptoms of mistuning and causes

Manufacturing tolerances

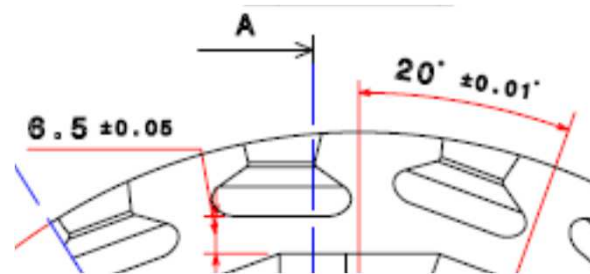


Assembly



Symptoms of mistuning and causes

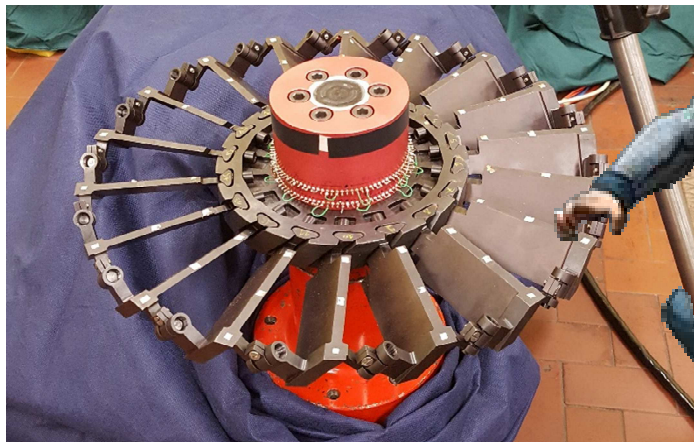
Manufacturing tolerances



Assembly

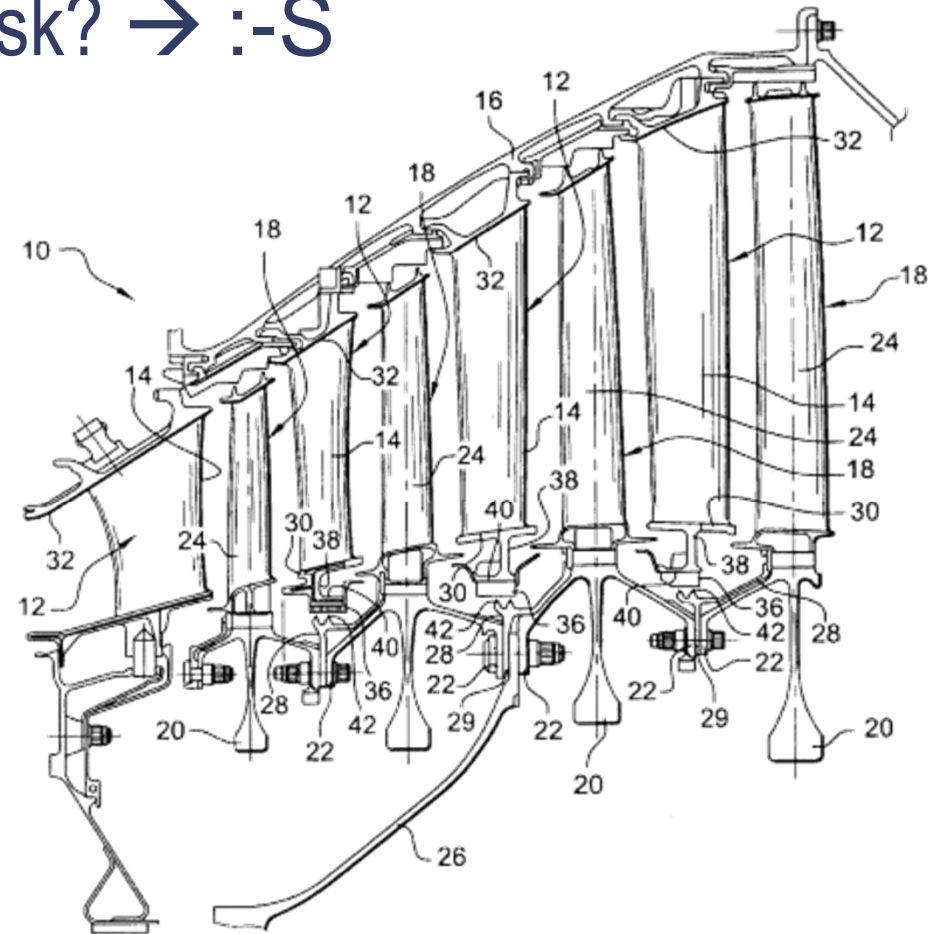
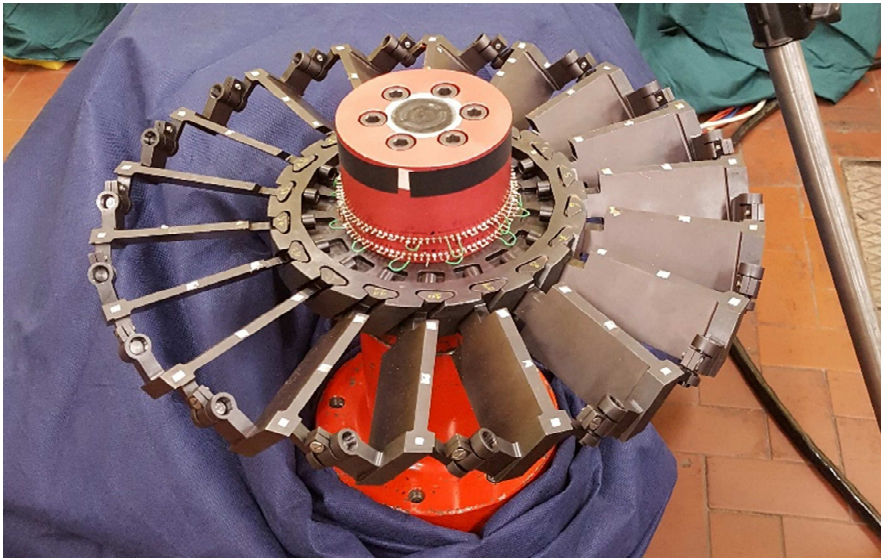


Wear in service



Symptoms of mistuning and causes

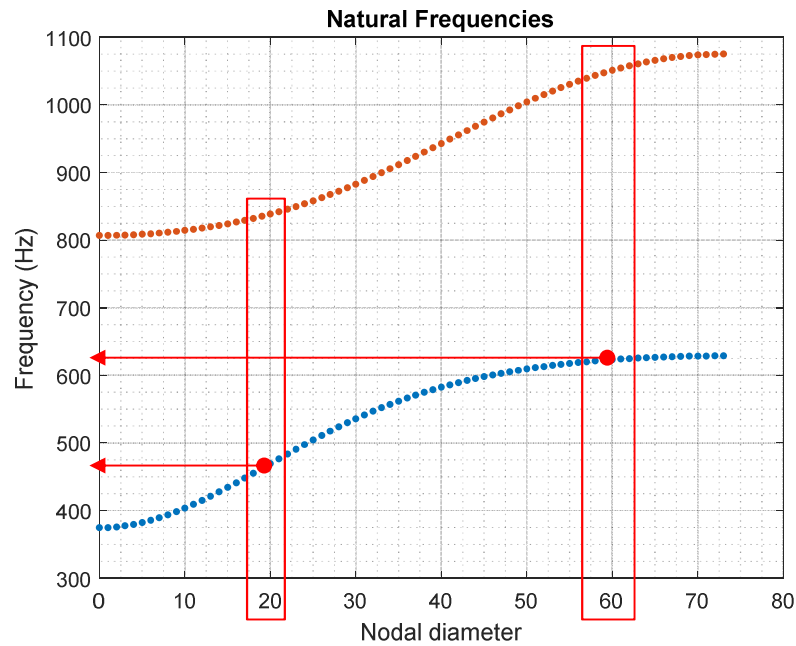
What if in a real bladed disk? \rightarrow :-S



Фиг. 1

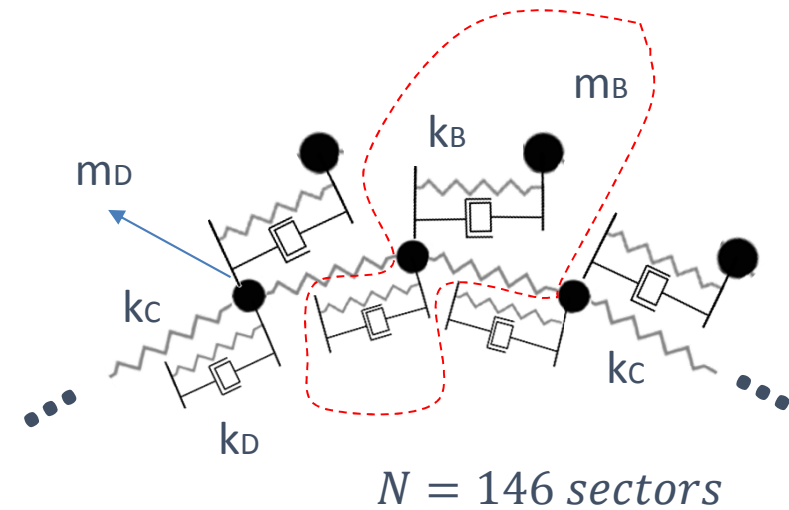
<http://russianpatents.com/patent/253/2532868.html>

Lumped parameters model



Isolated mode

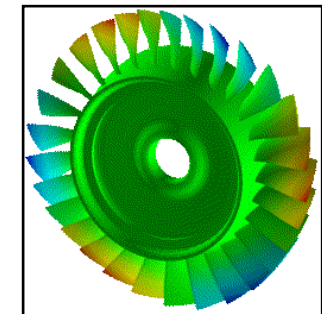
High modal density region



Excitation: travelling force with a given waveform along the hoop direction. The number of waves is called Engine Order (EO).

$$EO = mN \pm ND$$

$$m = 0 \rightarrow EO = ND = 20, 60$$



McGill University

Lumped parameters model

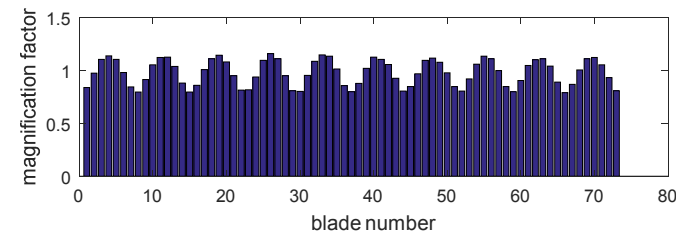
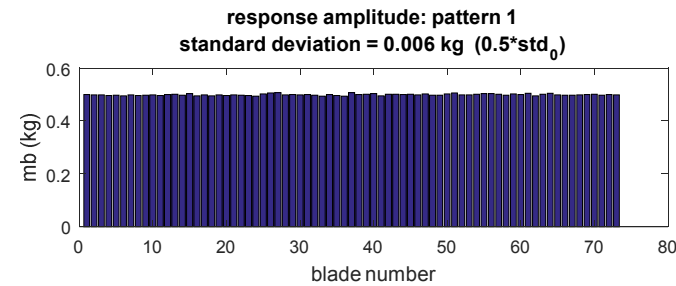
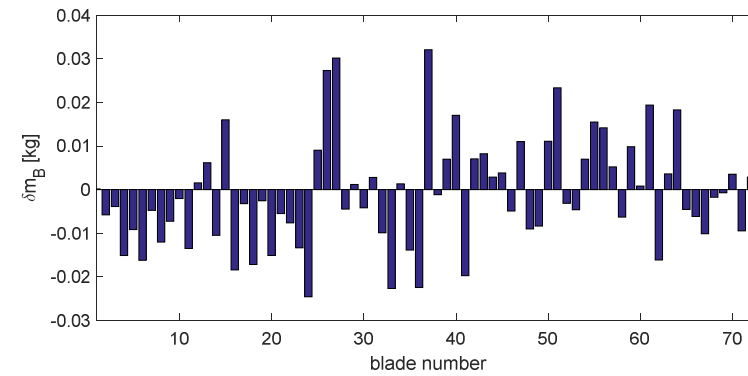
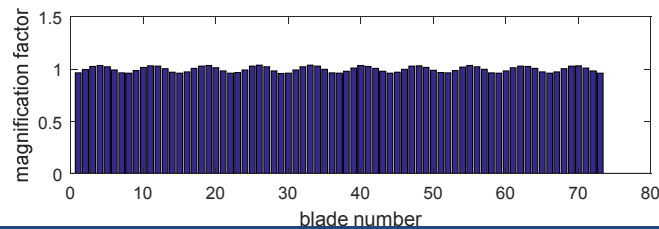
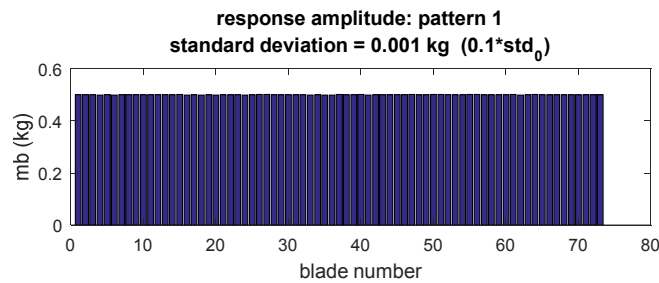
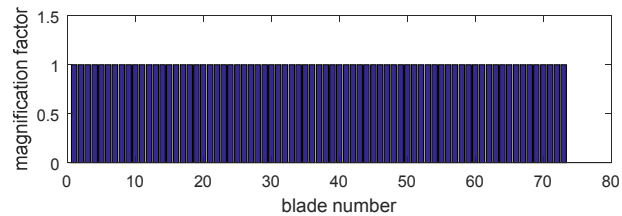
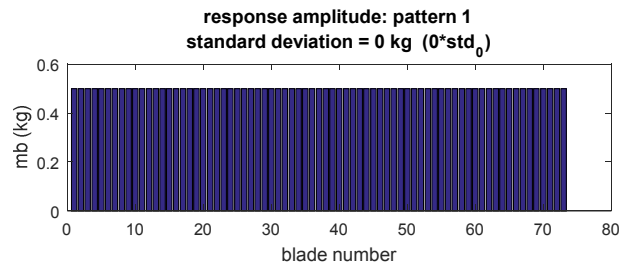
Isolated mode, first family

$$EO = ND = 20$$

Tuned response, first 73 blades plotted

A mistuning pattern is added on m_B with 0 mean value and standard deviation of 1.3% of the tuned blade mass (small mistuning)

Tuned

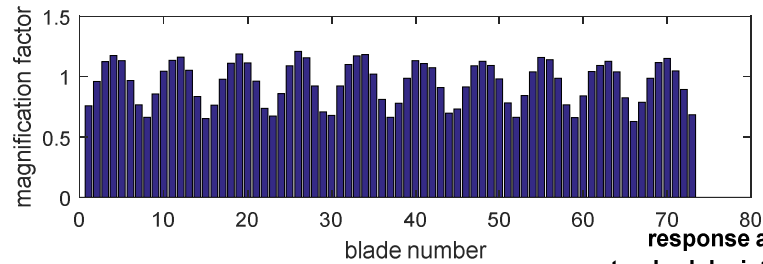
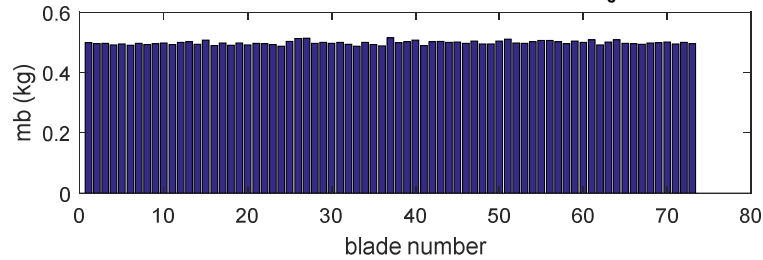


Lumped parameters model

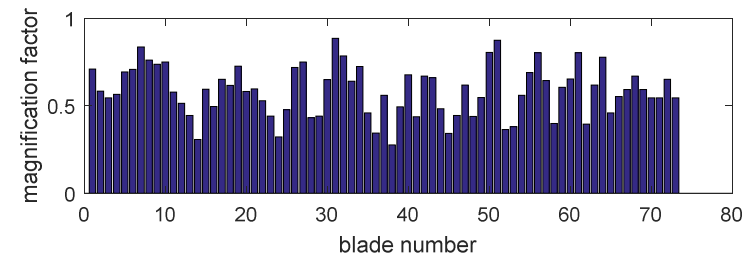
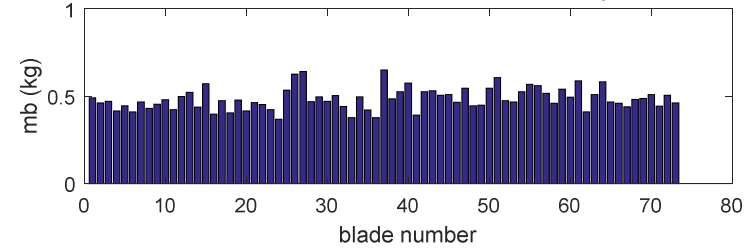
Isolated mode, first family

$$EO = ND = 20$$

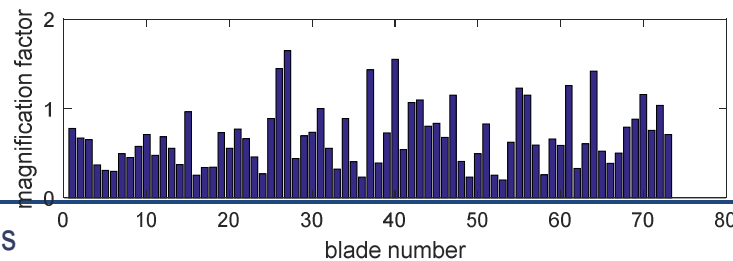
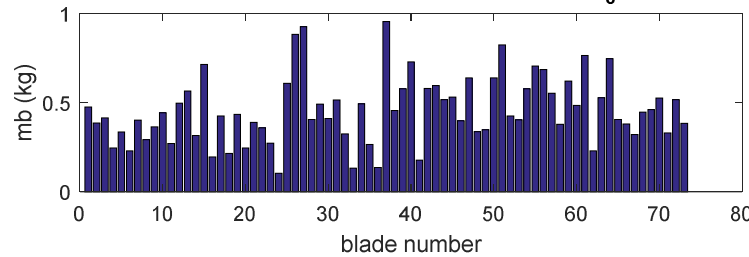
response amplitude: pattern 1
standard deviation = 0.013 kg ($1 \cdot \text{std}_0$)



response amplitude: pattern 1
standard deviation = 0.128 kg ($10 \cdot \text{std}_0$)



response amplitude: pattern 1
standard deviation = 0.383 kg ($30 \cdot \text{std}_0$)



Large mistuning!



<http://avherald.com/h?article=42290a67/0000>

Lumped parameters model

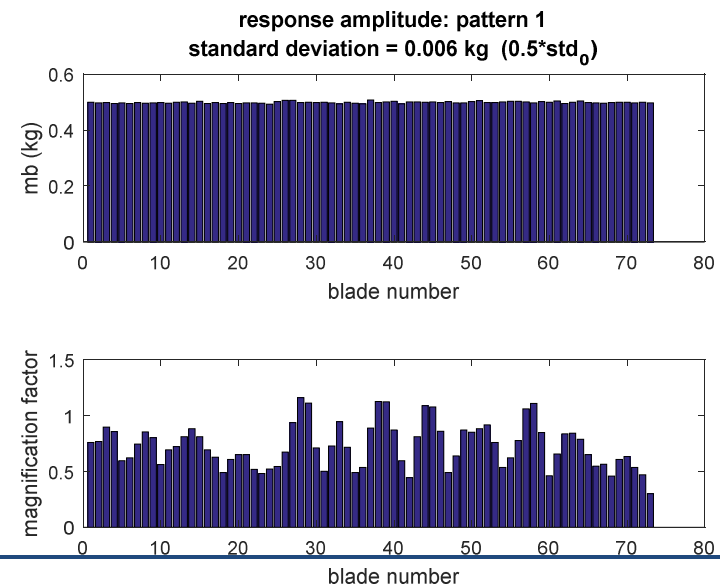
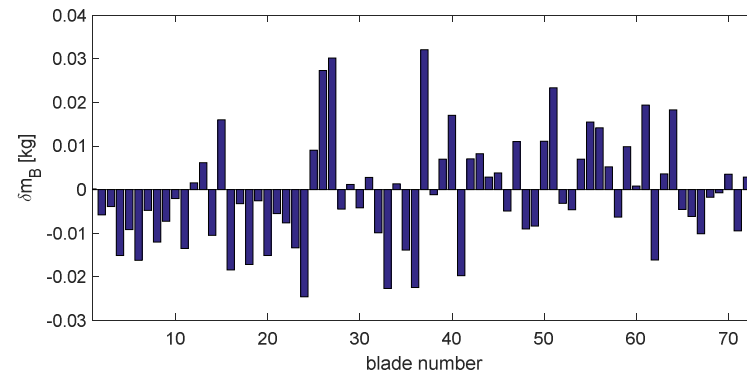
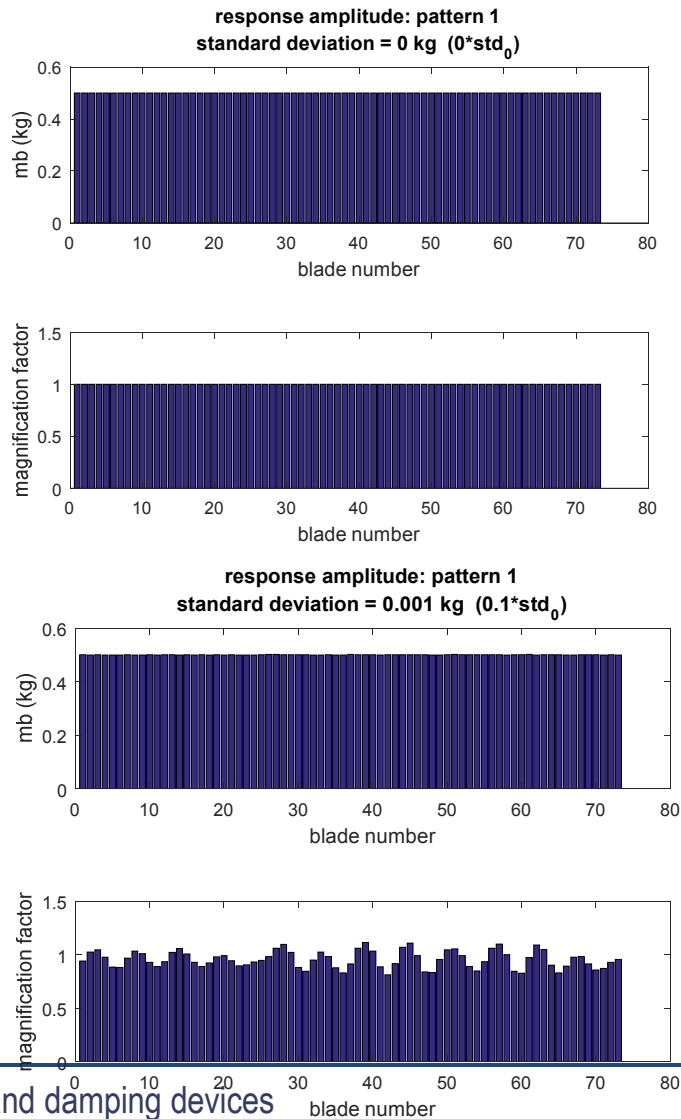
High modal density region, first family

$$EO = ND = 60$$

Tuned response, first 73 blades plotted

A mistuning pattern is added on m_B with 0 mean value and standard deviation of 1.3% of the tuned blade mass (small mistuning)

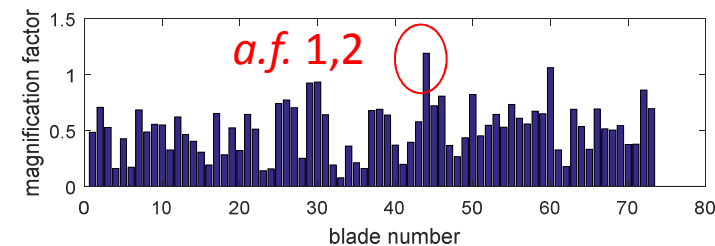
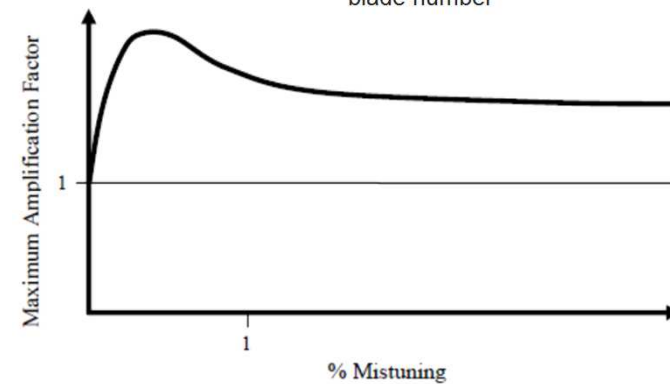
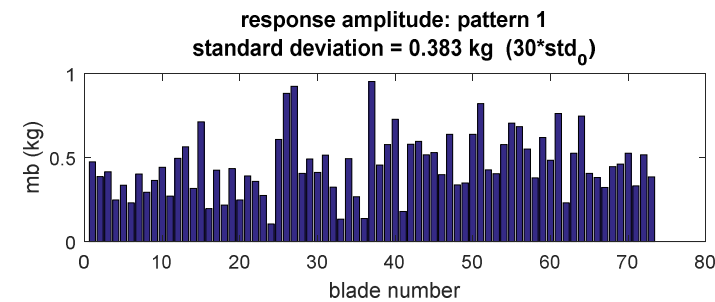
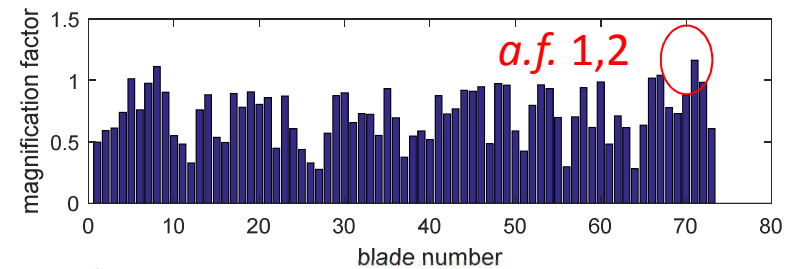
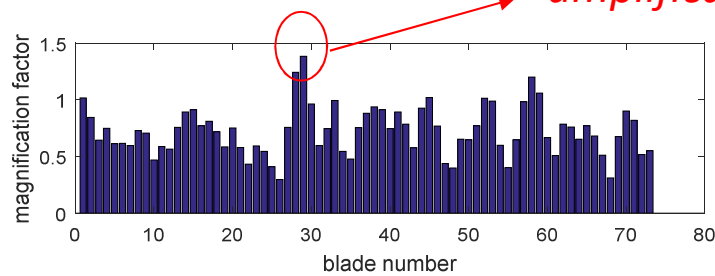
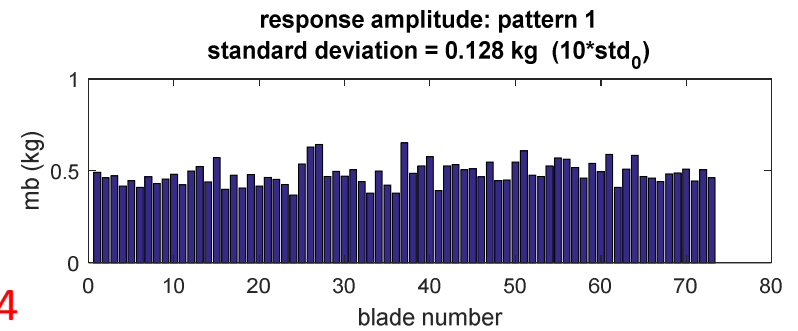
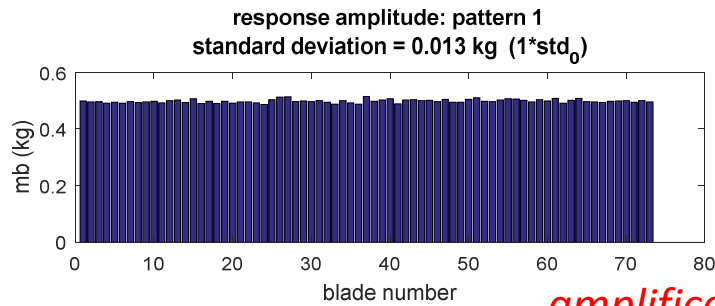
Tuned



Lumped parameters model

High modal density region, first family

$$EO = ND = 60$$



Whitehead amplification factor (1966):

$$\max a.f. = \frac{1 + \sqrt{N}}{2}$$

Numerical techniques to take into account mistuning: a literature overview

Mistuning models

- Carnegie Mellon University (USA) – Griffin
- University of Michigan (USA) – Castanier, Pierre, Epureanu
- Imperial College (UK) – Ewins, Petrov
- Brandenburg University of Technology Cottbus – Kühhorn, Beirov

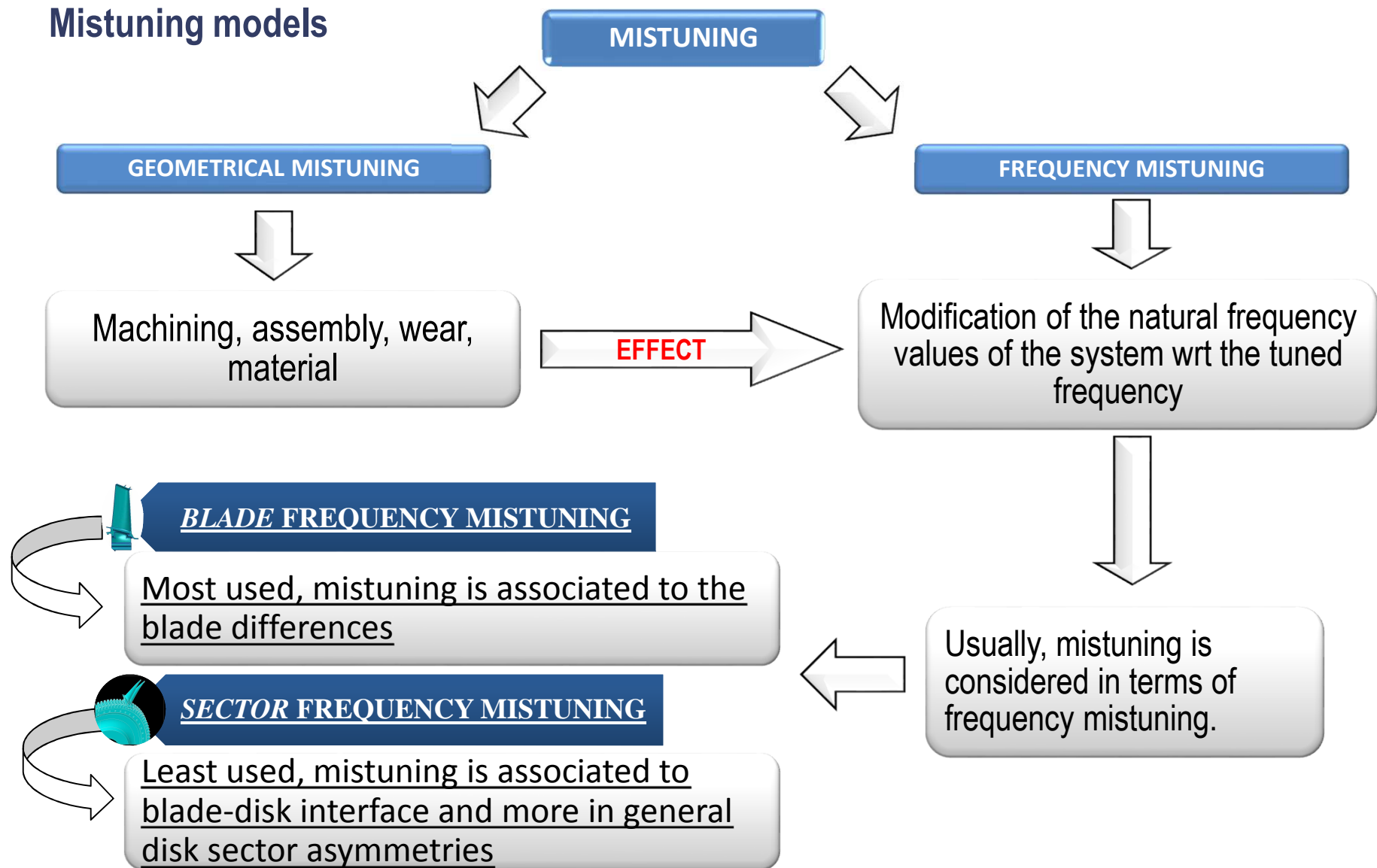
Reduction Techniques

- Carnegie Mellon University (USA) – Griffin
- University of Michigan (USA) – Castanier, Pierre
- Imperial College (UK) – Ewins, Petrov
- Politecnico di Torino (ITA) – Vargiu
- Université Paris-Est (FR) – Soize

Mistuning Identification

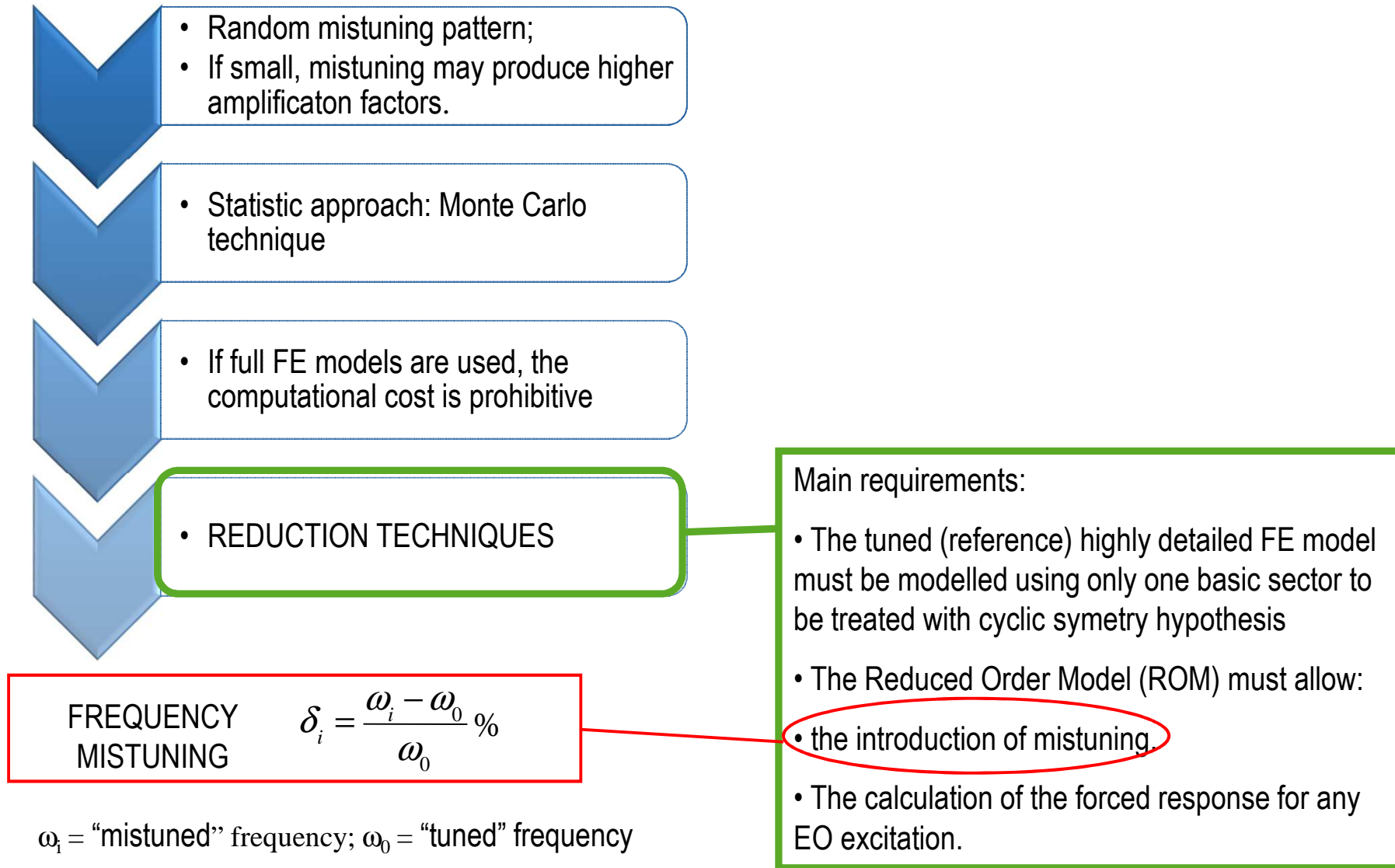
- Carnegie Mellon University (USA) – Griffin
- Ecole Centrale de Lyon (FR) – Thouverez
- Brandenburg University of Technology Cottbus – Kühhorn, Beirov

Numerical techniques to take into account mistuning: a literature overview



Numerical techniques to take into account mistuning: a literature overview

Reduction techniques: useful during design



Numerical techniques to take into account mistuning: a literature overview

Reduction techniques: useful during design

$$\begin{array}{c}
 \underbrace{([K] - \omega^2[M] + i\omega[C])}_{N \times N} \cdot \underbrace{\{x\}}_{N \times 1} = \underbrace{\{0\}}_{N \times 1} \\
 \xrightarrow{n \ll N} \\
 \underbrace{([\Psi]^T [K] [\Psi])}_{n \times n} - \omega^2 \underbrace{([\Psi]^T [M] [\Psi])}_{n \times n} + i\omega \underbrace{([\Psi]^T [C] [\Psi])}_{n \times n} \cdot \underbrace{\{q\}}_{n \times 1} = \underbrace{\{0\}}_{n \times 1} \\
 \underbrace{\{x\}}_{N \times 1} = \underbrace{[\Psi]}_{N \times n} \cdot \underbrace{\{q\}}_{n \times 1}
 \end{array}$$

Component Mode Synthesis (C.M.S.)

Example: Craig-Bampton (1968).

Bladed disk divided into its main components: Disk and blades

$\{q\} \Rightarrow$

- ✓ Modal coordinates (slave modes);
- ✓ Physical dofs (master nodes).

Features:

- Tuned system representation improves with the number of dofs;
- Frequency mistuning.

Mistuning:

Large number of master dofs

REDUCE, C.M.M.

Generalized, Normal Mode Reduction

Bladed disk studied as one body

$\{q\} \Rightarrow$

- ✓ modal coordinates;

Features:

- Very good accuracy of the *tuned system*;
- Geometrical mistuning.

Mistuning:

Product of matrices with big size.

S.N.M., F.M.M., MIST.RES.

Numerical techniques to take into account mistuning: a literature overview

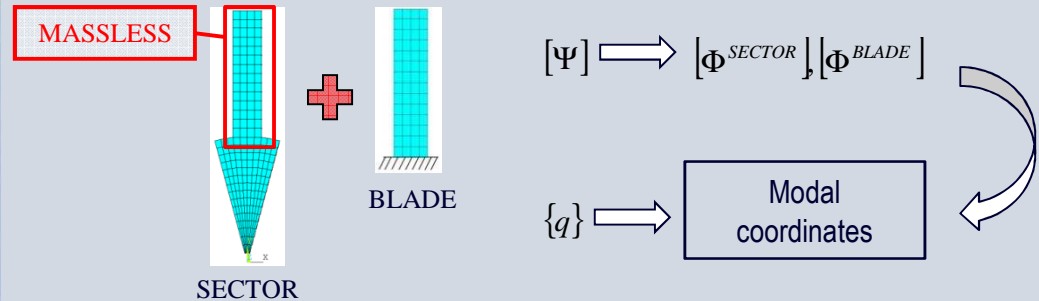
Reduction techniques: useful during design

REDUCE

Pierre, 1997

Idea

Blade displacements are a linear combination of two contributions: cantilever (mistuned) blade motion and motion driven by the disk.

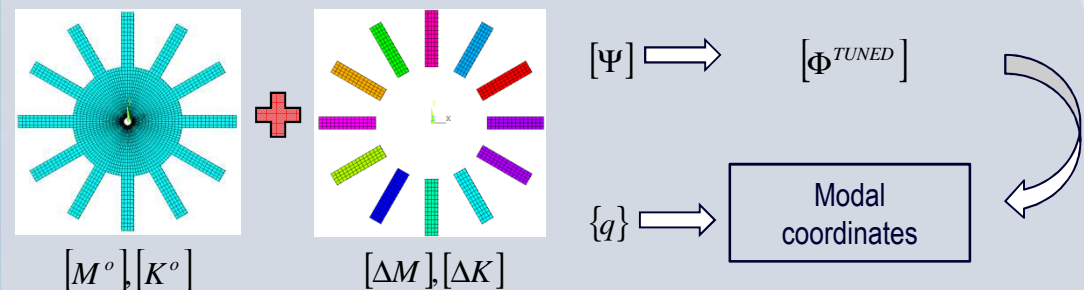


C.M.M. (Component Mode Mistuning)

Pierre, 2007

Idea

Matrix perturbation of the tuned condition = separate component with an interface with the tuned bladed disk.



I.M.M. (Integral Mistuning Model) Vargiu, 2012

N.E.W.T. (Nodal Energy Weight Transformation) Fitzner, 2014

Idea Mistuning can be associated to the disk sector and not only to the cantilever blade

Numerical techniques to take into account mistuning: a literature overview

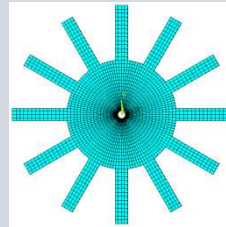
Reduction techniques: useful during design

S.N.M. (Subset of Nominal Modes)

Griffin, 2001

Idea

Mistuned modal shapes = linear combination of tuned mode shapes within the same frequency range.



$$[M^o] + [\Delta M], [K^o] + [\Delta K]$$

$$[\Psi] \Rightarrow [\Phi^{TUNED}]$$

$$\{q\} \Rightarrow \text{Modal coordinates}$$

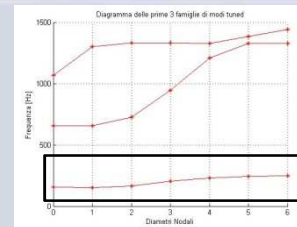
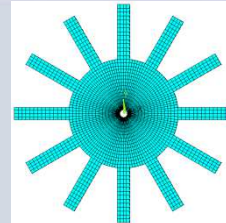


F.M.M. (Fundamental Mistuning Model)

Griffin, 2002

Idea

Application to a single modal family, isolate (no veering regions), flat.



$$[M^o] + [\Delta M], [K^o] + [\Delta K]$$

$$[\Psi] \Rightarrow [\Phi^{TUNED}]$$

$$\{q\} \Rightarrow \text{Modal coordinates}$$



MIST.RES.

Ewins, 2002

Idea

Sherman-Morrison-Woodbury formula to invert the dynamic stiffness matrix of the mistuned system.

$$[D(\omega)]^{-1} = ([D_o] + [U \cdot V^T])^{-1} = [D_o]^{-1} - [D_o]^{-1} \cdot [U] \cdot ([I] + [V]^T \cdot [D_o]^{-1} \cdot [U])^{-1} \cdot [V]^T \cdot [D_o]^{-1}$$

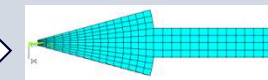


$$[\Delta D]$$

$$\{x\} = f(x_o, D_o^{-1})$$

$$\Rightarrow [\Phi^{TUNED}]$$

$$\Rightarrow$$



$$\{q\} \Rightarrow \text{Physical dofs}$$



Cyclic symmetry

Numerical techniques to take into account mistuning: a literature overview

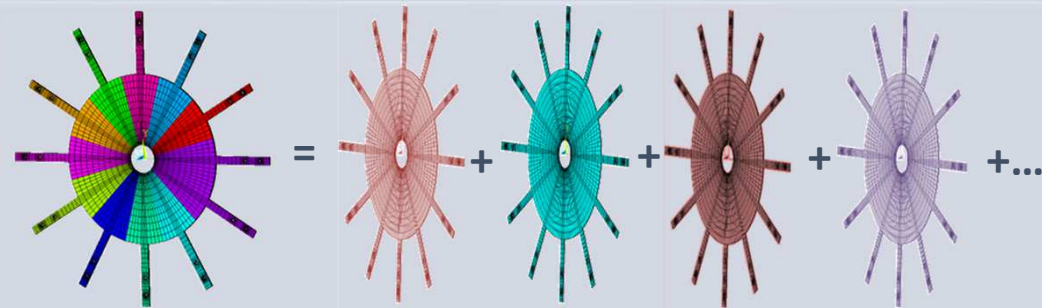
Reduction techniques: useful during design

LARGE MISTUNING (Subset of Normal Modes)

Mbaye, Soize, 2010

Idea

Each mistuned sector is used to build a 'tuned' disk and a modal basis is obtained as a set of cyclically symmetric mode shapes.

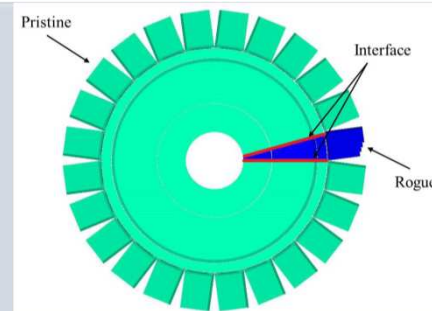


P.R.I.M.E. (Large mistuning)

Madden, 2012

Idea

Pristine-Rogue-Interface basic component, in this case the projection of the mistuned model is made using sector level mode shapes (low computational cost).



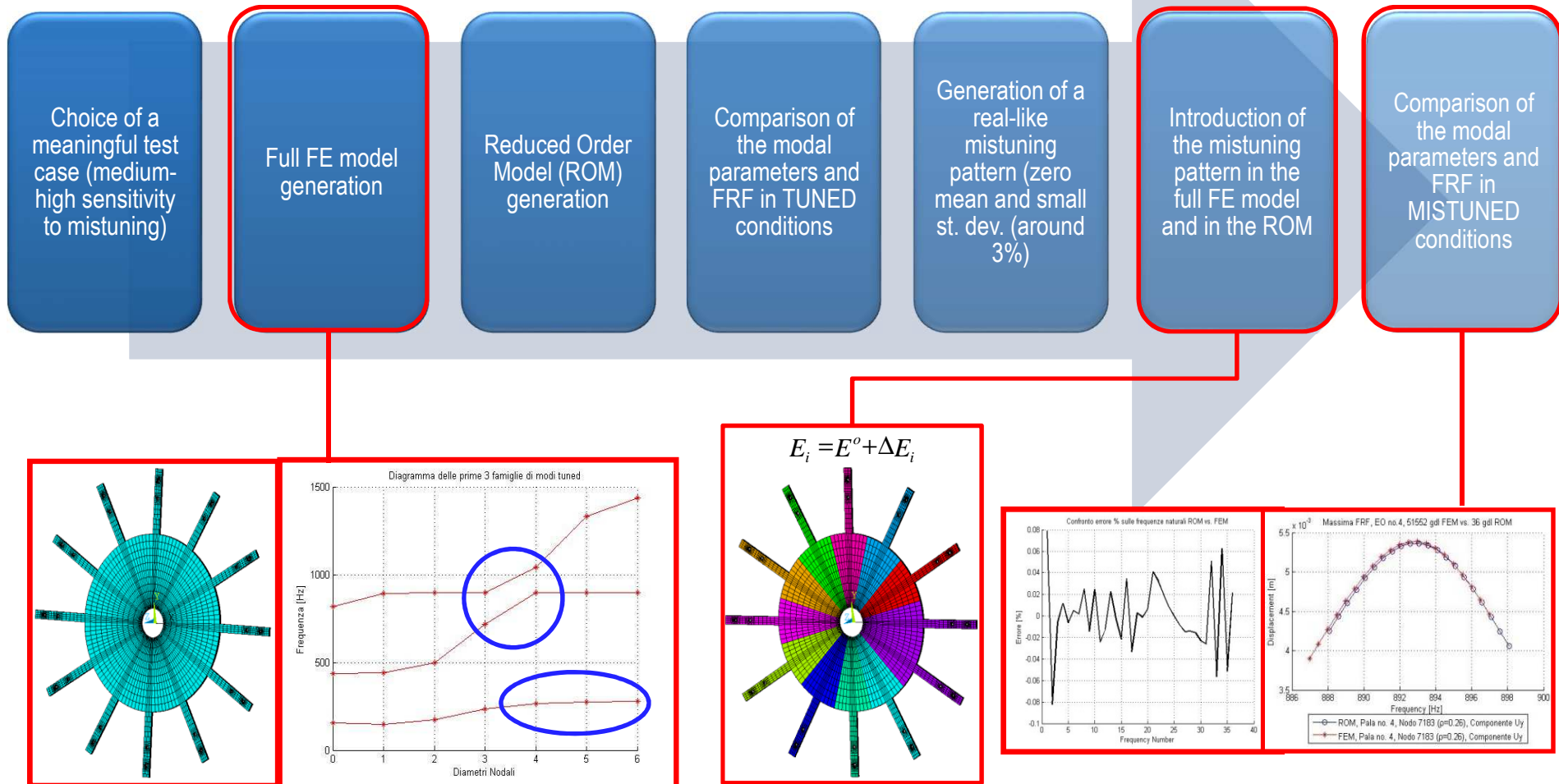
N-PRIME (small and Large Mistuning) Madden, 2012

N.E.W.T. + P.R.I.M.E. reduction techniques

Idea The mistuning pattern is added directly to the Reduced Order Model for Monte Carlo simulations

Numerical techniques to take into account mistuning: a literature review

Reduction techniques: numerical validation



Numerical techniques to take into account mistuning: a literature review

Reduction techniques: parameter for the comparison

NATURAL FREQUENCIES

- Absolute percentage error:

$$\varepsilon = \left| \frac{f_{ROM} - f_{FEM}}{f_{FEM}} \right| \cdot 100$$

- Frequency split error:

$$\varepsilon_{split}^{FEM} = \varepsilon - \left| \delta_{split}^{FEM} / 2 \right|$$

MODE SHAPES

- M.A.C.

$$MAC = \frac{|\phi^T \cdot \psi^*|}{(\phi^T \cdot \phi^*)(\psi^T \cdot \psi^*)}$$

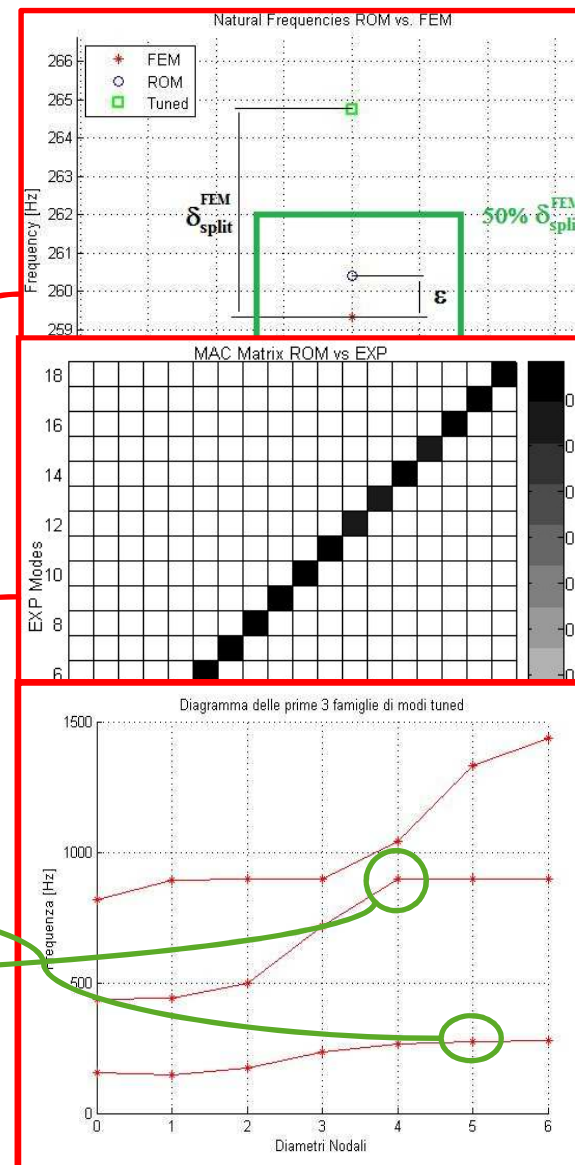
FORCED RESPONSE

- Engine order 5 out-of-plane

- Engine order 4 in-plane

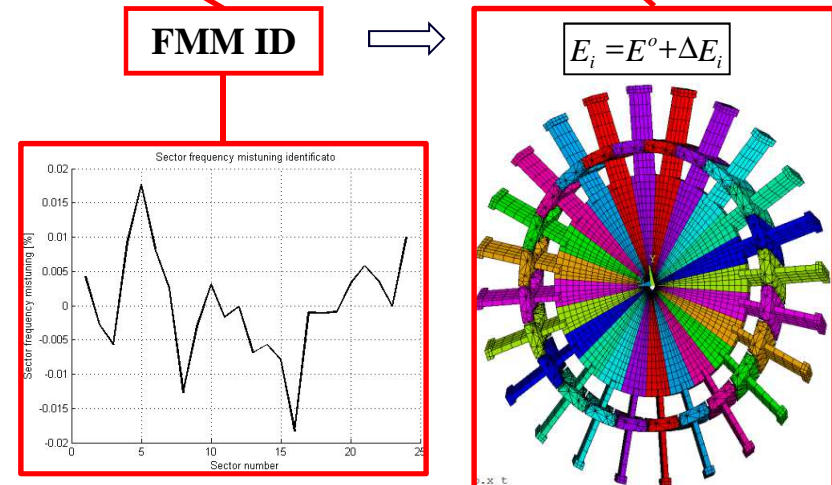
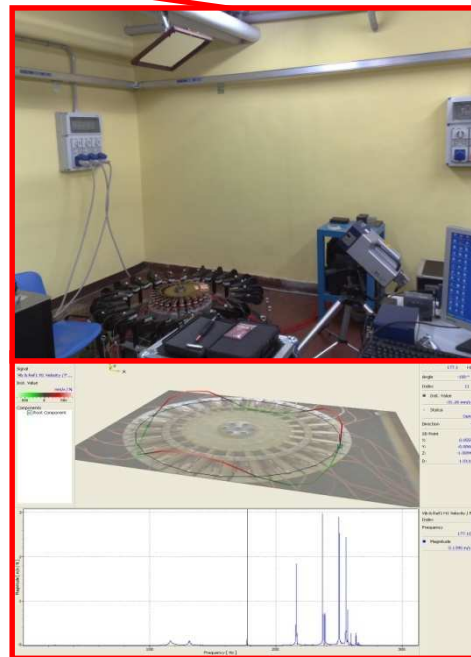
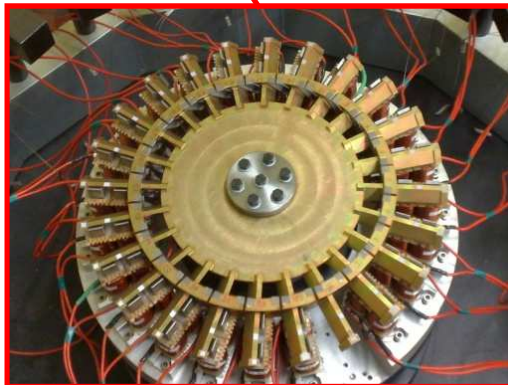
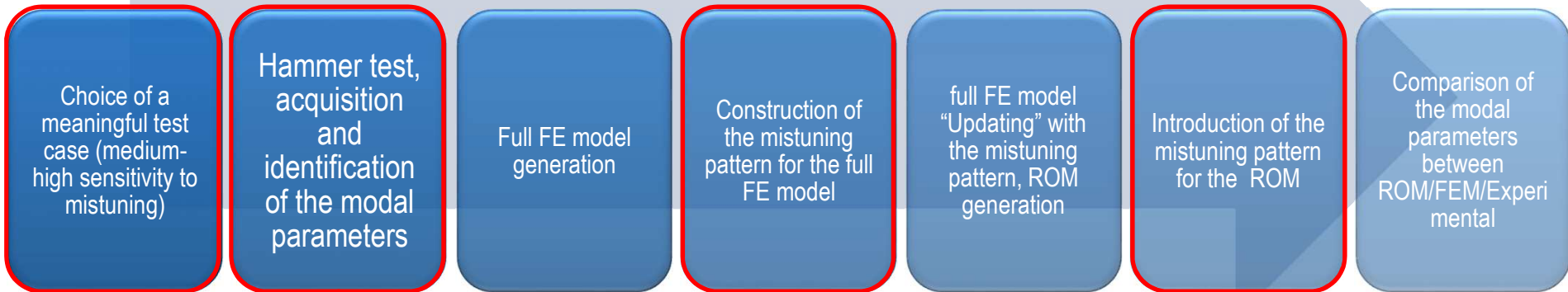
- Amplification factor:

$$A = x_{MAX}^{mistuned} / x_{MAX}^{tuned}$$



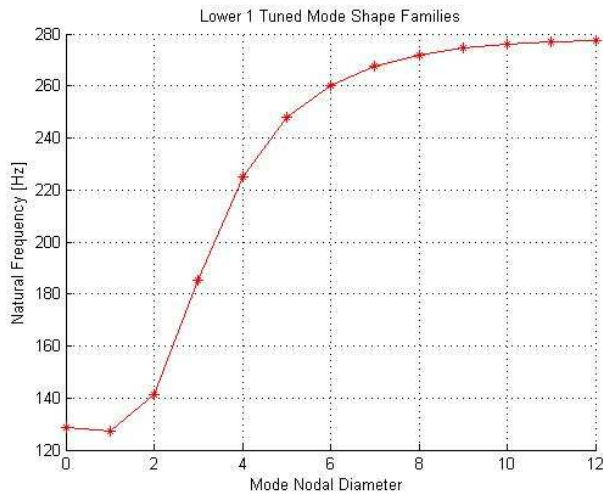
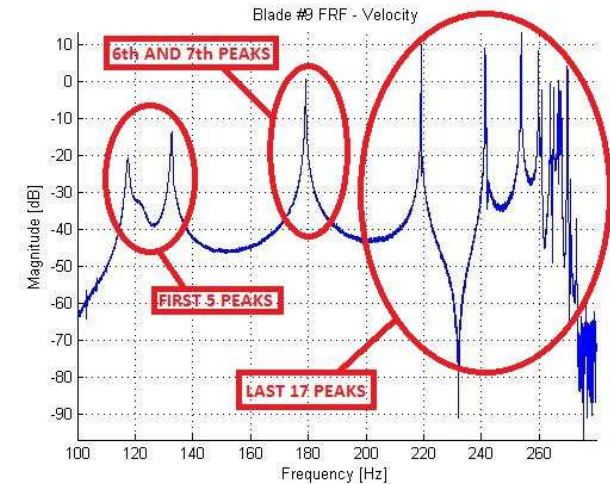
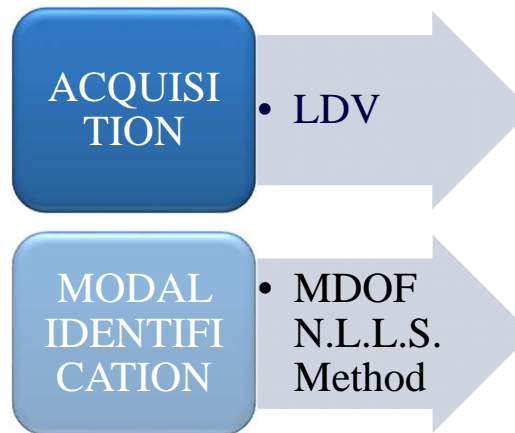
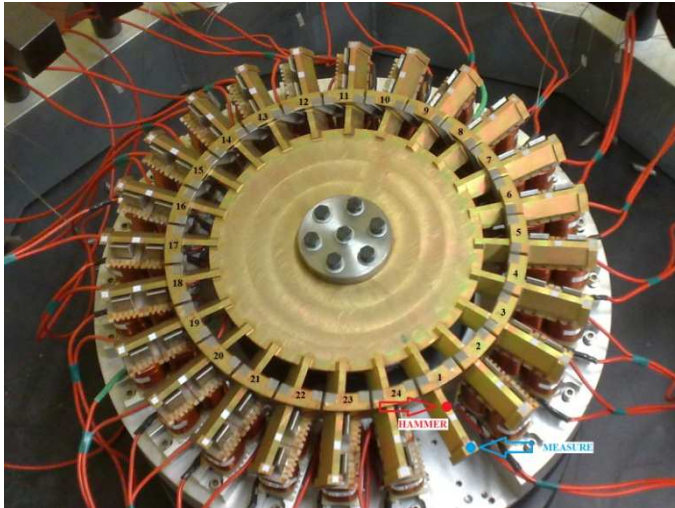
Numerical techniques to take into account mistuning: a literature review

Reduction techniques: experimental validation



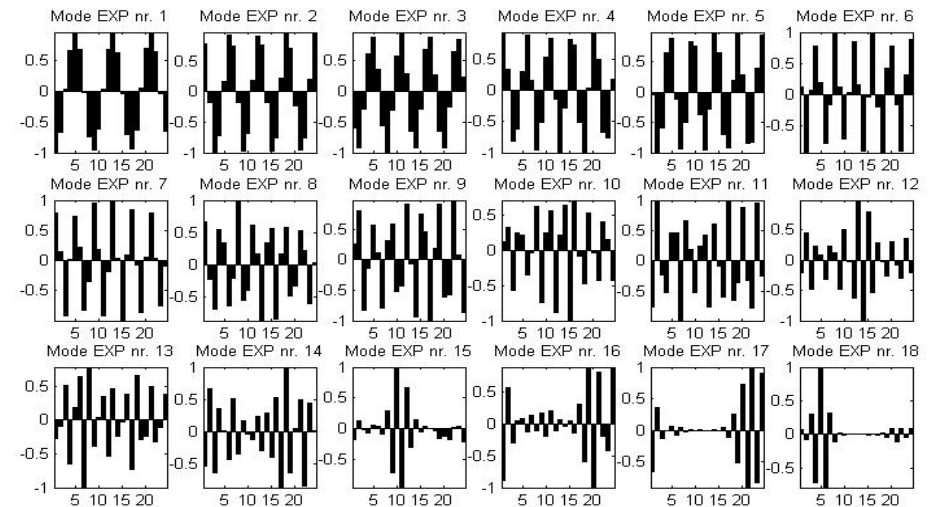
Numerical techniques to take into account mistuning: a literature review

Measurement – Hammer-test



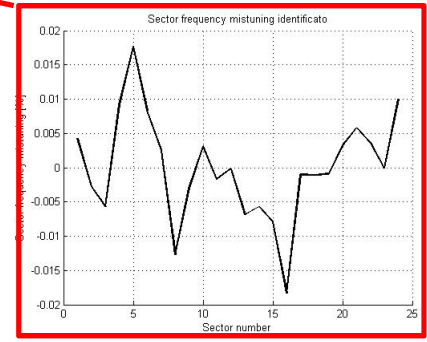
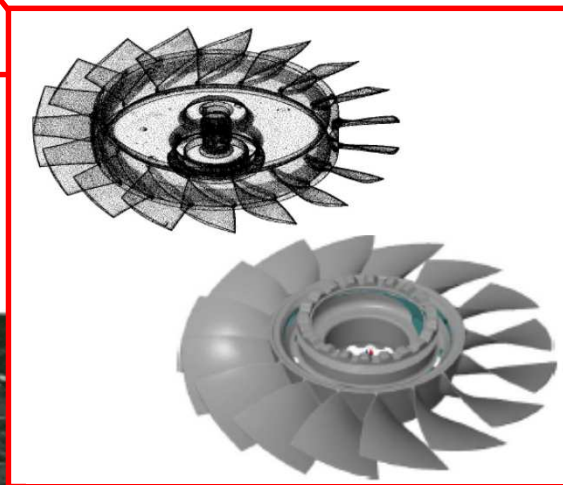
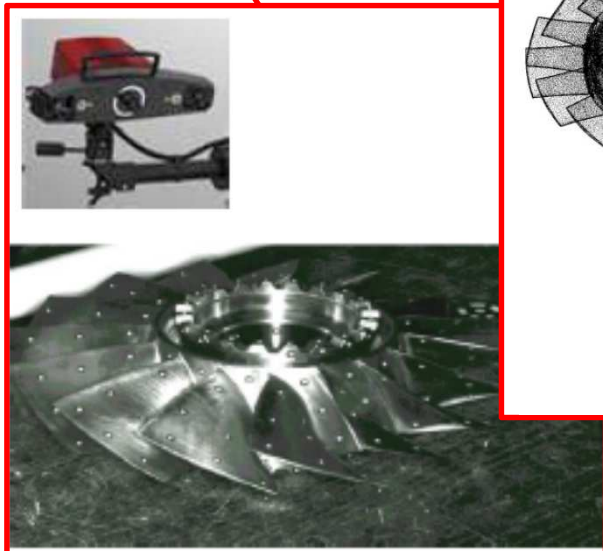
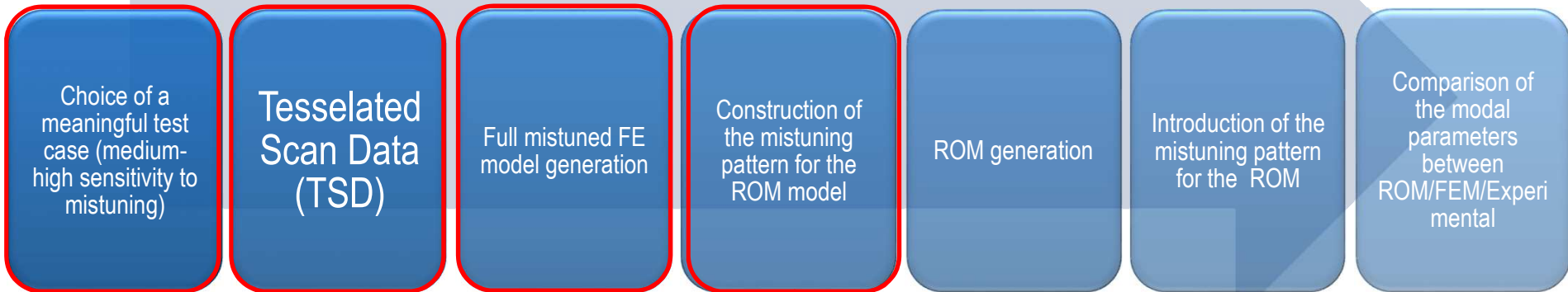
Frequencies [Hz]

- 179.08
- 219.07
- 219.24
- 241.27
- 242.04
- 253.43
- 253.72
- 259.73
- 260.82
- 263.83
- 264.94
- 266.57
- 266.89
- 267.69
- 269.70
- 269.81
- 270.87
- 272.95



Numerical techniques to take into account mistuning: a literature review

Reduction techniques: experimental validation (alternative)

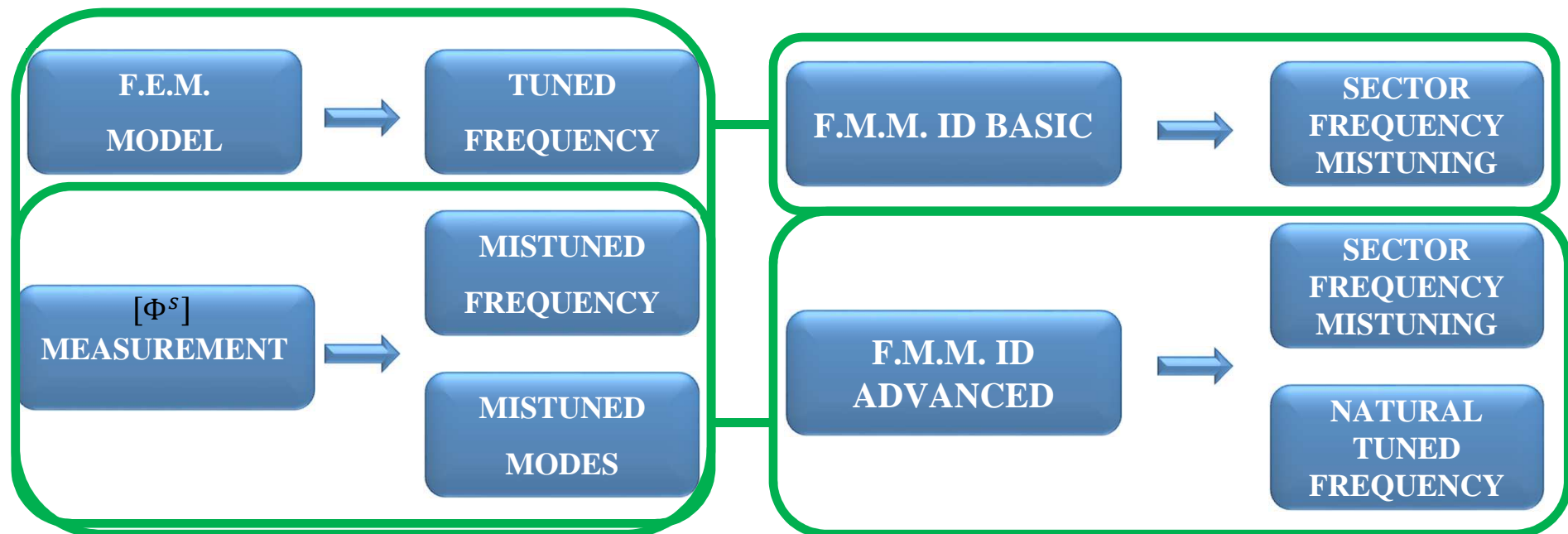


Jean de Cazenove , Scott Cogan Moustapha Mbaye (2013)
Alexander A. Kaszynski Joseph A. Beck, Jeffrey M. Brown (2014)

Numerical techniques to take into account mistuning: a literature review

F.M.M. ID is an identification technique for mistuned bladed disks developed at the Carnegie Mellon University (Griffin). It can be used for:

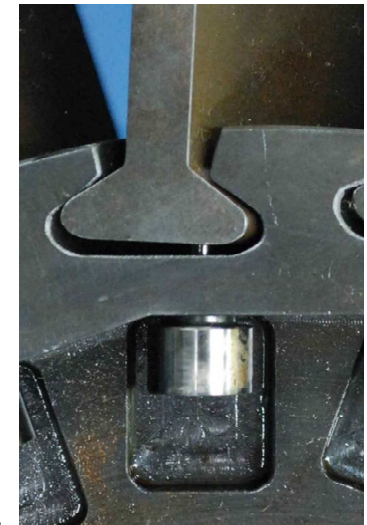
1. Isolated modal families;
2. Blade dominated modes.



The accuracy of the mistuning pattern identified by means of the F.M.M. ID strongly depends on the accuracy of the identified modal parameters in the experiments.

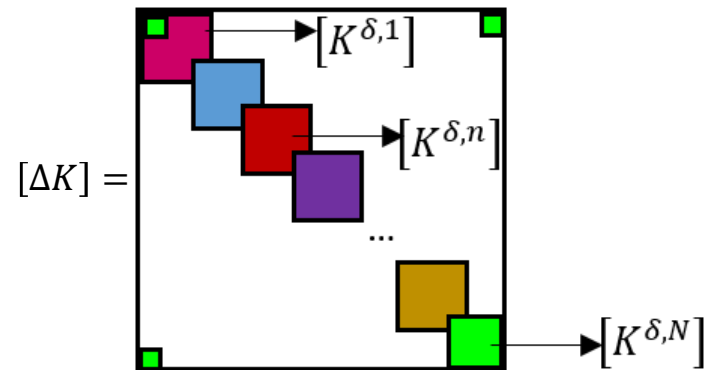
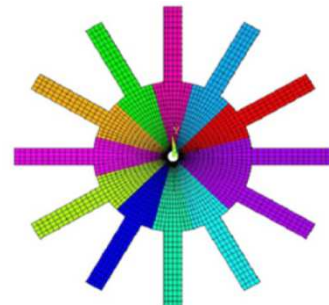
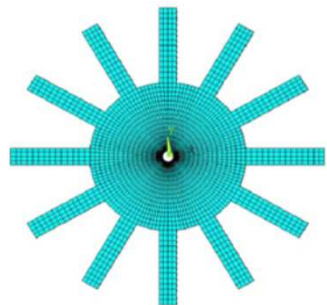
Numerical techniques to take into account mistuning in the presence of friction contacts

Blade root joint as a stiffness affected by mistuning: I.M.M. ROM



Tuned bladed disks

Perturbations of the single sectors



$[M], [K]$ Tuned system

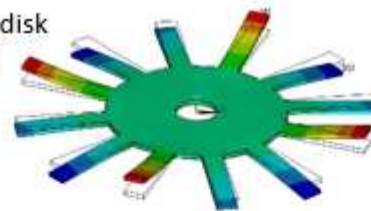
$[\Delta M], [\Delta K]$

$[\Lambda^s]$ Tuned eigenvalues

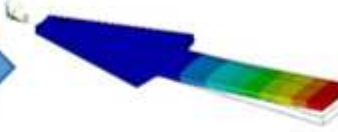
$[\Phi^s]$ Tuned eigenvectors

Key idea:

Tuned bladed disk
with N blades



n-th sector

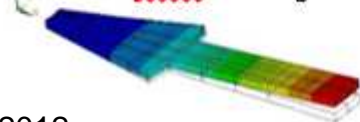


||

single sector – free interfaces

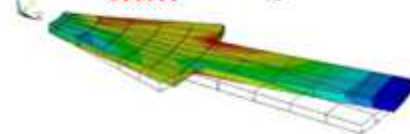
$[\Phi^{0,n}]$

Out of plane bending



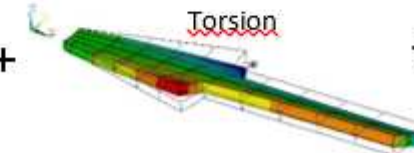
+

In plane bending



+

Torsion

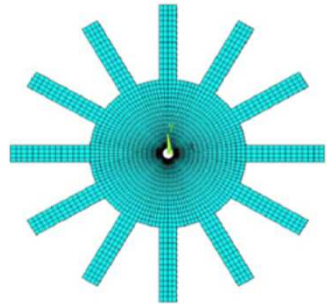


+ ...

Numerical techniques to take into account mistuning in the presence of friction contacts

Blade root joint as a stiffness affected by mistuning

Tuned bladed disks

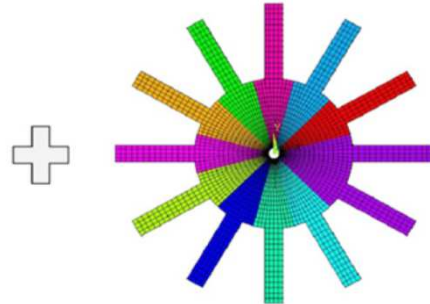


$[M], [K]$ Tuned system

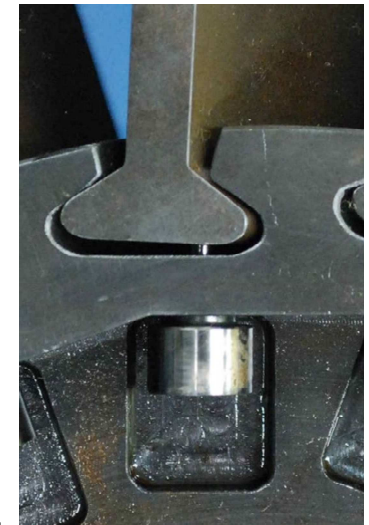
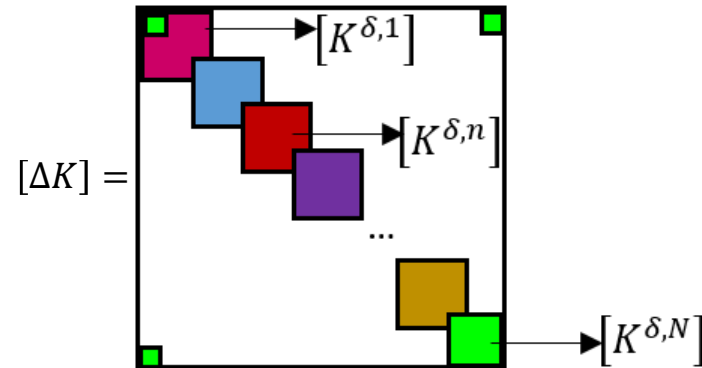
$[\Lambda^s]$ Tuned eigenvalues

$[\Phi^s]$ Tuned eigenvectors

Perturbations of the single sectors



$[\Delta M], [\Delta K]$



Prohibitive time cost
for computation

$$[M^{mist}] = [M] + [\Delta M] \quad \Rightarrow \quad [\Phi^s]^T [M^{mist}] [\Phi^s] = \mu^{rom} = I + [\Phi^s]^T [\Delta M] [\Phi^s]$$

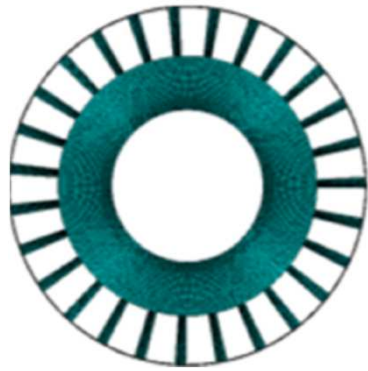
$$[K^{mist}] = [K] + [\Delta K] \quad \Rightarrow \quad [\Phi^s]^T [K^{mist}] [\Phi^s] = k^{rom} = \Lambda^s + [\Phi^s]^T [\Delta K] [\Phi^s]$$

$$\begin{aligned} [\Phi^s]^T [\Delta K] [\Phi^s] &= \sum_{n=1, \dots, N} [\Phi^{s,n}]^T [K^{\delta,n}] [\Phi^{s,n}] \approx \sum_{n=1, \dots, N} [\Phi^{0,n} q^n]^T [K^{\delta,n}] [\Phi^{0,n} q^n] = \\ &= \sum_{n=1, \dots, N} [q^n]^T [\Phi^{0,n}]^T [K^{\delta,n}] [\Phi^{0,n}] [q^n] = \sum_{n=1, \dots, N} [q^n]^T \text{diag}_{p=1, \dots, P} (\delta_p^n \cdot \lambda_p) [q^n] \end{aligned}$$

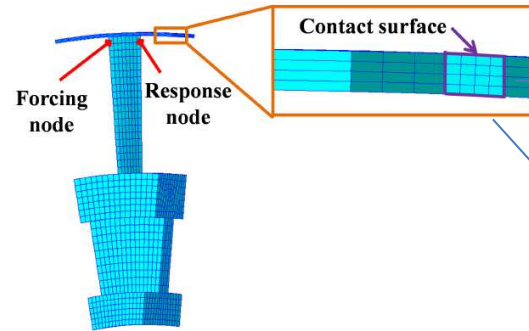
Vargiu, Firrone, Zucca, 2012

Numerical techniques to take into account mistuning in the presence of friction contacts

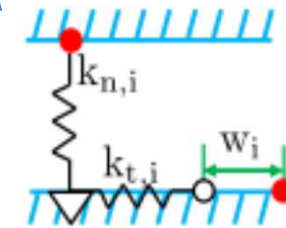
Shroud contact: stiffness affected by mistuning and nonlinear forces



a CMS – CB ROM is produced

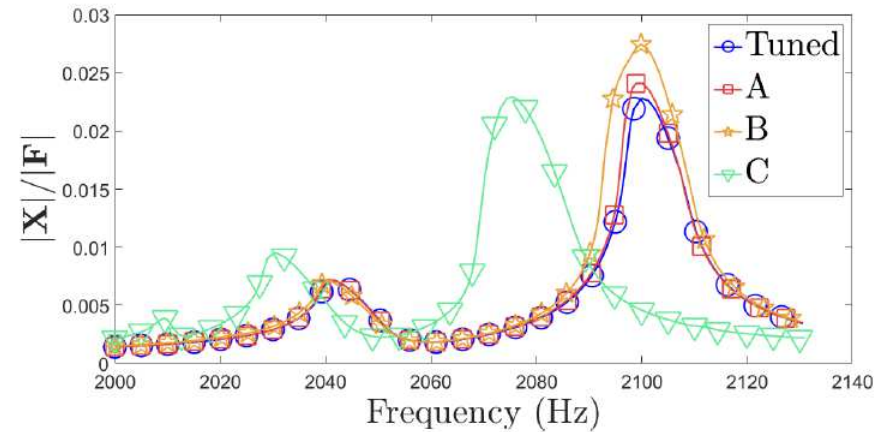
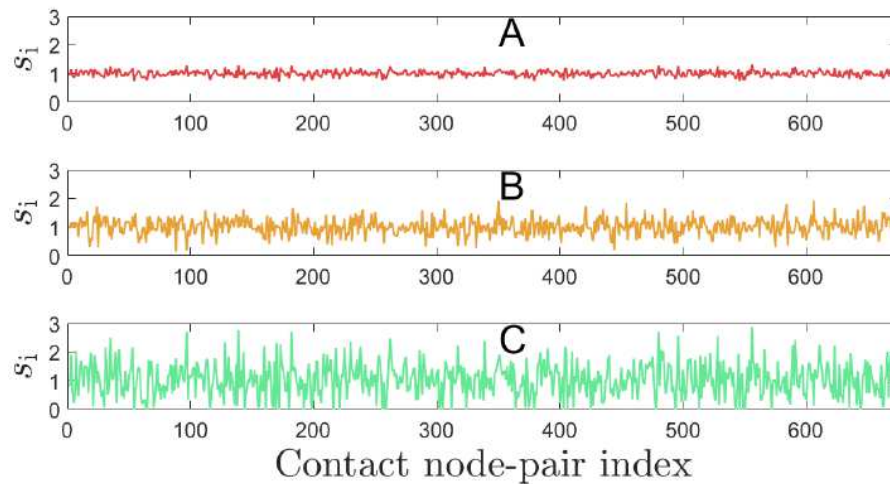


Master nodes



Friction coefficient

Mistuning pattern on contact stiffness



RESPONSE TO EO 12 EXCITATION

REFERENCES

- [1] Mead, D.J., *A General Theory of Harmonic Wave Propagation in Linear Periodic Systems with Multiple Coupling*, Journal of Sound and Vibration (1973) **27**(2), 235-260.
- [2] Ottarsson, G.S. and Pierre, C., *A Transfer Matrix Approach to Free Vibration Localization in Mistuned Blade Assemblies*, Journal of Sound and Vibration, (1996) **197**(5), 589-618.
- [3] Pierre, C. and Castanier, M.P., *Individual and Interactive Mechanisms for Localization and Dissipation in a Mono-Coupled Nearly-Periodic Structure*, Journal of Sound and Vibration, (1993) **168**(3), 479-505.
- [4] Ottarsson, G.S., *Dynamic Modeling and Vibration Analysis of Mistuned Bladed Disks*, PhD Thesis, (1994).
- [5] Pierre, C., Ottarsson, G.S. and Castanier, M.P., *A Reduced Order Modeling Technique for Mistuned Bladed Disks*, ASME Journal of Sound and Vibration, (1997) **119**(3), 439-447.
- [6] Pierre, C. and Kruse, M.J., *Forced Response of Mistuned Bladed Disks Using Reduced-Order Modeling*, Proceeding of the 37th ALAA/ASME/ASCE/AHS/ASC Structures, Structural Dynamics, and Materials Conference, Salt Lake City, Utah, 4, pp. 1938-1950.
- [7] Pierre, C., Castanier, M.P. and Bladh, R., *Reduced Order Modeling and Vibration Analysis of Mistuned Bladed Disk Assemblies with Shrouds*, ASME Journal of Engineering for Gas Turbines and Power, (1999) **121**(3), 515-522.
- [8] Griffin, J.H. and Yang, M.-T., *A Normalized Modal Eigenvalue Approach for Resolving Modal Interaction*, ASME Journal of Engineering for Gas Turbines and Power, (1997) **119**, 647-650.
- [9] Griffin, J.H. and Yang, M.-T., *A Reduced-Order Model of Mistuning Using a Subset of Nominal System Modes*, Journal of Engineering for Gas Turbines and Power, (2001) **123**(4), 893-900.
- [10] Griffin, J.H. and Feiner, D.M., *A Fundamental Model of Mistuning for a Single Family of Modes*, Journal of Turbomachinery, (2002) **124**(4), 597-605.

REFERENCES

- [11] Ewins, D.J., Petrov, E.P. and Sanliturk, K.Y., *A New Method for Dynamic Analysis of Mistuned Bladed Disks Based on the Exact Relationship Between Tuned and Mistuned Systems*, Journal of Engineering for Gas Turbines and Power, (2002) **124**(3), 586-597.
- [12] Pierre, C. and Kruse, M.J., *An Experimental Investigation of Vibration Localization in Bladed Disks, Part I: Free Response*, (1997) ASME Paper 97-GT-501.
- [13] Pierre, C. and Kruse, M.J., *An Experimental Investigation of Vibration Localization in Bladed Disks, Part II: Forced Response*, (1997) ASME Paper 97-GT-501.
- [14] Pierre, C., Castanier, M.P. and Baik, S., *Mistuning Sensitivity Prediction of Bladed Disks Using Eigenvalue Curve Veerings*, Proceedings of the 9th National Turbine Engine High Cycle Fatigue Conference, Pinehurst, NC, March 2004.
- [15] Thomas, D.L., *Dynamics of Rotationally Periodic Structures*, International Journal For Numerical Methods In Engineering, (1979) **14**, 81-102.
- [16] Pierre, C., *Mode Localization and Eigenvalue Loci Veering Phenomena in Disordered Structures*, Journal of Sound and Vibration, (1988) **126**(3), 485-502.
- [17] Pierre, C. and Castanier, M.P., *Modeling and Analysis of Mistuned Bladed Disk Vibration: Status and Emerging Directions*, Journal of Propulsion and Power, (2006) **22**(2), 384-396.
- [18] Bladh, R., Castanier, M.P. and Pierre, C., *Component-Mode-Based Reduced Order Modeling Techniques for Mistuned Bladed Disks – Part I: Theoretical Models*, Journal of Engineering for Gas Turbines and Power, (2001) **123**(1), 89-99.
- [19] Bladh, R., Castanier, M.P. and Pierre, C., *Component-Mode-Based Reduced Order Modeling Techniques for Mistuned Bladed Disks – Part II: Application*, Journal of Engineering for Gas Turbines and Power, (2001) **123**(1), 100-108.

REFERENCES

- [20] Lim, S.-H., Castanier, M.P. and Pierre, C., *Predicting Mistuned Blade Amplitude Bounds and Stress Increases from Energy Formulations*, (2005).
- [21] Lim, S.-H., Castanier, M.P. and Pierre, C., *Mistuning Identification and Reduced-Order Model Updating for Bladed Disks Based on a Component Mode Mistuning Technique*, (2005).
- [22] Jean de Cazenove, Scott Cogan Moustapha Mbaye, *Finite-element Modelling Of An Experimental Mistuned Bladed Disk And Experimental Validation*, ASME Turbo Expo 2013, GT2013-95985
- [23] Alexander A. Kaszynski, Joseph A. Beck, Jeffrey M. Brown, *Automated Finite Element Model Mesh Updating Scheme Applicable To Mistuning Analysis*, ASME Turbo Expo 2014, GT2014-26925
- [24] Weihang Tang, Seunghun Baek, Bogdan I. Epureanu, *Reduced Order Models for Blisks with Small and Large Mistuning and Friction Dampers*, ASME Turbo Expo 2016, GT2016-57850
- [25] P. Vargiu , C.M.Firrone, S.Zucca, M.M.Gola, *A reduced order model based on sector mistuning for the dynamic analysis of mistuned bladed disks*, International Journal of Mechanical Sciences 53 (2011) 639–646
- [26] Mitra, M., Zucca, S., Epureanu, B.I., *Effects of contact mistuning on shrouded blisk dynamics*, ASME Turbo Expo 2016, GT2016-57812
- [27] Malte Krack, Lars Panning-von Scheidt, Joerg Wallaschek, Andreas Hartung, *Robust Design of Friction Interfaces of Bladed Disks With Respect to Parameter Uncertainties*, DOI10.1115/GT2012-68578, ASME Turbo Expo 2012
- [28] Christian Soize, *A nonparametric model of random uncertainties for reduced matrix models in structural dynamics*, <https://hal-upec-upem.archives-ouvertes.fr/hal-00686293>

KICK-OFF TRAINING

TUM - Garching-bei-München
2018 Jan 8-12

Forced response measurement of bladed disks

Teresa Berruti, Christian Firrone
Politecnico di Torino
teresa.berruti@polito.it

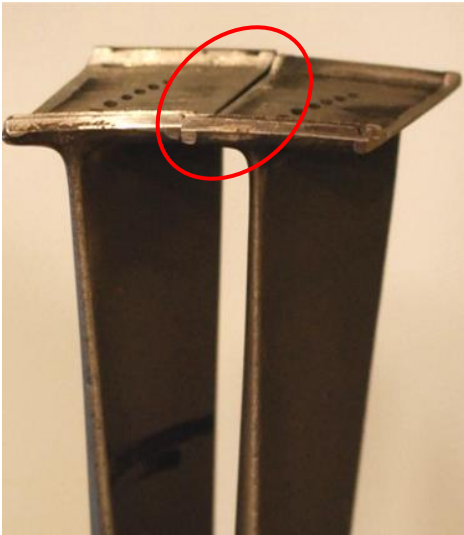
- Typical friction contacts in bladed disks
- The experimental validation by bladed disk test rigs
- Example of test rigs with bladed disks in the world
- Some important diagrams
- The bladed disk test rigs at Politecnico di Torino

Typical friction contacts in bladed disks

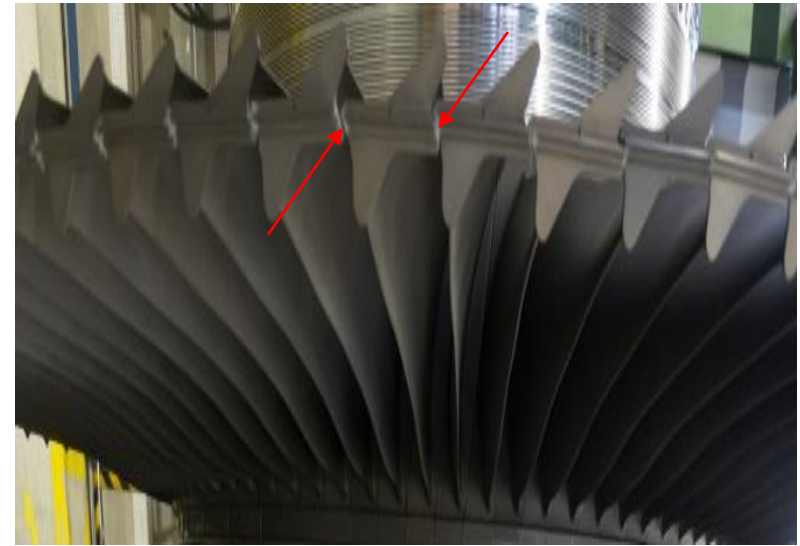
Typical friction contacts in bladed disks

Blade to blade

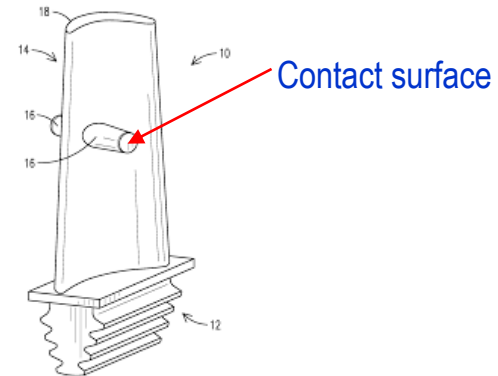
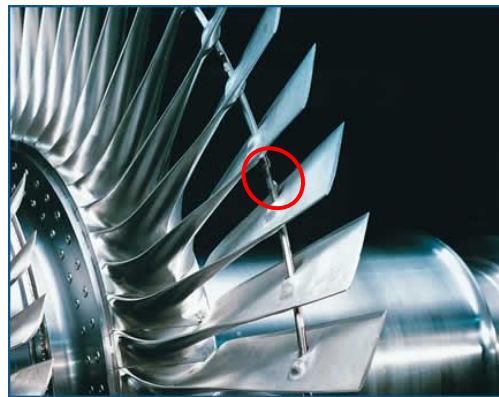
Shroud



Shroud with interlocking



Snubbers



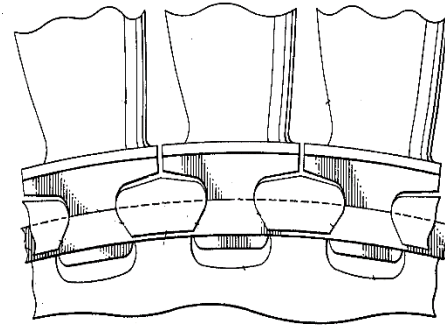
Typical friction contacts in bladed disks

Blade to disk

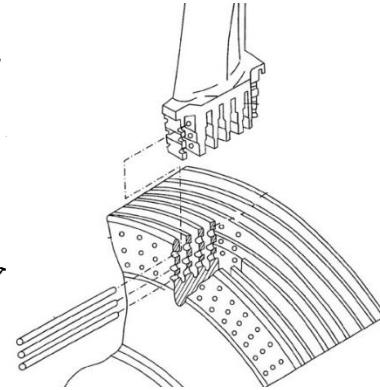
fir tree



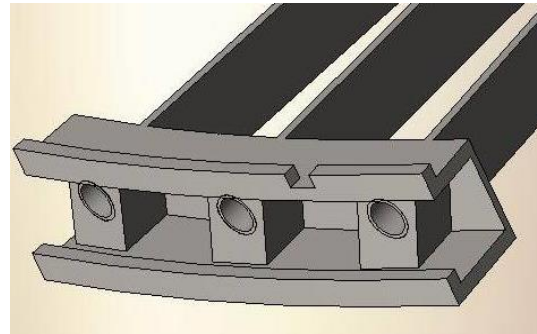
dove tail



pinned root



Blade root

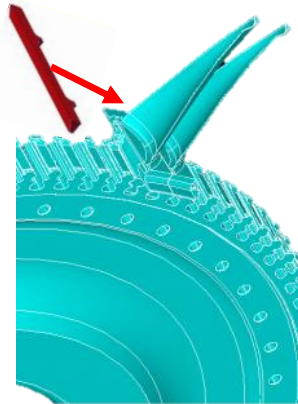


Hooks

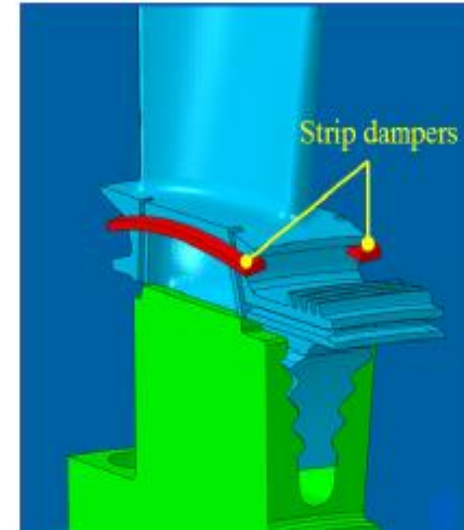
Typical friction contacts in bladed disks

Blade to damper

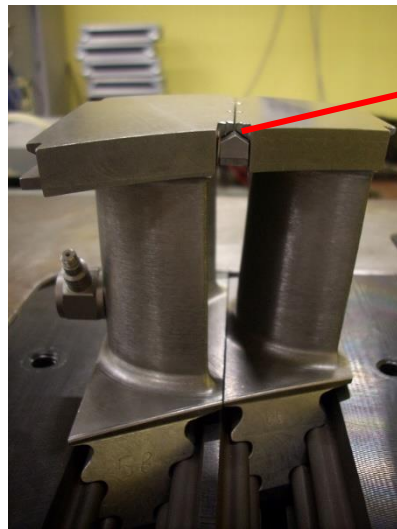
Rigid damper



Flexible damper /strip damper



Underplatform dampers

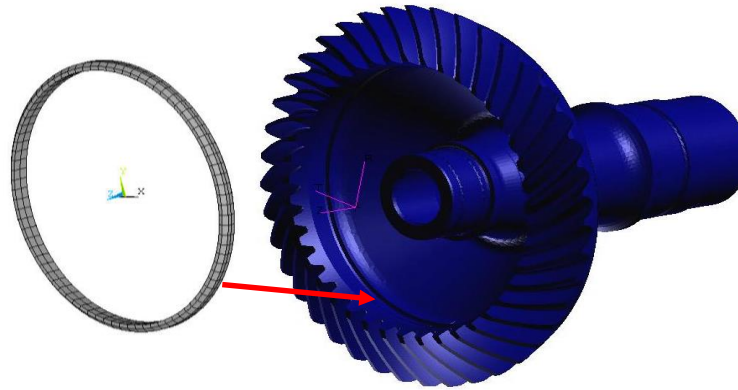


Tip dampers

Typical friction contacts in bladed disks

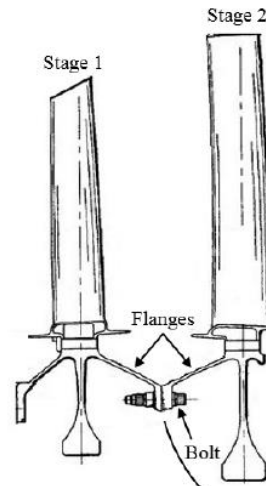
Disk to damper

Ring damper



Disk to Disk

Bolted flanges between disks

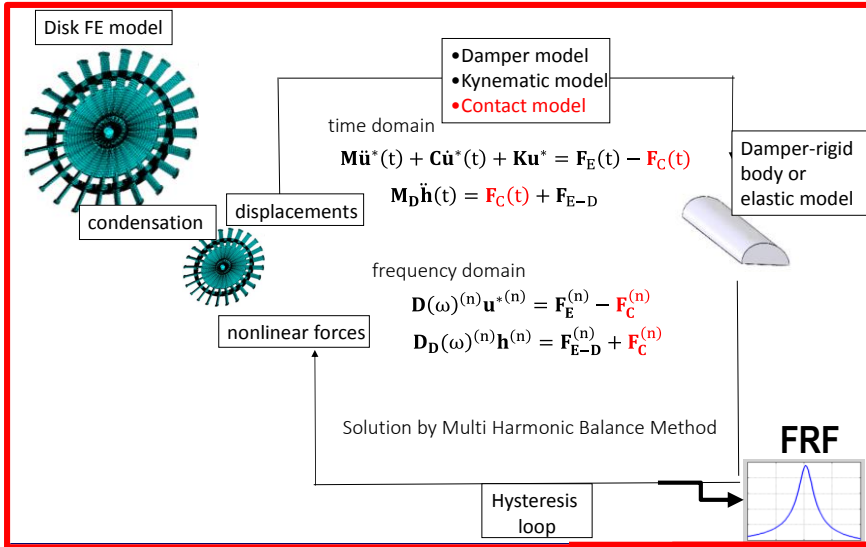


The experimental validation by bladed disk test rigs

Prediction of non linear dynamic of bladed disks with friction damping

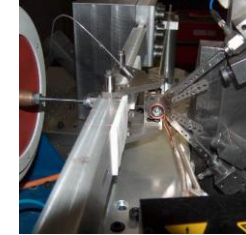
Example : case of disk with underplatform damper

Numerical calculation



Experiments

Contact parameters



1st Experimental validation



Experimental validation with real disk



Experimental validation with dummy disk in lab condition



1

3

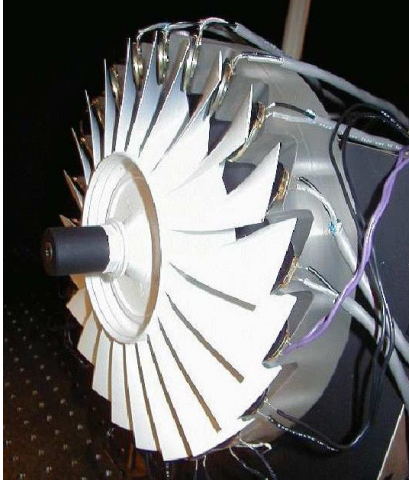
2

Example of test rigs with bladed disks in the world

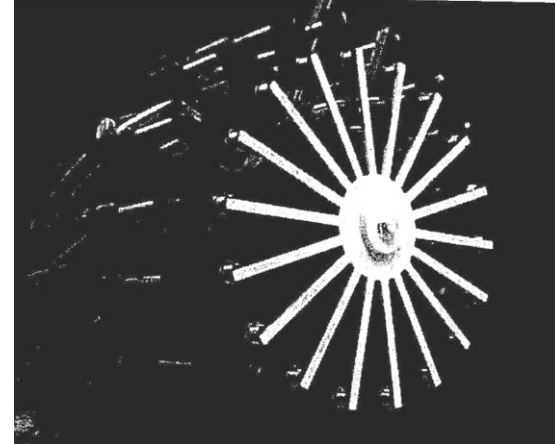
Example of test rigs for bladed disks in the world

Static rigs (not rotating)

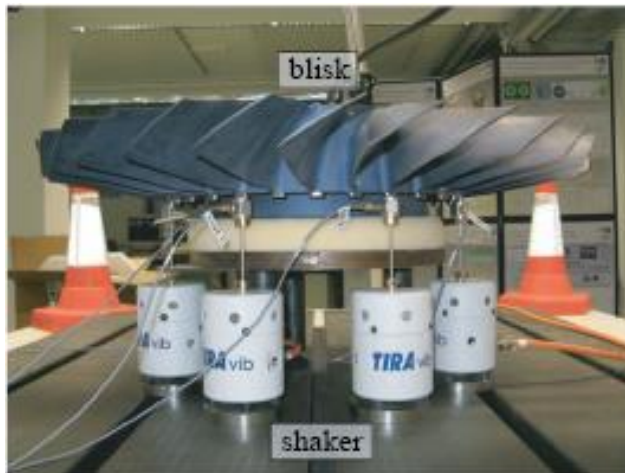
Pierre C., Ceccio S.L., et al.
University of Michigan, 2003.



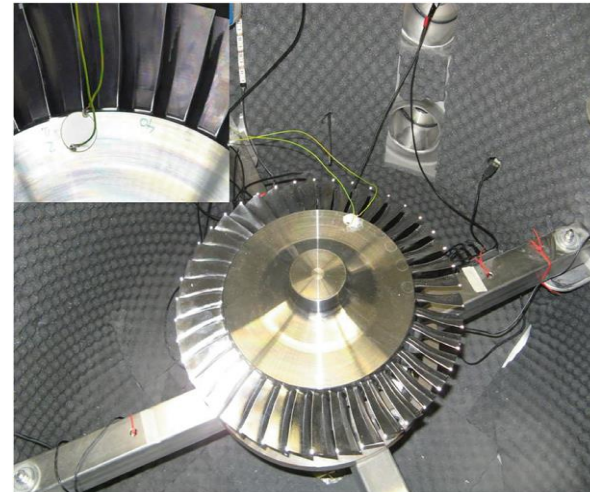
Jones K.W. , Cross C.J.
US Air Force Res.Lab. 2003



Strehlau U., Kuhhorn A.
Brandenburg Univ. of Tech. , 2010



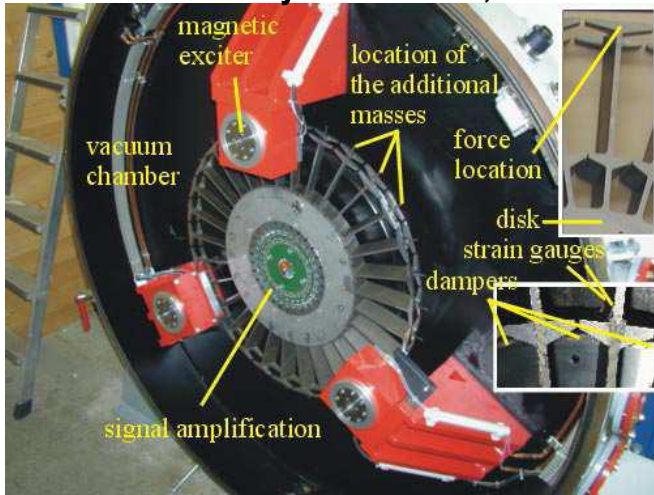
Beirow B. et al.
Brandenburg Univ. of Tech., 2018



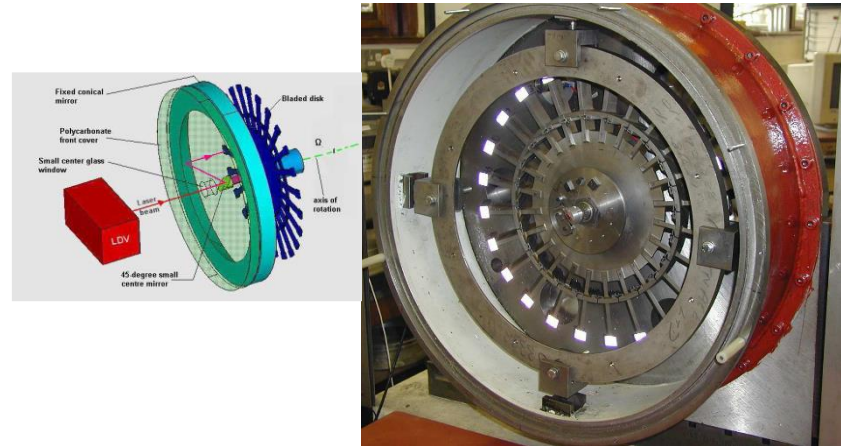
Example of test rigs for bladed disks in the world

Rotating rigs

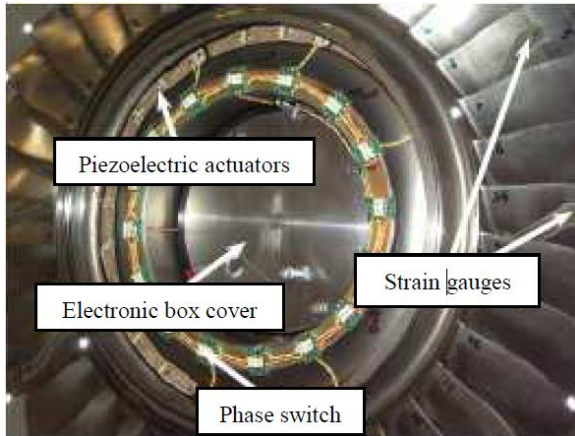
Gotting F., Sextro W., Panning L., Popp K.,
University of Hannover, 2004.



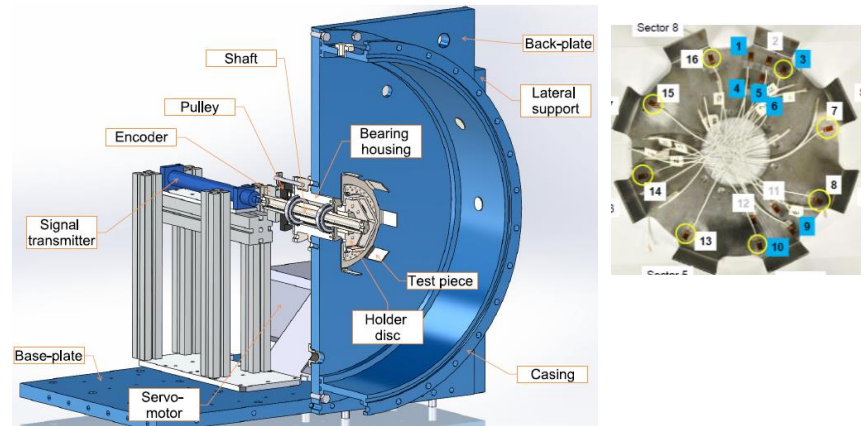
Ewins J., et al. Imperial College London, 2004



Gibert C., Thouverez F. et al. Lab. of Tribology and Sys.
Dynamics, Ecole Centrale de Lyon, 2010



Ruffini, V., Schwingshackl, C. W., and Green, J. S.,
Imperial College London, 2017



Main common features of the rigs

Static rigs (not rotating)

Rotating rigs

The disk is simplified in order to highlight a particular phenomenon

- Travelling excitation force
- Non contact excitation systems (acoustic speakers, electromagnet) or with low impact on the structure (piezoelectric actuators)
- Measurement of the response: laser vibrometer or strain gages



Manly used to validate mistuning model (linear cases)

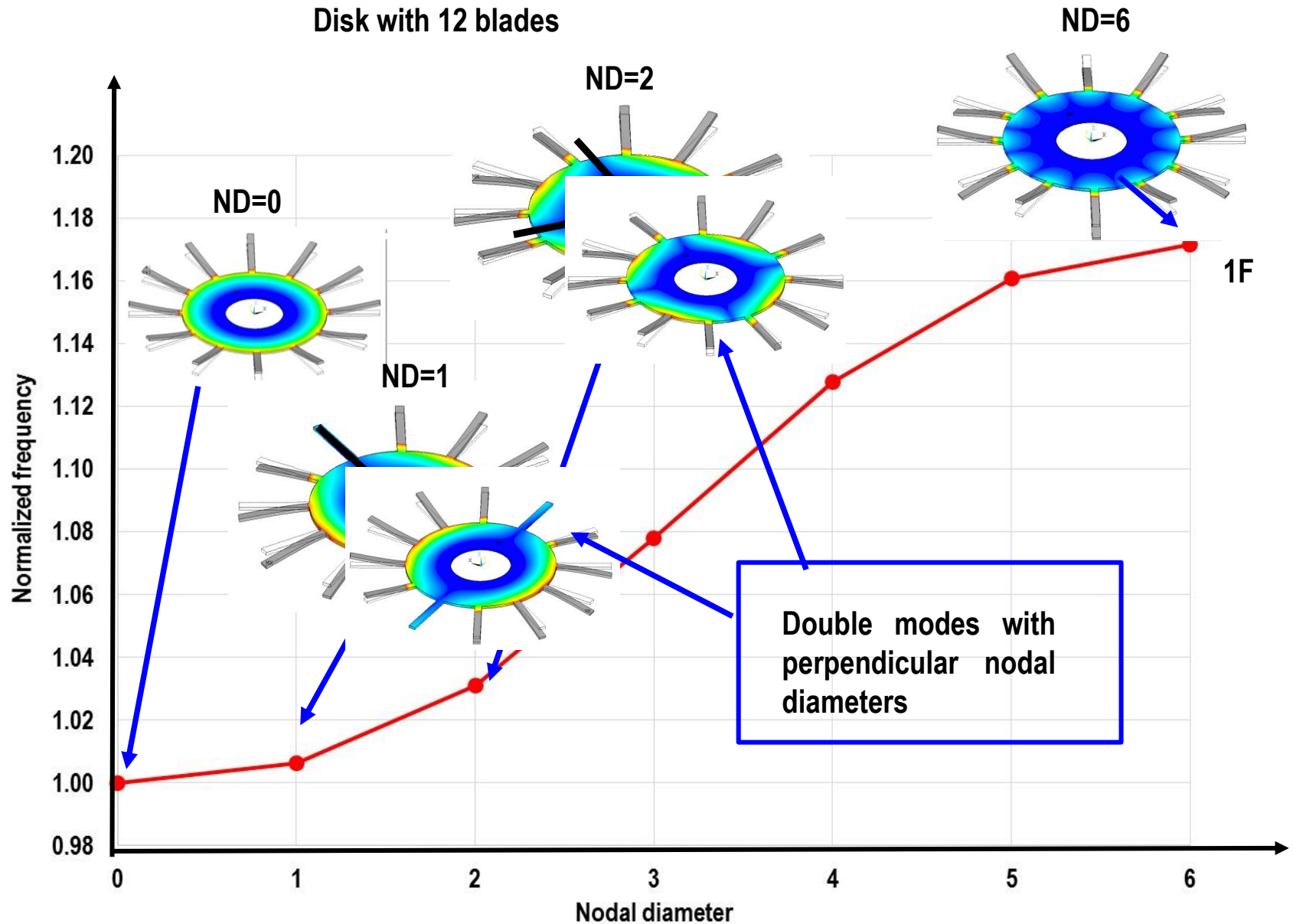
- Excitation of the blades by permanent magnets (synchronous excitation) , electromagnet or piezo actuators (also asynchronous excitation)
- Most of them rotates in vacuum
- Measurement of the response: by strain gages or tip timing system



Manly used to validate mistuning models (linear cases), interaction with mistuning and rotation speed (Coriolis effect) , damping characterization (friction damping devices)

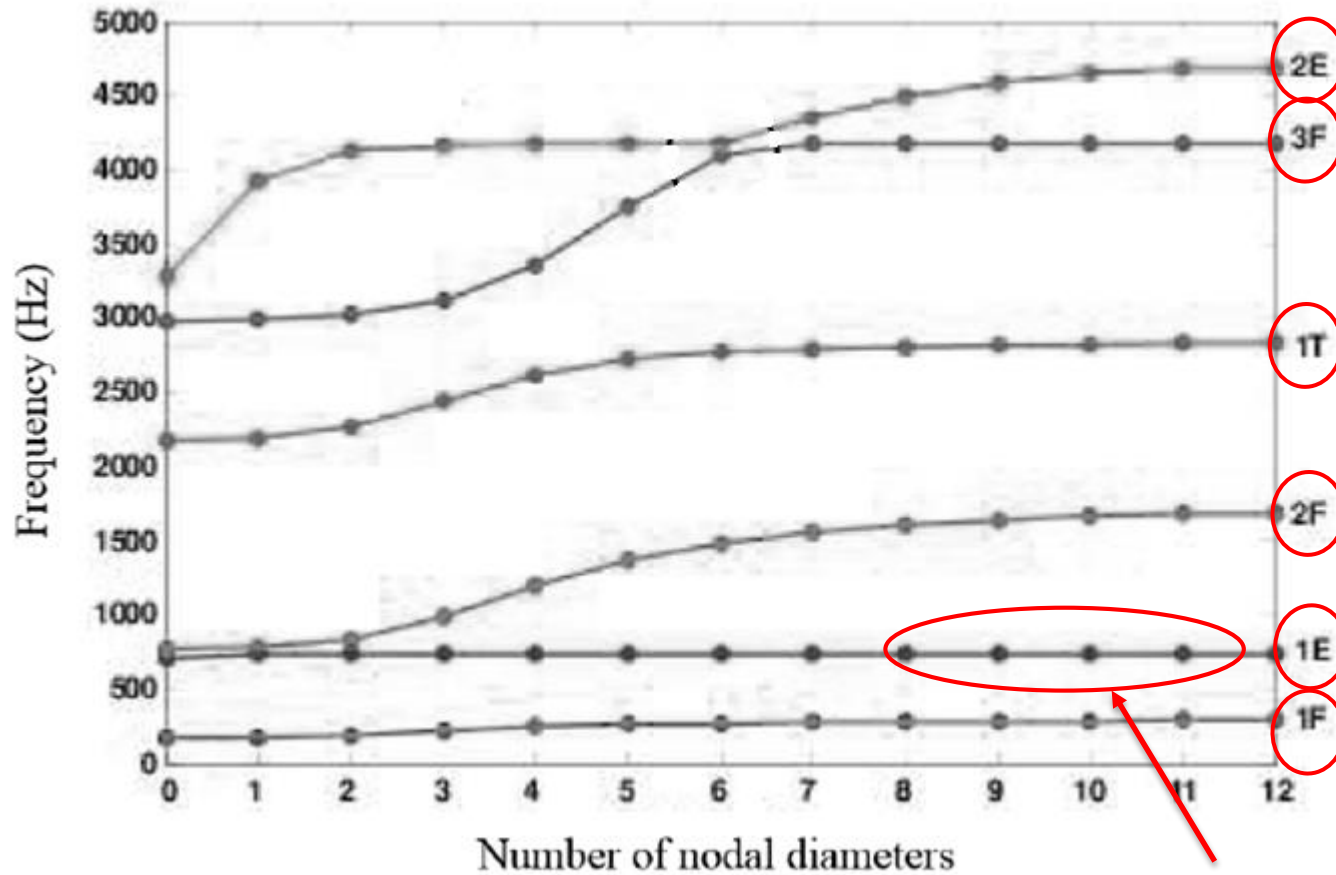
Some important diagrams

The Frequency-Nodal Diameter diagram (FREND)



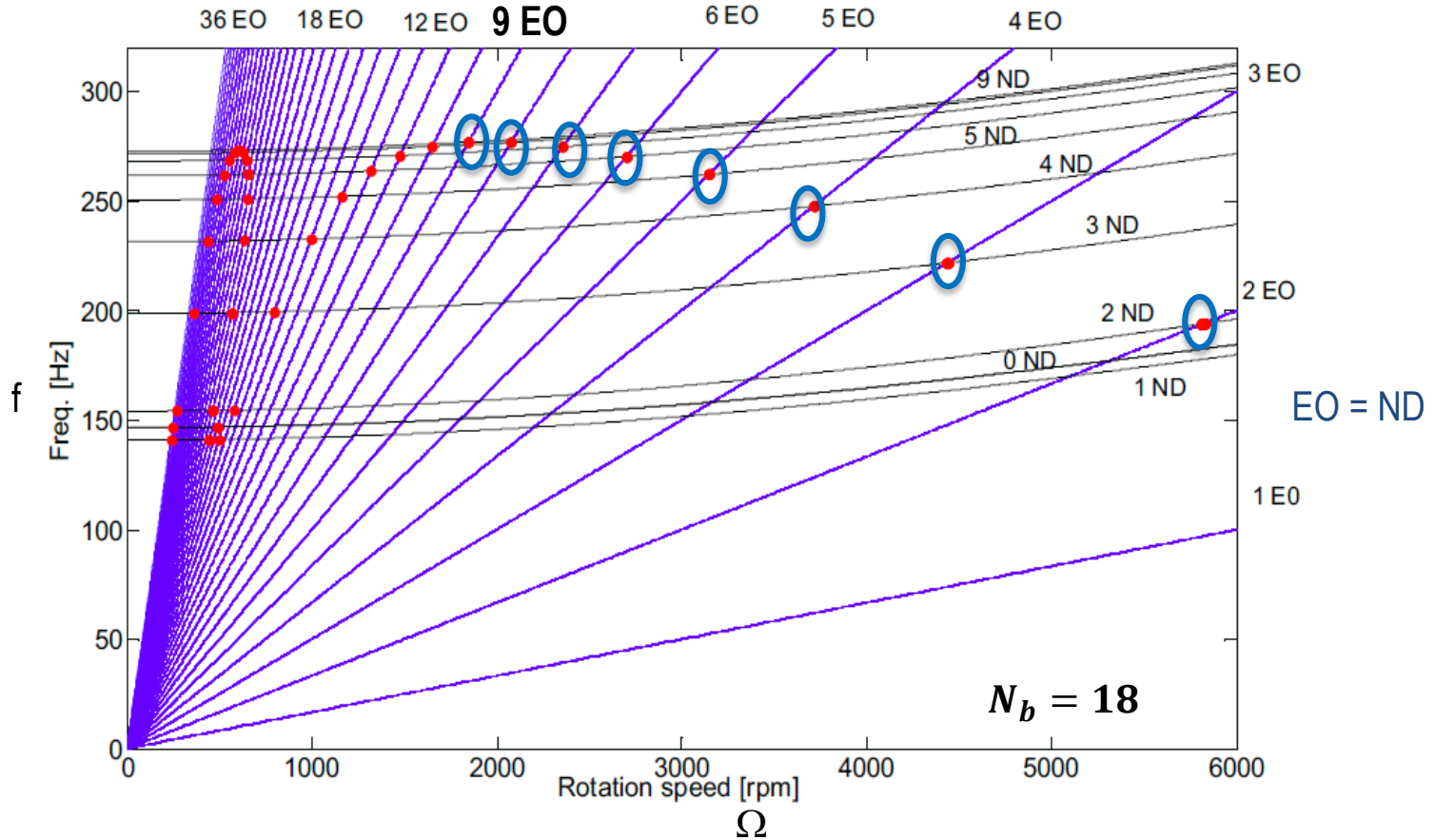
The Frequency-Nodal Diameter diagram (FREND)

Disk with 24 blades different modal families



High modal density region

The Campbell diagram



● Resonance
:

frequency of the force = natural frequency $EO \cdot \Omega = f$

shape of the force = shape of the excited mode

Forcing Function

Mode Shape

The Campbell diagram

Resonance when

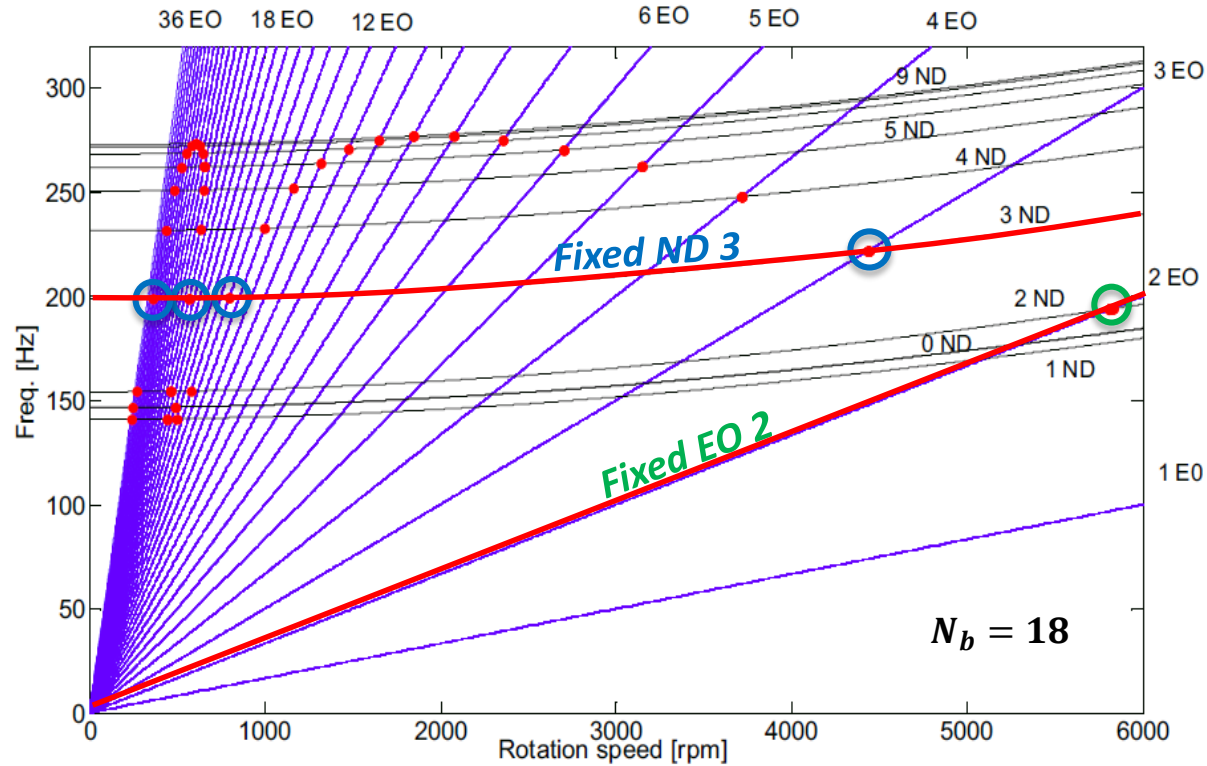
- $EO = ND$

but also

- $EO = j \cdot N_b \pm ND$

By looking at a generic Campbell diagram it can be noticed that each mode corresponding to a certain ND line intersects different EO lines

..while each EO line intersects just one ND line.



Example

Fixed EO



$$2 = 0 \cdot 18 + 2$$

$$2 = 1 \cdot 18 - 16$$

$$2 = 2 \cdot 18 - 34$$

⋮

Only ND 2 satisfies the equation



ND 16 & ND 34 do not exist!

Fixed ND



$$3 = 0 \cdot 18 + 3$$

$$15 = 1 \cdot 18 - 3$$

$$21 = 1 \cdot 18 + 3$$

⋮



The same ND can be excited by different EOs

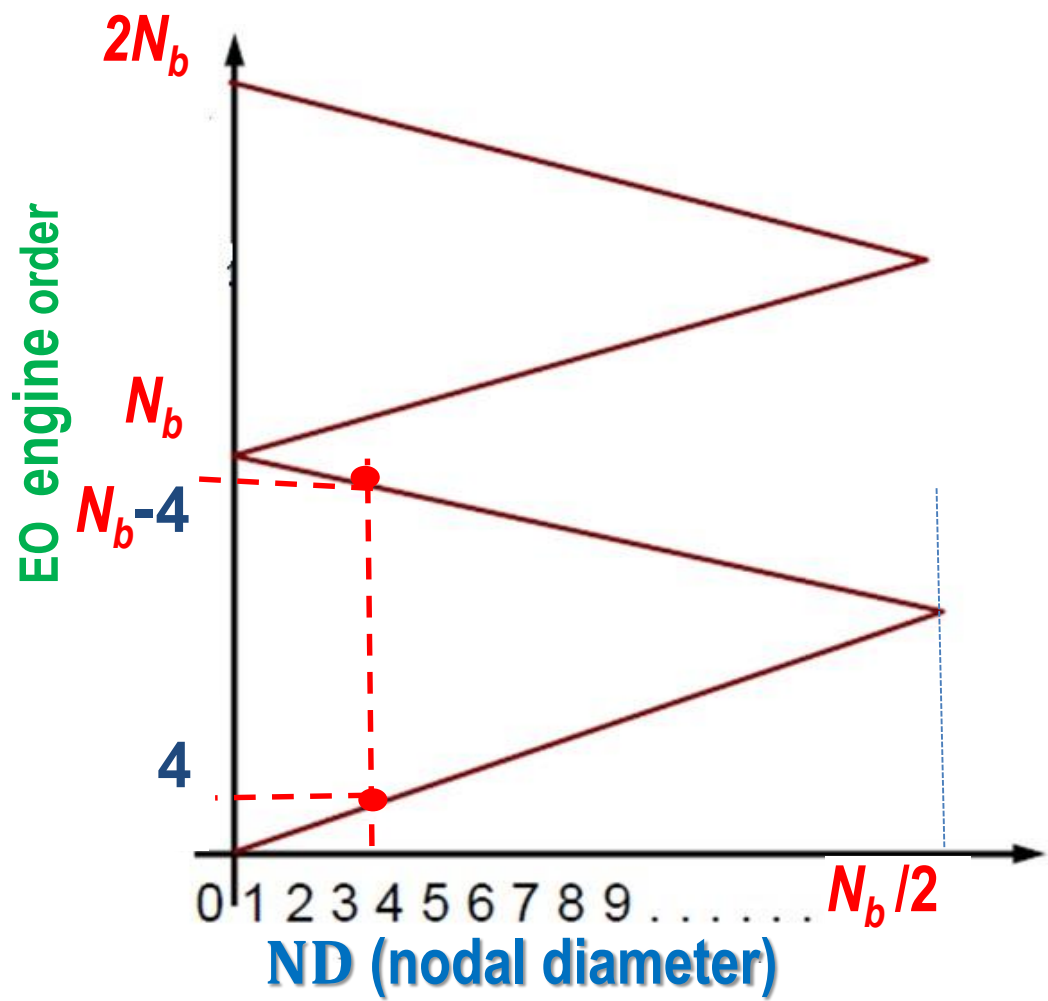
EO: Engine Order

N_b : # Blades

ND: # Nodal Diameters

$j = 0, 1, 2, 3, \dots$

The Zig-Zag diagram – SAFE diagram



$$EO = j \cdot N_b \pm ND$$

Example

$N_b=24$ number of blades

To excite $ND=4$

- $EO=4$
- $EO=24-4=20$

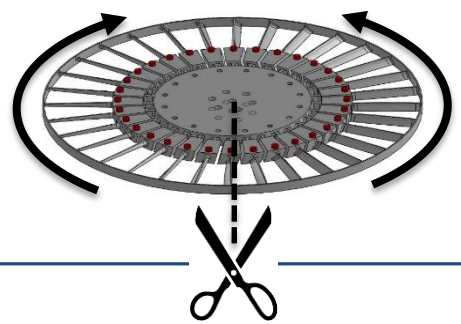
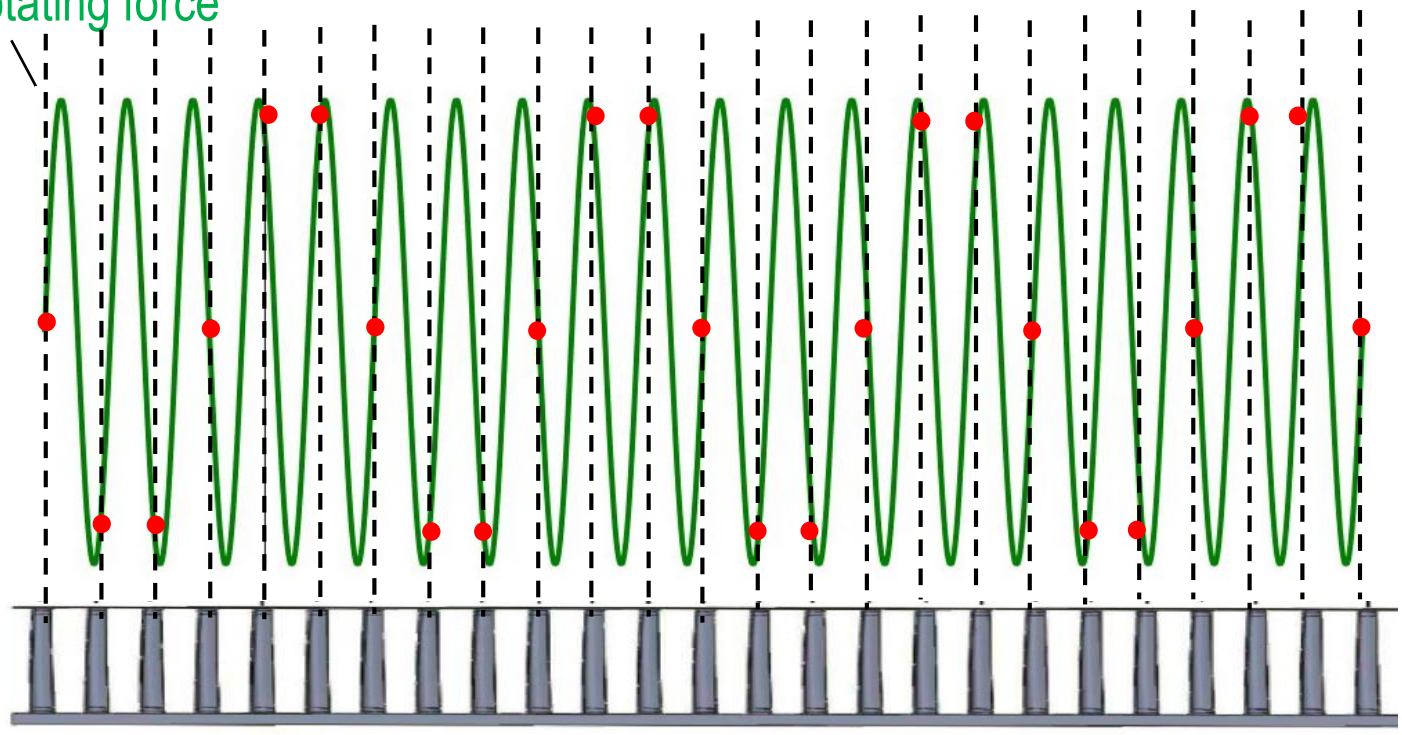
Why $EO=20$ can excite $ND=4$

M.P.Singh, J. (2002). SAFE diagram- A design and reliability tool for turbine blading. Proceeding of the 17th Turbomachinery Symposium.

Explanation of the Zig-Zag diagram

It is do to the Aliasing phenomenon.....

EO = 20 rotating force



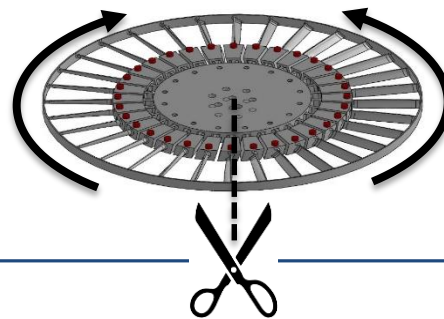
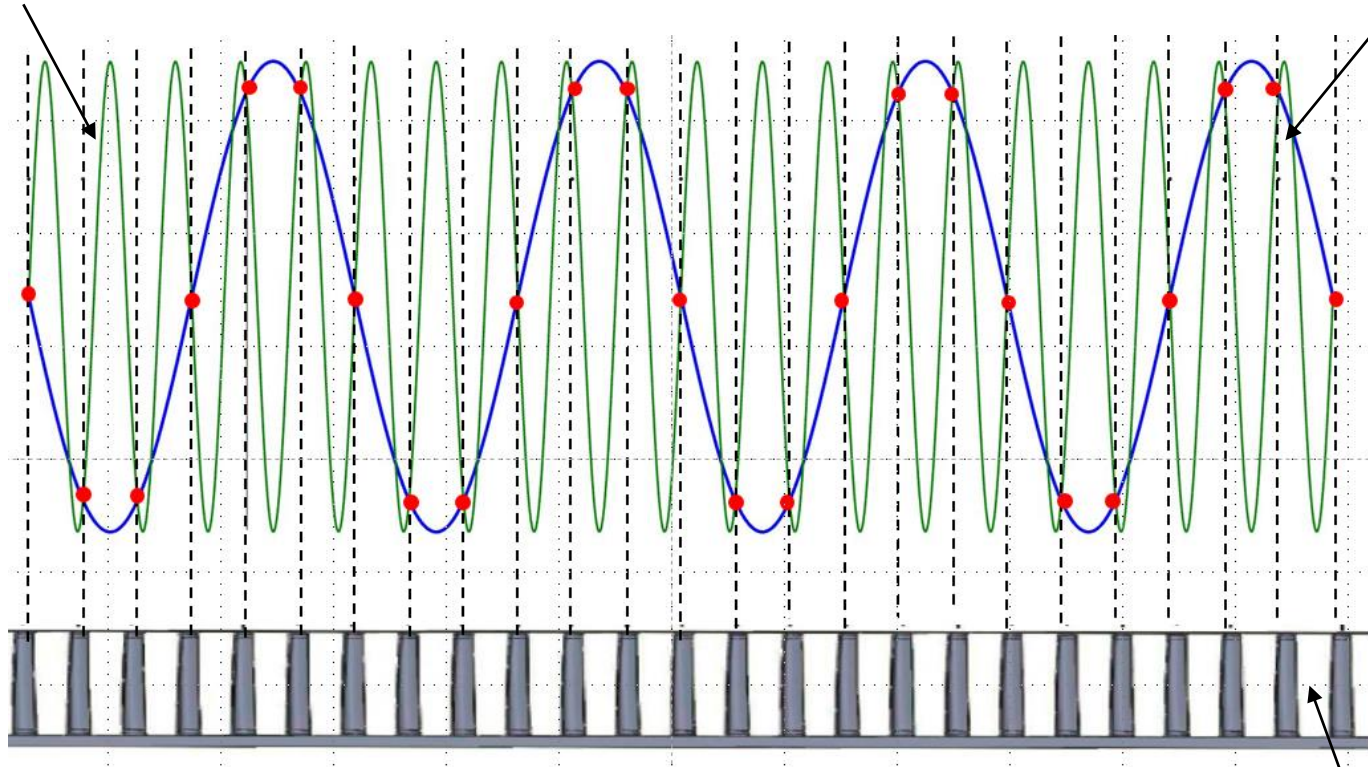
24 blades

Explanation of the Zig-Zag diagram

It is do to the Aliasing phenomenon.....

EO = 20 rotating force

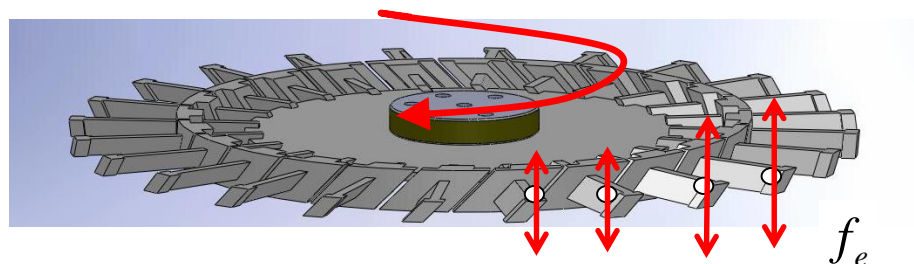
ND = 4



24 blades

TRAVELLING WAVE EXCITATION on a NON ROTATING DISK

TRAVELLING FORCE



Travelling Excitation force

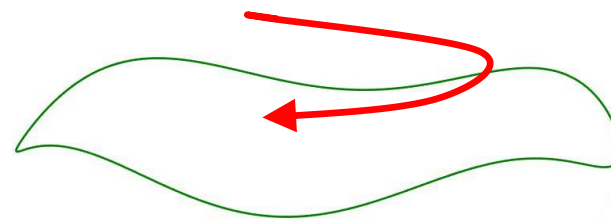
$$f_e = F_E \cos(\omega_m t + (n-1) \cdot \varphi_m)$$

$n = 1, \dots, N_b = 24$ Number of the blade

EO engine order index

$$\varphi_m = \frac{2\pi}{N_b} EO \quad \text{Inter Blade excitation angle}$$

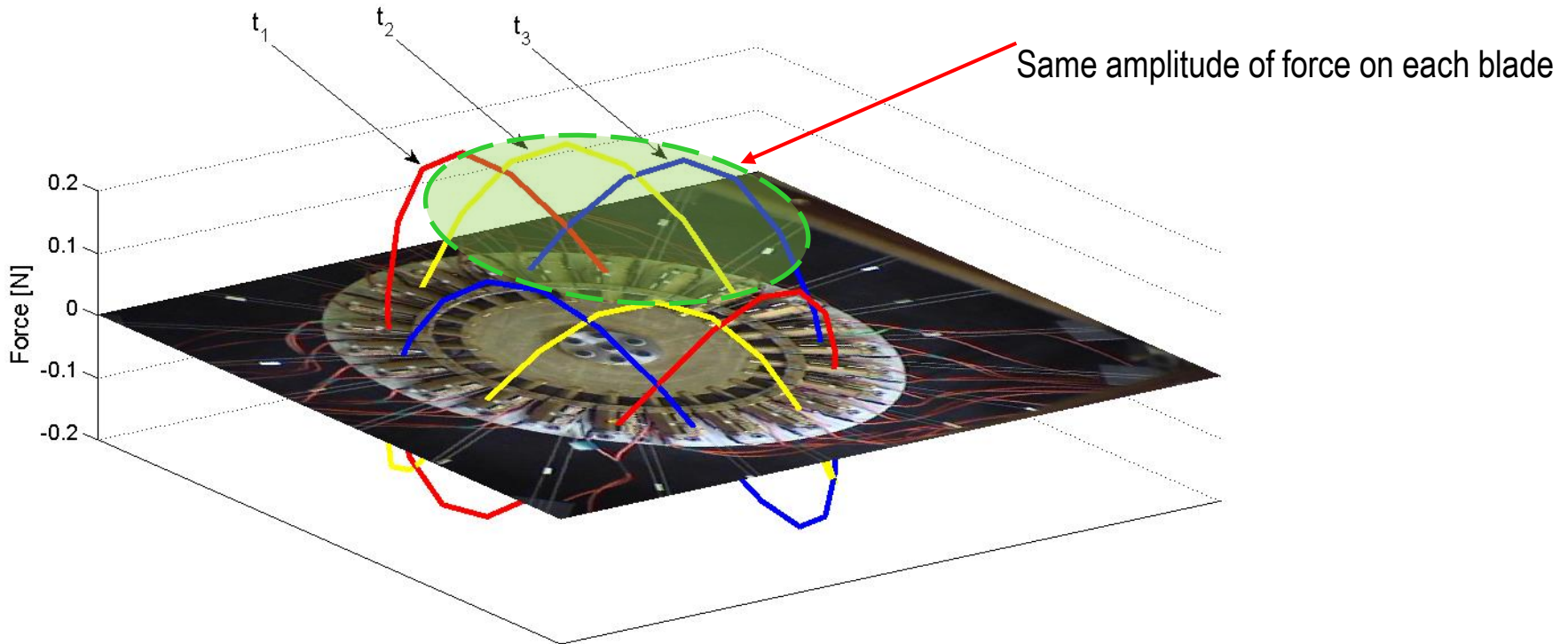
Example $EO = 0 \quad \varphi_m = 0$ $EO = \frac{N_b}{2} \quad \varphi_m = \pi$



TRAVELLING WAVE EXCITATION on a NON ROTATING DISK

$$f_e = F_e \cos(\omega_m t + (n-1) \cdot \varphi_m)$$

Plot of the force at time t_1, t_2, t_3



The force can also be written as the sum of two orthogonal waves

$$\begin{aligned} f_e &= F_e \cos(\omega_m t + (n-1) \cdot \varphi_m) \\ &= \underline{F_e \cos((n-1) \cdot \varphi_m)} \cdot \underline{\cos(\omega_m t)} - \underline{F_e \sin((n-1) \cdot \varphi_m)} \cdot \underline{\sin(\omega_m t)} \end{aligned}$$

TRAVELLING WAVE EXCITATION on a NON ROTATING DISK

RESPONSE TO A TRAVELLING FORCE

$$x = X \cos(\omega_m t + (n-1) \cdot \varphi_m) \quad n = 1, \dots, N_b = 24$$

$$x = \underbrace{X \cos((n-1) \cdot \varphi_m)}_{\text{red}} \cdot \underbrace{\cos(\omega_m t) - X \sin((n-1) \cdot \varphi_m) \cdot \sin(\omega_m t)}_{\text{yellow}} \quad \varphi_m = \frac{2\pi}{N_b} \text{EO}$$

EO engine order index

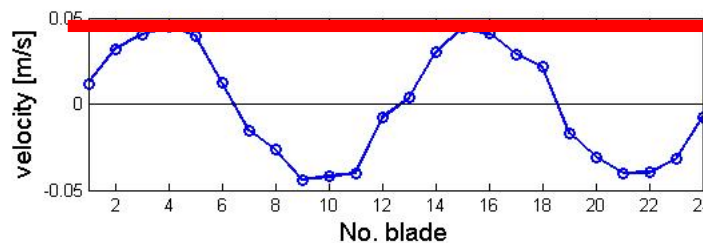
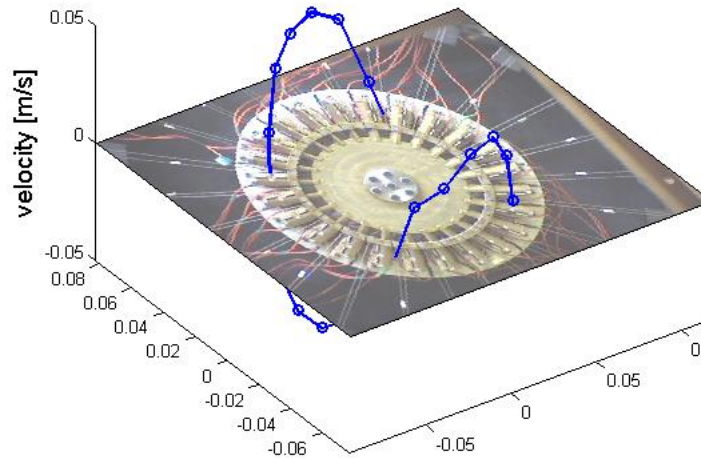
TRAVELLING WAVE EXCITATION on a NON ROTATING DISK

RESPONSE TO A TRAVELLING FORCE

$$x = X \cos(\omega_m t + (n-1) \cdot \varphi_m) \quad n = 1, \dots, N_b = 24$$

$$x = X \cos((n-1) \cdot \varphi_m) \cdot \cos(\omega_m t) - X \sin((n-1) \cdot \varphi_m) \cdot \sin(\omega_m t) \quad \varphi_m = \frac{2\pi}{N_b} \text{EO}$$

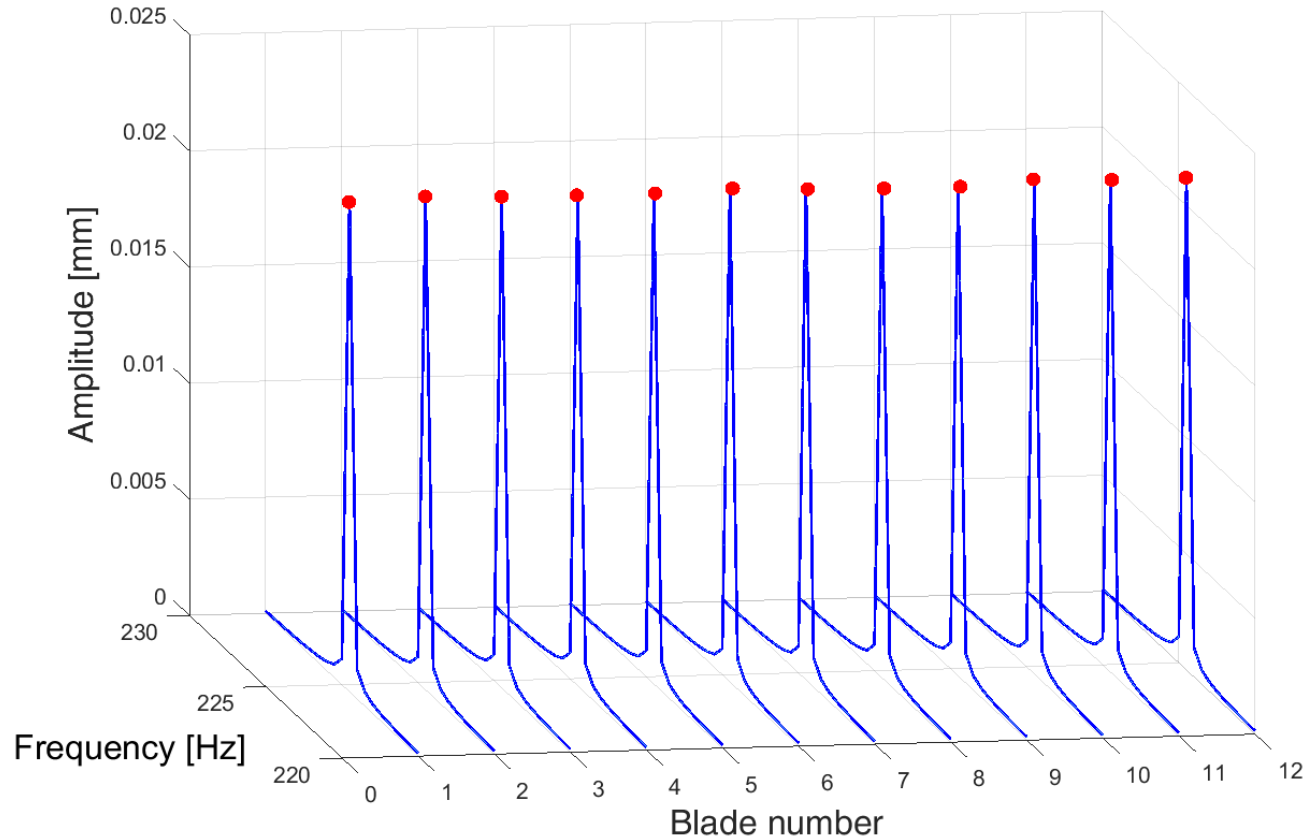
EO engine order index



In an ideal perfectly tuned disk it is a straight line

TRAVELLING WAVE EXCITATION on a NON ROTATING DISK

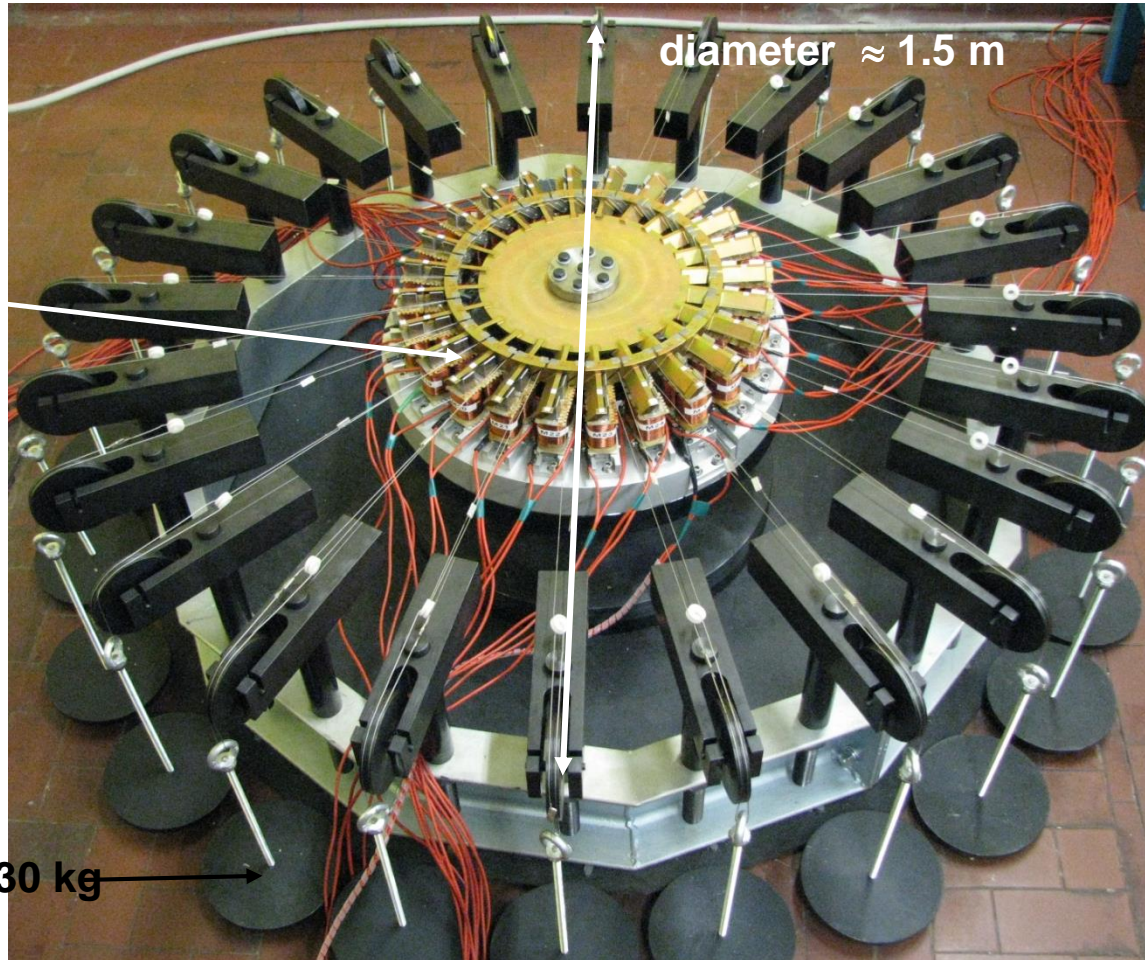
BLADES' RESPONSE IN FREQUENCY



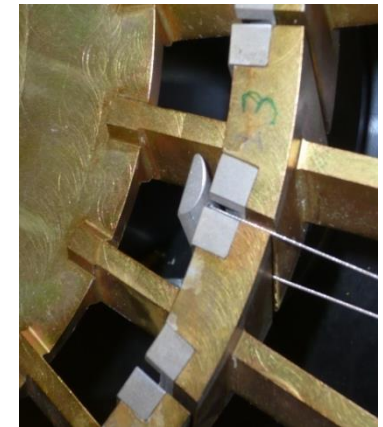
In a tuned disk subjected to a rotating force I expect to find the same response for each blade

The test rigs for bladed disks at Politecnico di Torino

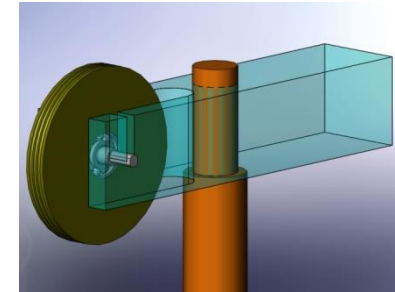
THE TEST RIG OCTOPUS at the Lab. AERMEC Politecnico di Torino



Underplatform damper loading system



arm structure



EXCITATION SYSTEM FEATURES

- absence of contact between blades and exciters
- same excitation force amplitude on each blade but different phase
- high excitation force amplitude
- accurate measurement of the force amplitude

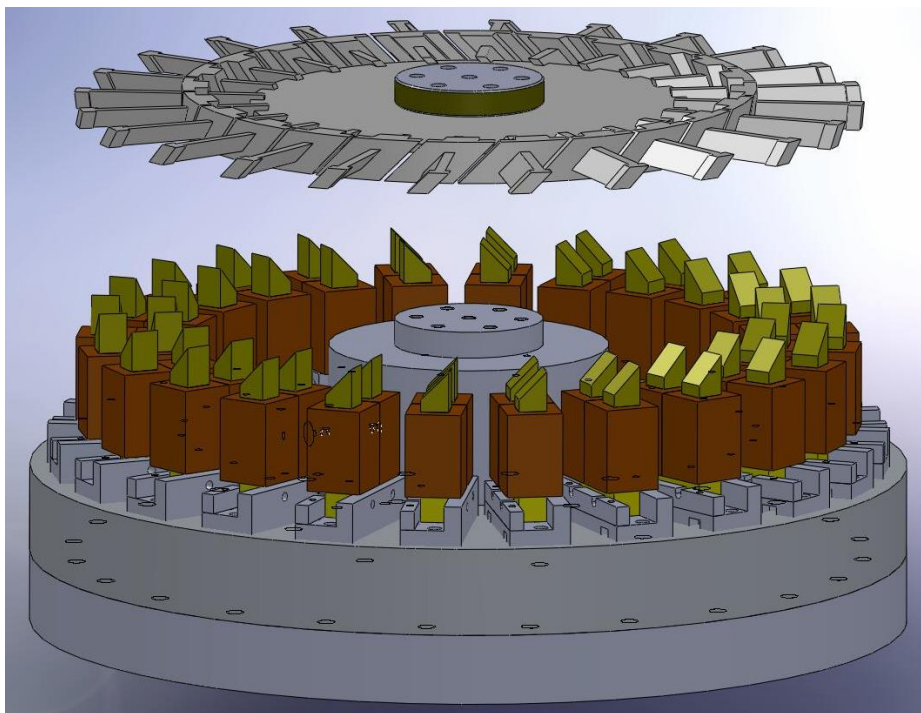
References

C.M. Firrone, T. Berruti, M.M. Gola, On force control of an engine order type excitation applied to a bladed disk with underplatform dampers, **JOURNAL OF VIBRATION AND ACOUSTICS**, 135(4), 041103 (2013) (9 pages) doi:10.1115/1.4023899.

C.M. Firrone, T. Berruti, - “An electromagnetic system for the non-contact excitation of bladed disks” *Experimental Mechanics*, DOI: 10.1007/s11340-011-9504-1, Volume 52, Issue 5 (2012), Page 447-459

T. Berruti, C.M. Firrone, M.M. Gola – “A test rig for non-contact travelling wave excitation of a bladed disk with underplatform dampers”, *Journal of Engineering for Gas Turbines and Power* vol 133 Transactions of the ASME, pp. 032502-1-8, ISSN 0742-4795, DOI: 10.1115/1.4002100 (2011).

THE EXCITATION SYSTEM



Electromagnets



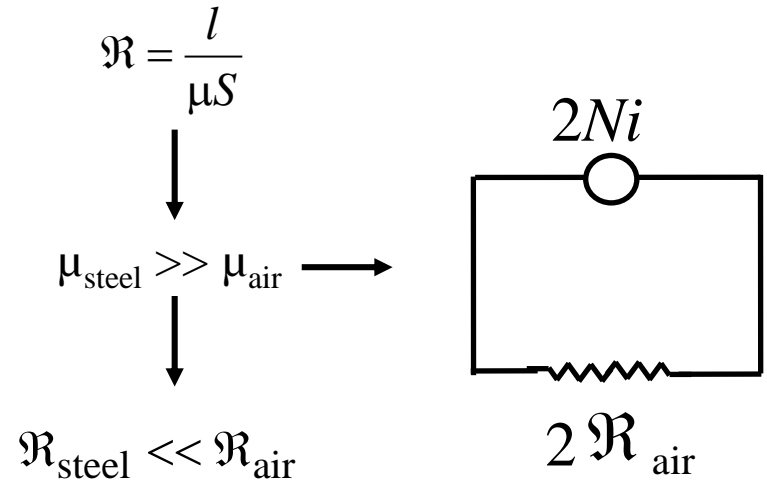
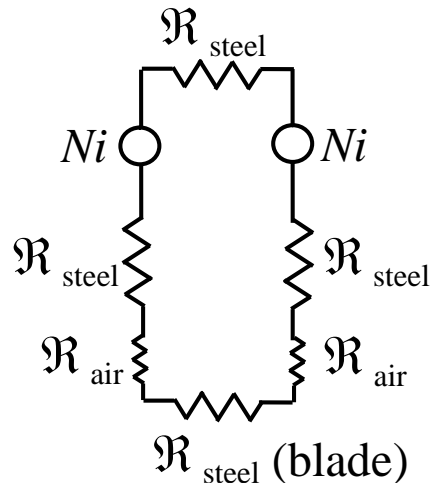
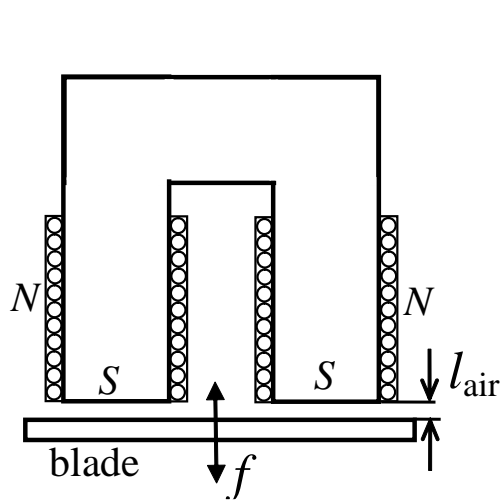
ferromagnetic extensions



Table I

Size (b x h x t)	48X64x16 mm
Core section	16x16 mm
turns per coil N	50
Maximum current I_{max}	10 A
Maximum alternating force amplitude F_a	15 N (@ 300Hz 5 N (@ 600Hz

THE THEORETICAL MODEL OF THE MAGNETIC FORCE



$i(t) = I \sin f_{el} t$ **alternate component of the force** $\rightarrow f_a = \frac{(N \cdot I)^2 \cdot \mu_{\text{air}} \cdot S'}{2l_{\text{air}}^2} \cos 2f_{el} t$

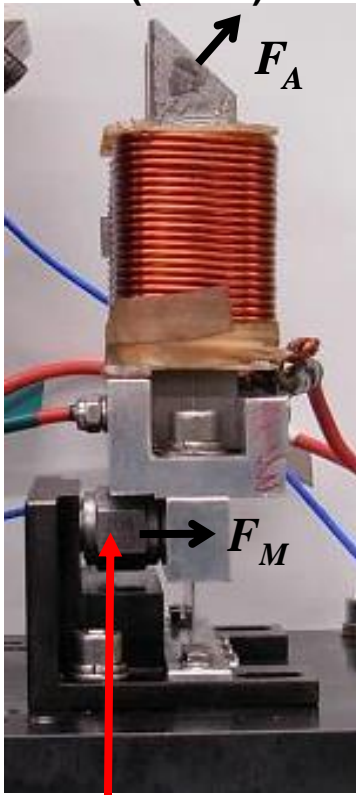
$V = \left(\sqrt{\frac{4 \cdot \pi^2 \cdot F_A \cdot L^2 \cdot l_{\text{air}}^2}{\mu_{\text{air}} N^2 \cdot S'}} \right) \cdot f_{el}$

$V = \left(\sqrt{\frac{4 \cdot \pi^2 \cdot f_{el}^2 \cdot L^2 \cdot l_{\text{air}}^2}{\mu_{\text{air}} N^2 \cdot S'}} \right) \cdot \sqrt{F_A}$

THE CONTROL OF THE EXCITATION FORCE AMPLITUDE

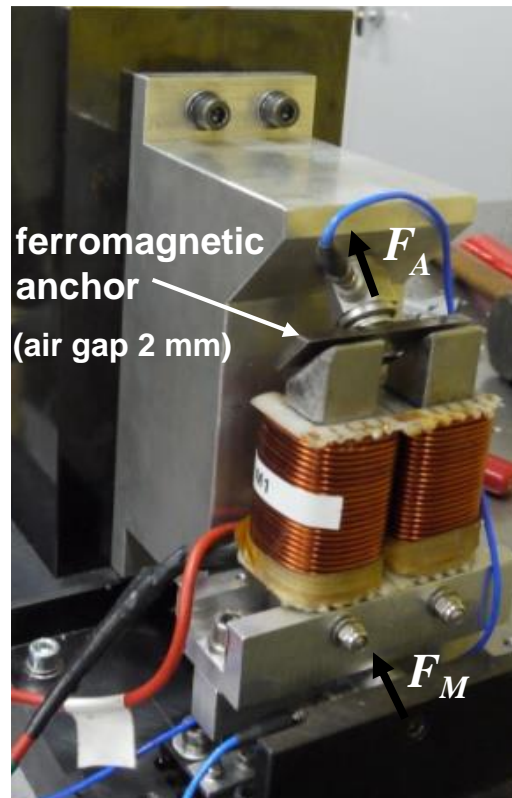
REFERENCE ELECTROMAGNET

The Force Measuring ElectroMagnet (FMEM)

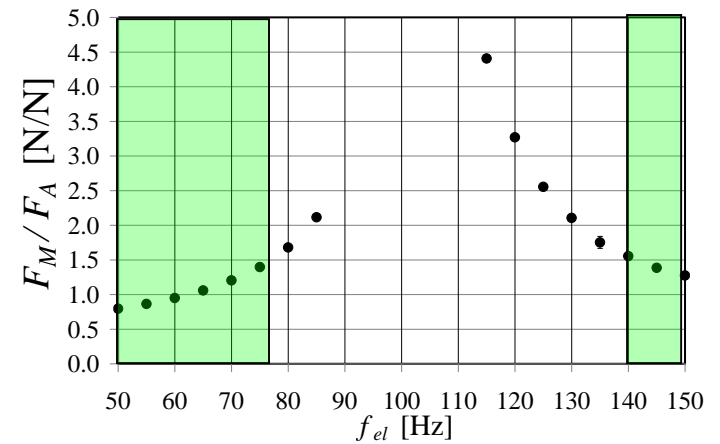


force transducer

FMEM calibration bench

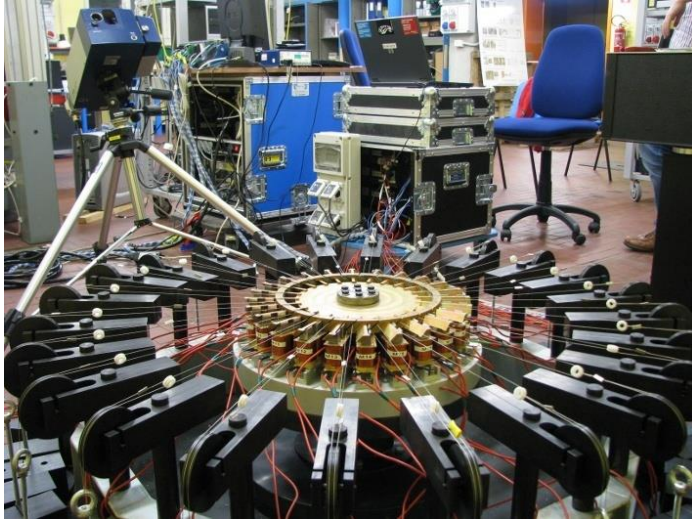


The FMEM calibration curve



$F_A = 5$ N (tol. 1%) controlled by a Labview routine

TEST FACILITIES



EMs power supply

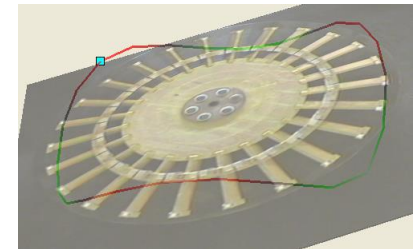
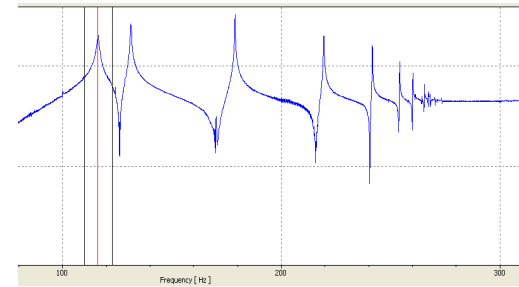
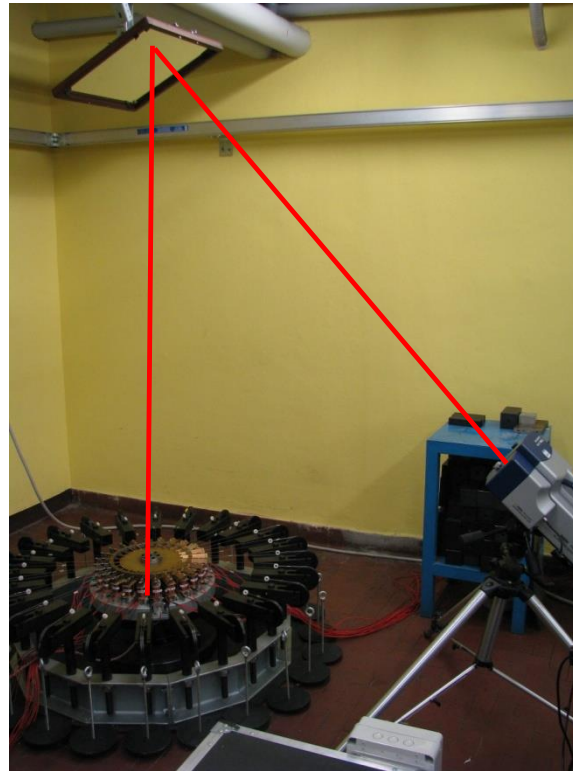
Signal generator
and controller
NI cRIO

12 amplifiers
2 channel (800 W)



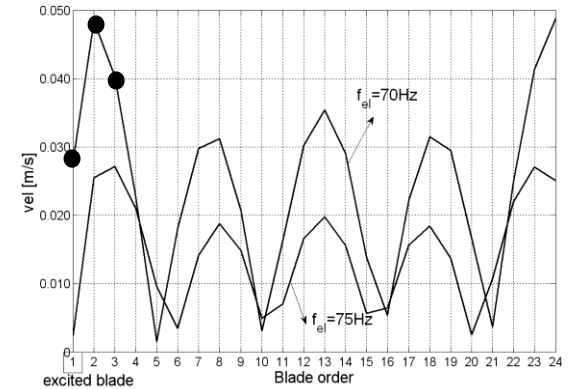
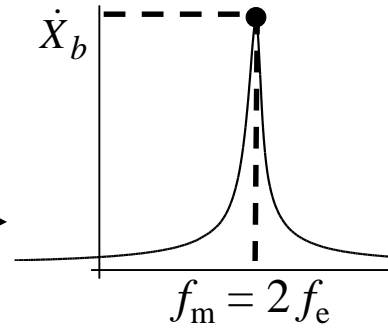
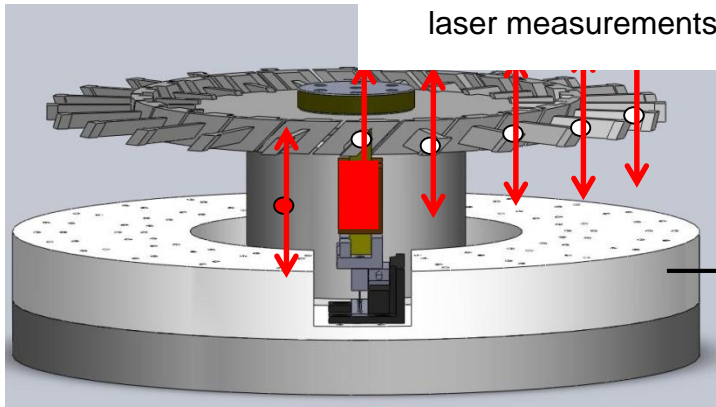
Dynamic response measurement

Laser scanning
vibrometer

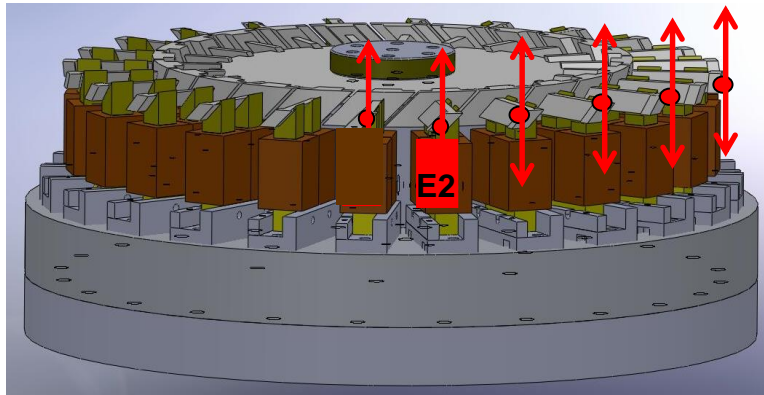


CALIBRATION vs. the REFERENCE ELECTROMAGNET

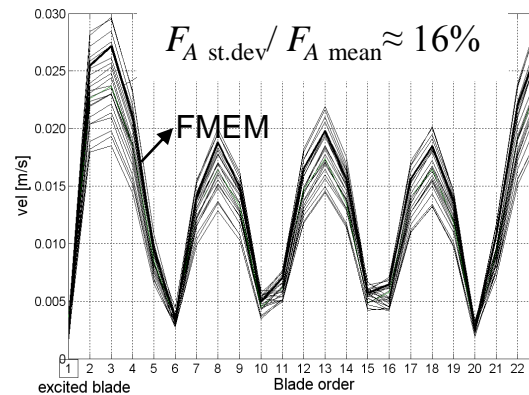
Configuration 1



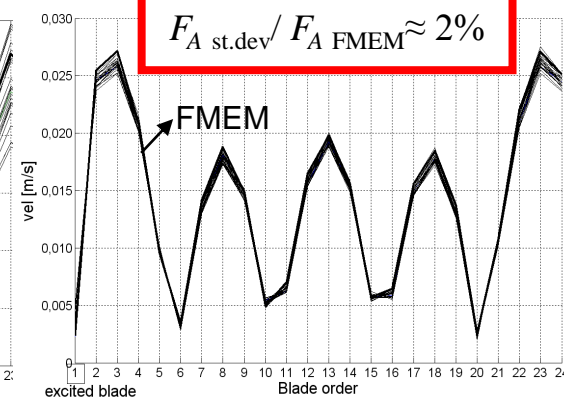
Configuration 2



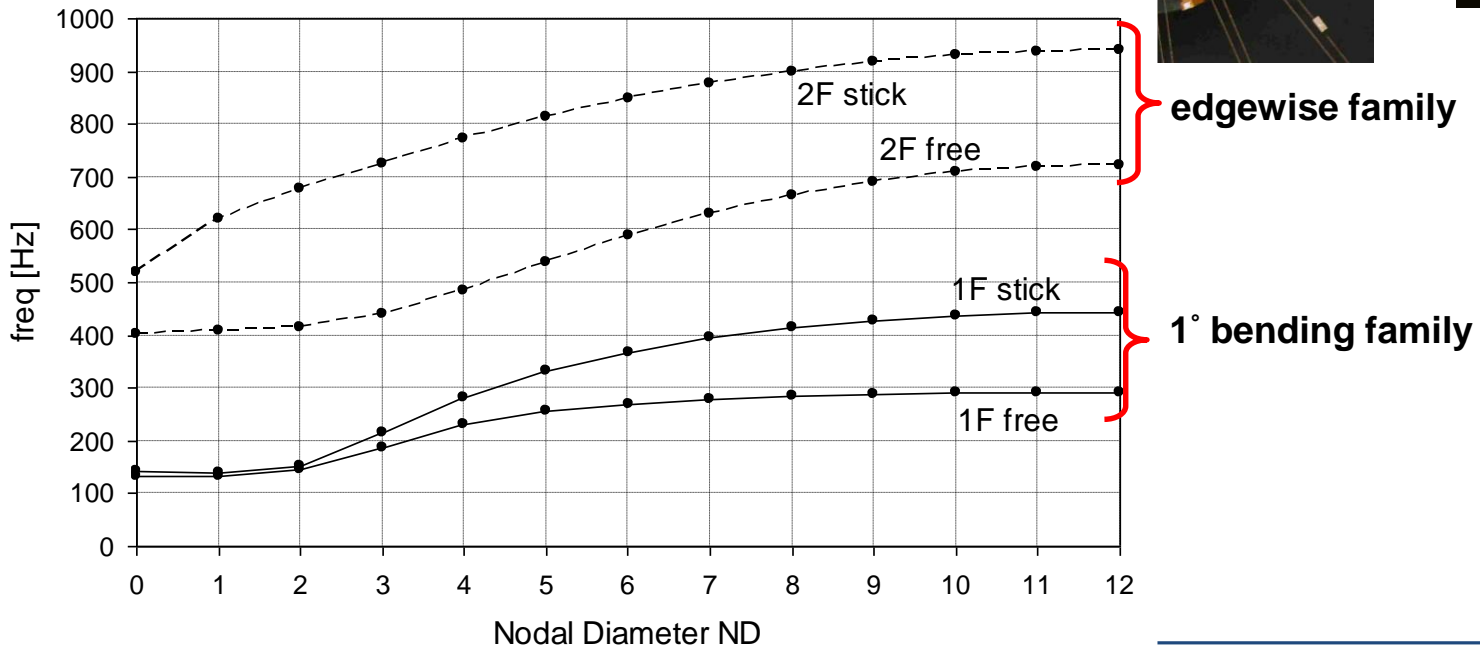
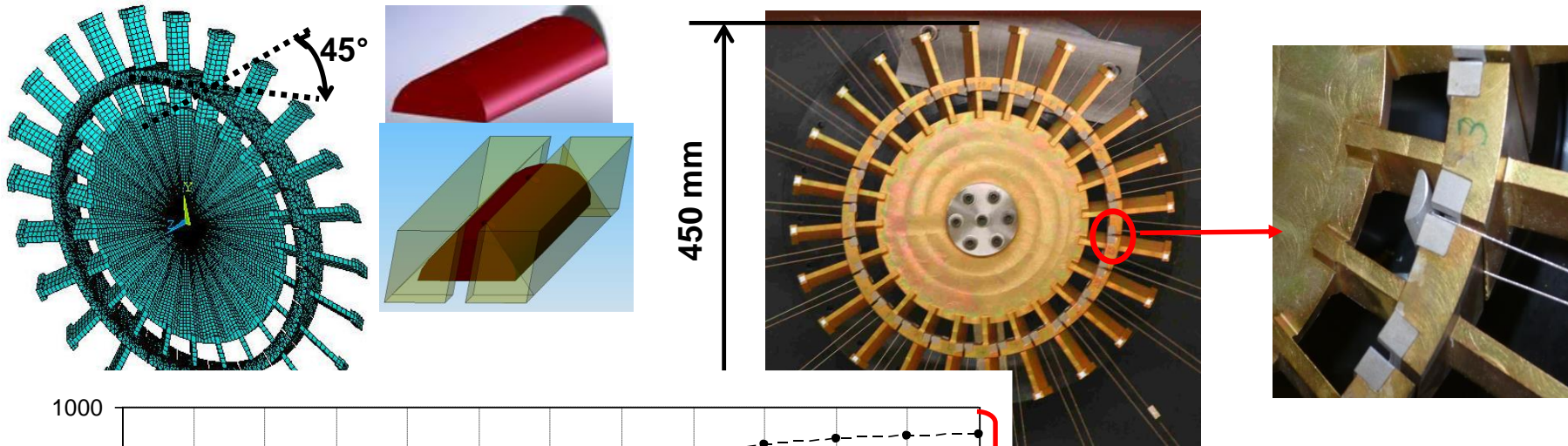
Before tuning



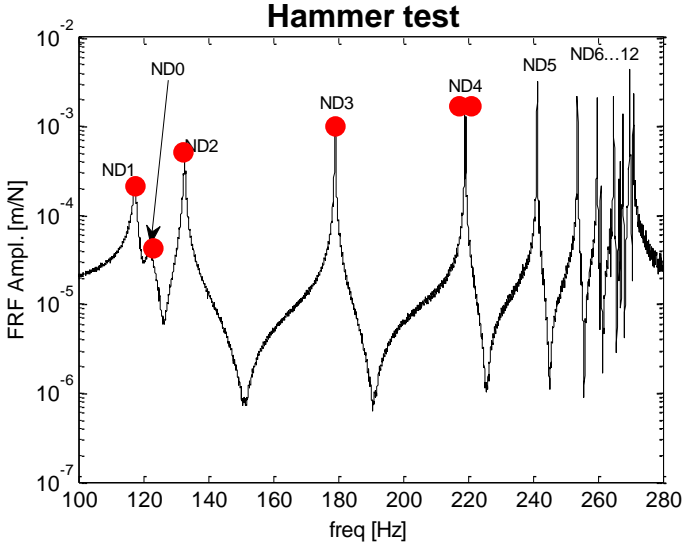
After tuning



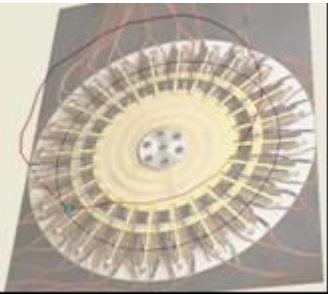
THE BLADED DISK



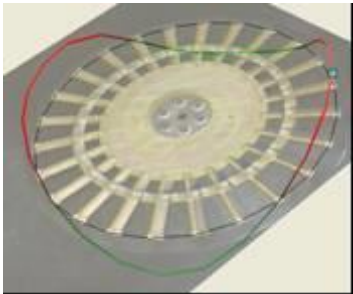
BLISK WITHOUT DAMPERS - HAMMER TEST



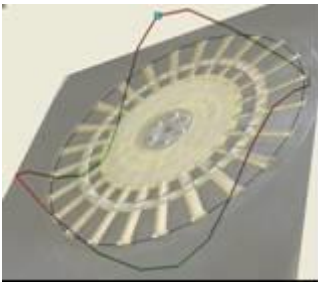
ND = 0



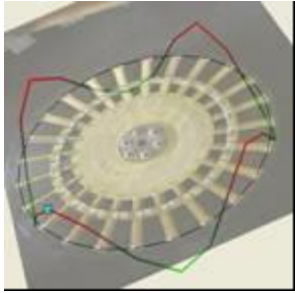
ND = 2



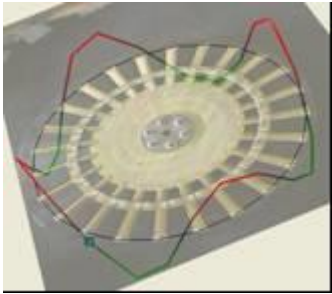
ND = 3



ND = 4
f = 219,1 HZ

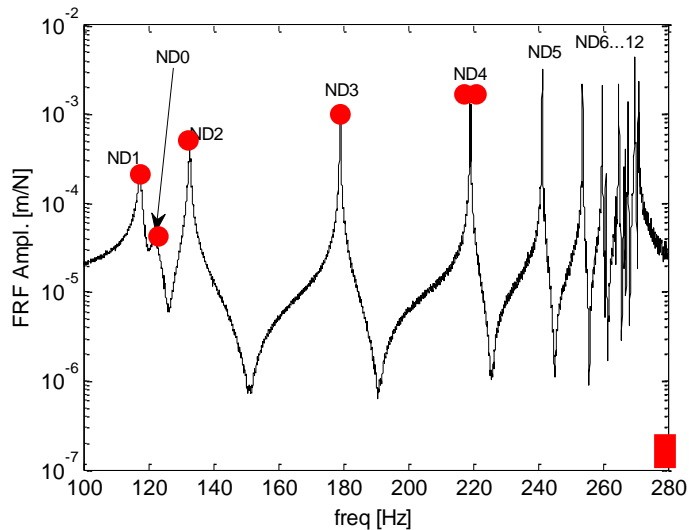


f = 219,2 HZ

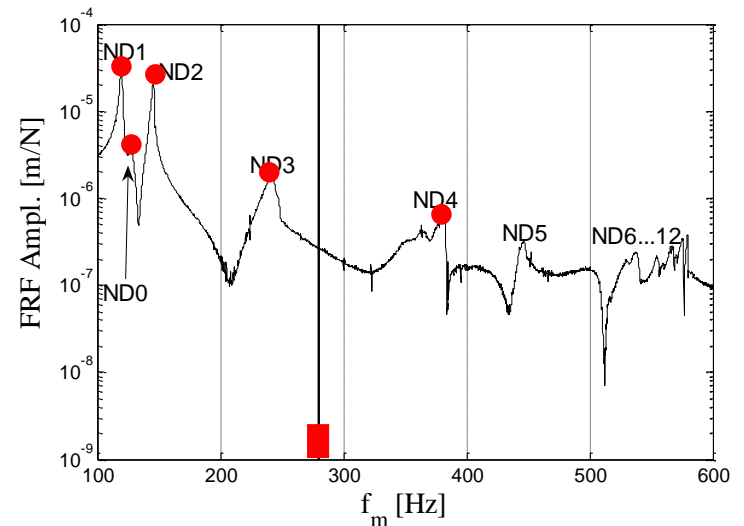
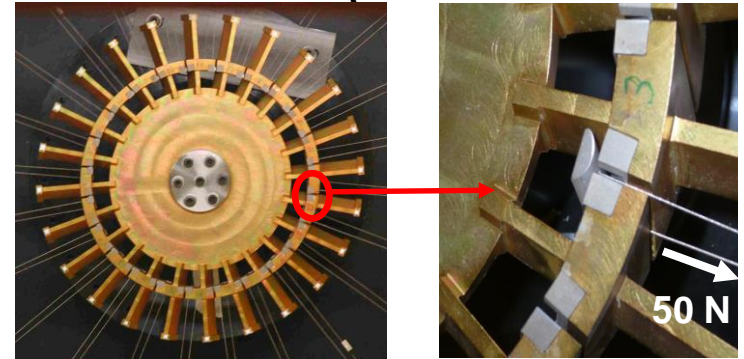


HAMMER TEST – BLISK WITHOUT and WITH DAMPERS

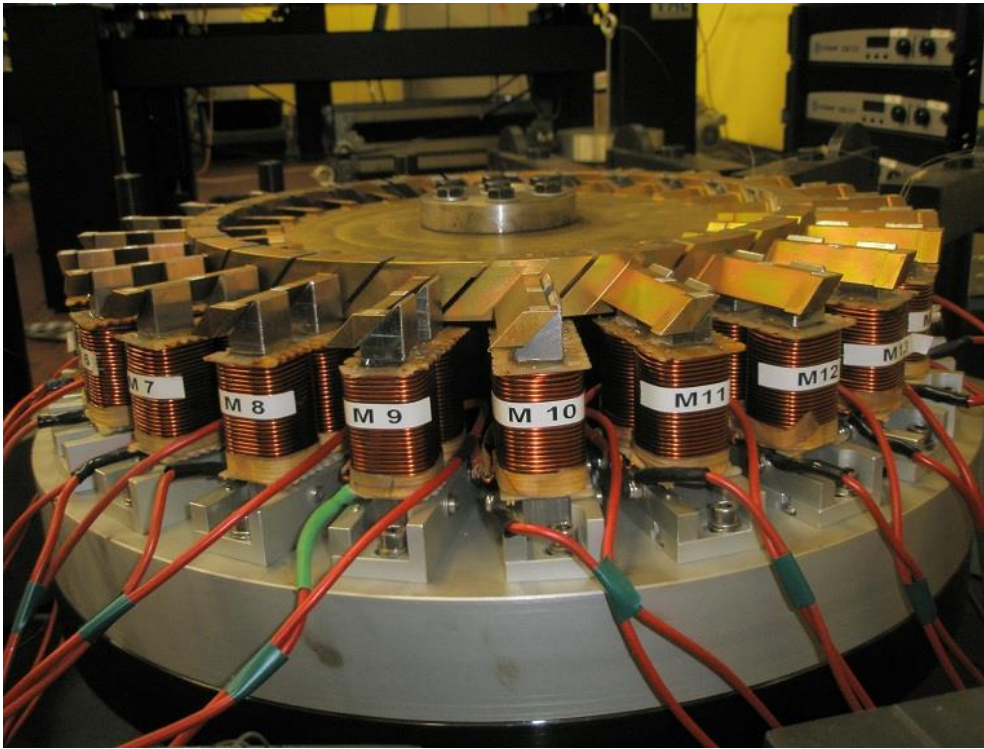
FRF without dampers (free)



FRF with dampers (50 N on each UPD)



TRAVELLING WAVE EXCITATION



TEST PARAMETERS

$$EO = ND = 2, 3, 4, 5, 6$$

$$F_A = 0.1 \text{ N}$$

Excitation force at a given EO

$$f_e = F_E \cos(\omega_m t + (n-1) \cdot \varphi_m)$$

$$n = 1, \dots, N_b = 24 \quad \text{number of the blade}$$

EO engine order index

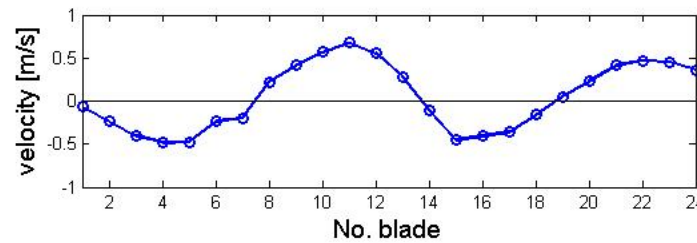
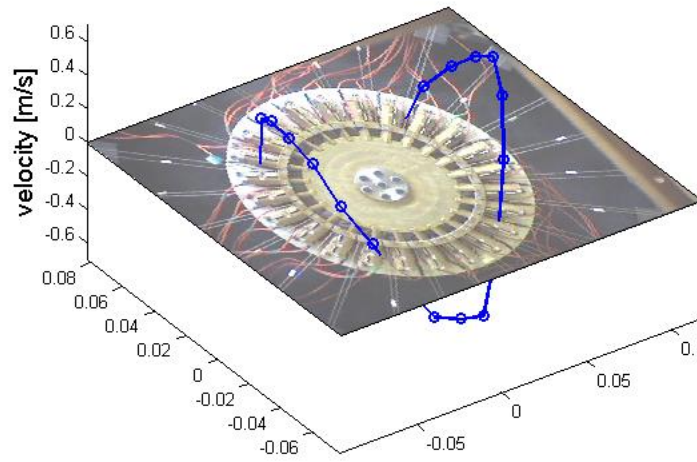
$$\varphi_m = \frac{2\pi}{N_b} EO$$

We choose $EO = ND$

$$\varphi_m = \frac{2\pi}{N_b} ND \quad \text{Inter Blade Phase Angle (IBPA)}$$

RESPONSE TO A TRAVELLING WAVE EXCITATION

CASE OF SMALL MISTUNING



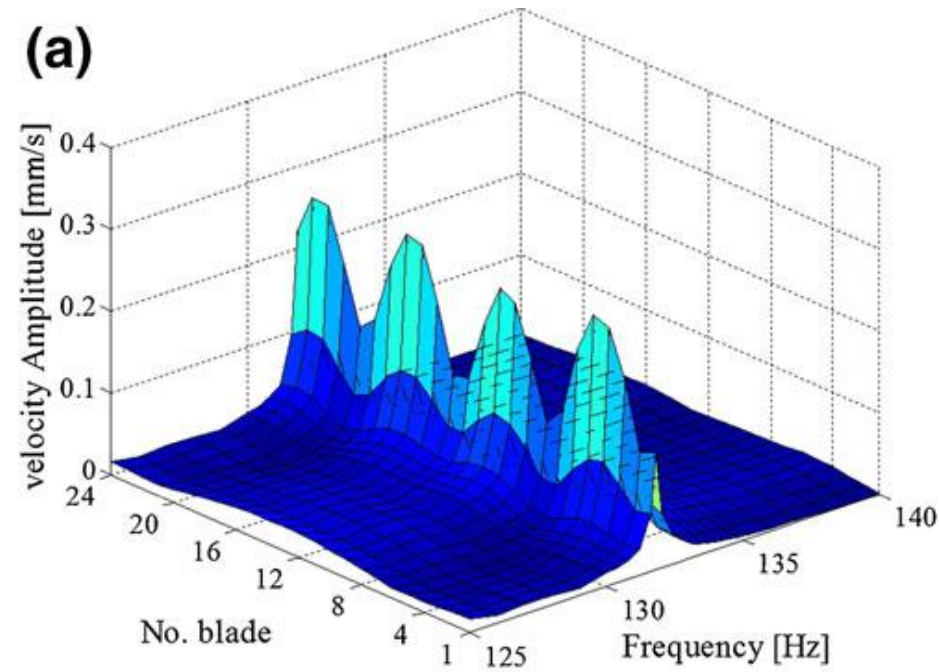
No more a straight line

FFT of the response of each blade

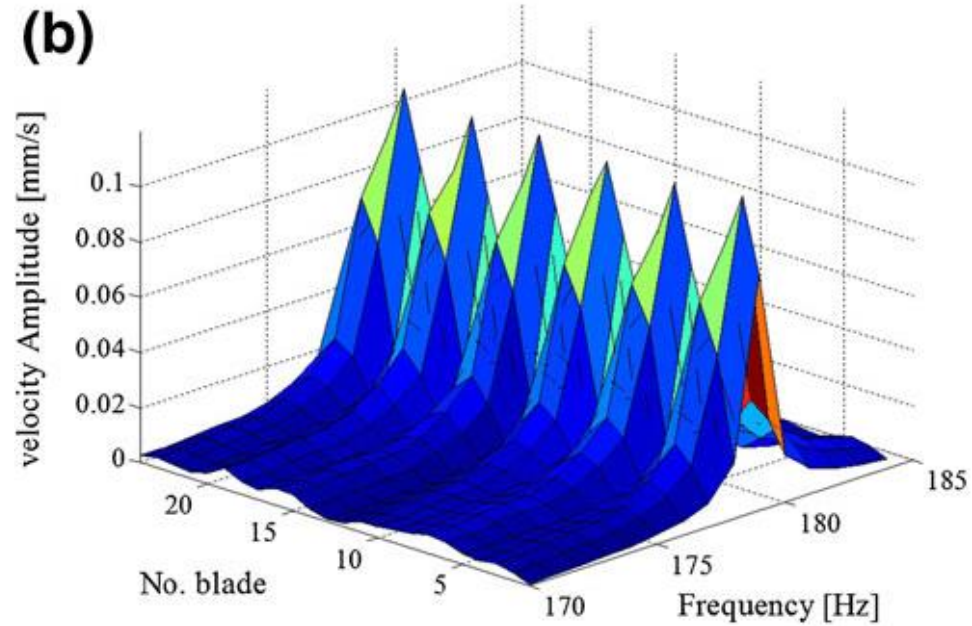
Small mistuning

Excitation at $EO = ND = 2$

Excitation at $EO = ND = 3$



Why 4 lobes?



Why 6 lobes?

EXPLANATION OF THE MODULATION OF THE RESPONSE

Equation of the travelling response of a tuned disk

$$x = X \cos(\omega_m t + (n-1) \cdot \varphi_m) \quad n = 1, \dots, N_b = 24$$

$$x = X \cos((n-1) \cdot \varphi_m) \cdot \cos(\omega_m t) - X \sin((n-1) \cdot \varphi_m) \cdot \sin(\omega_m t) \quad \varphi_m = \frac{2\pi}{N_b} EO$$

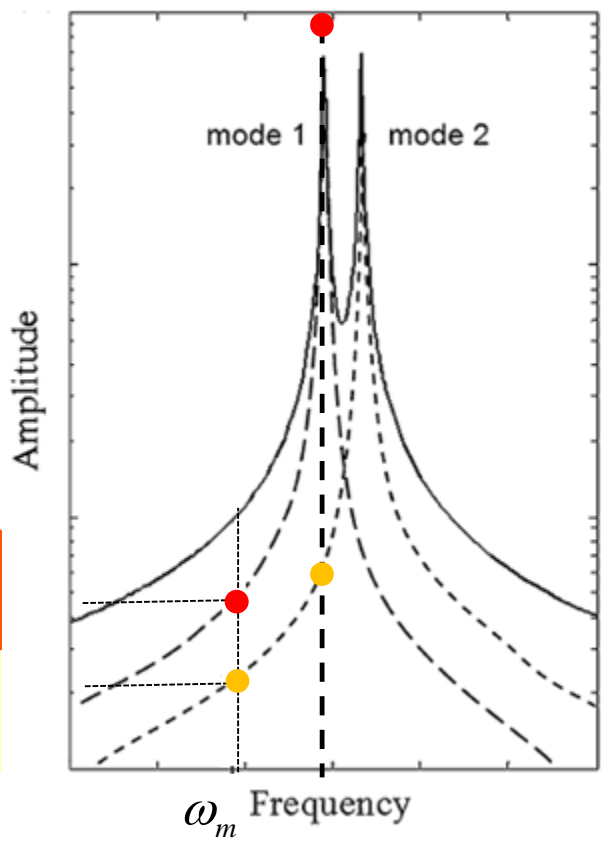
EO engine order index

Response of a “small” mistuned disk

$$x = X_1 \cos((n-1) \cdot \varphi_m) \cdot \cos(\omega_m t) - X_2 \sin((n-1) \cdot \varphi_m) \cdot \sin(\omega_m t)$$

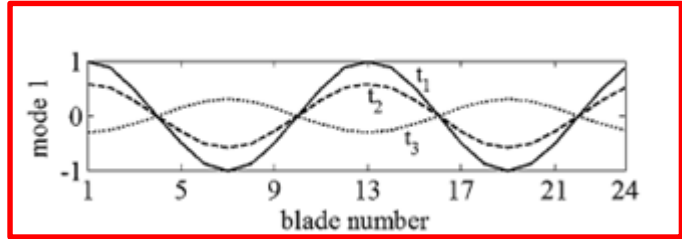
Graphical explanation of the lobes

$$x = X_1 \cos((n-1) \cdot \varphi_m) \cdot \cos(\omega_m t) - X_2 \sin((n-1) \cdot \varphi_m) \cdot \sin(\omega_m t)$$

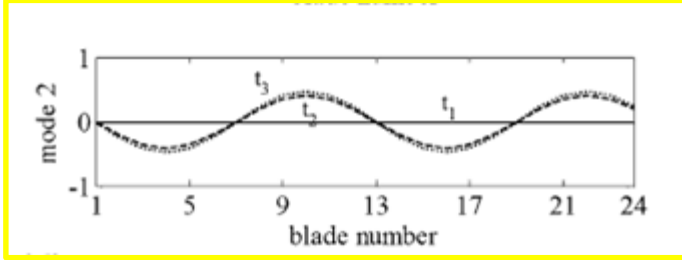


X_1

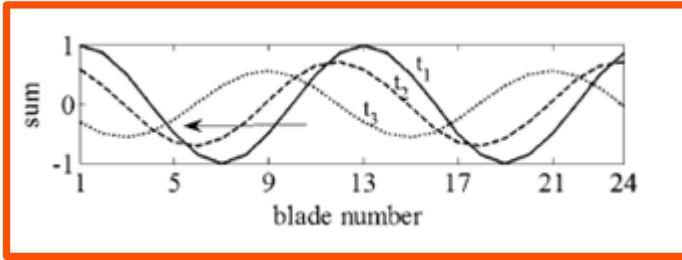
X_2



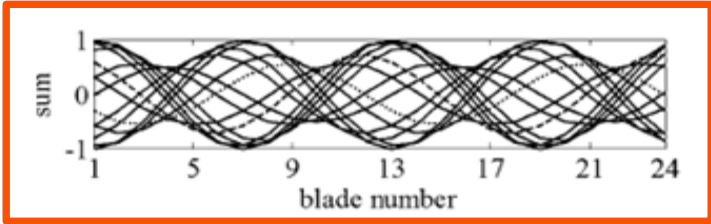
Wave ND2, phase 0°



Wave ND2, phase 90°



Sum of the 2 waves

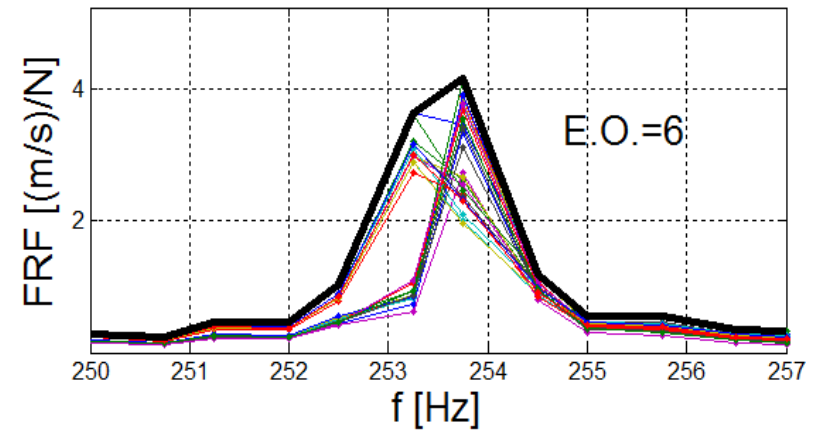
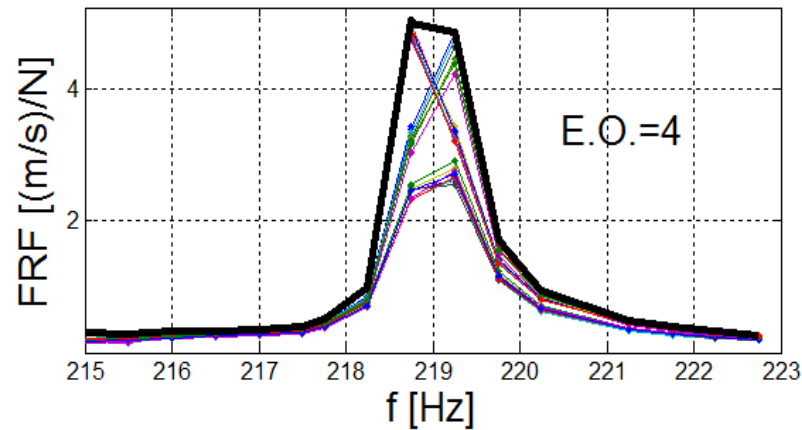
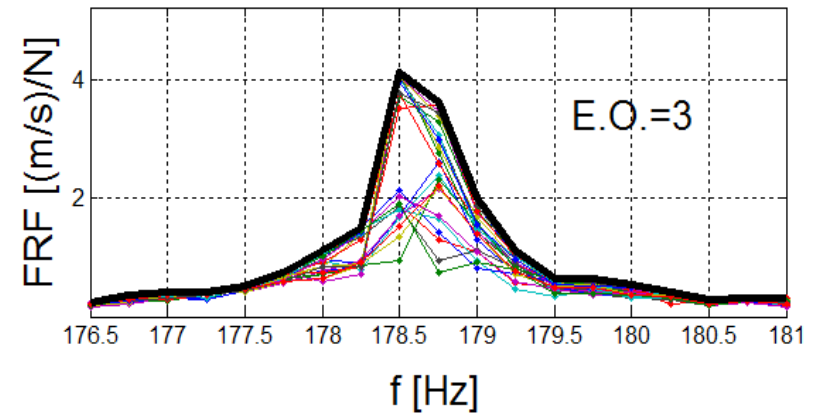
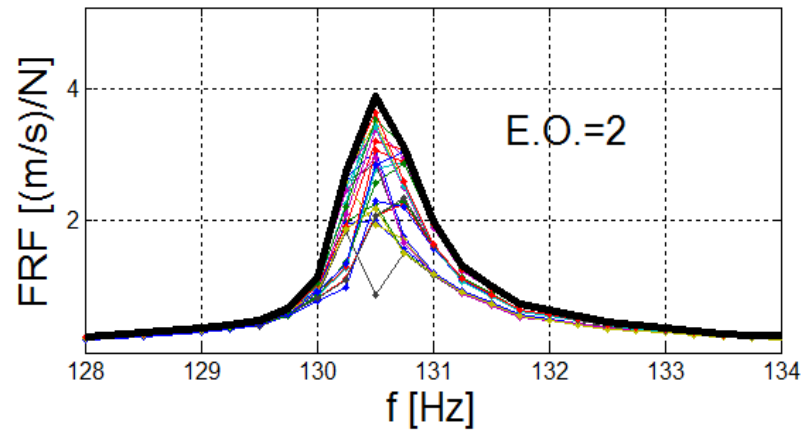


Amplitude modulation

4 LOBES

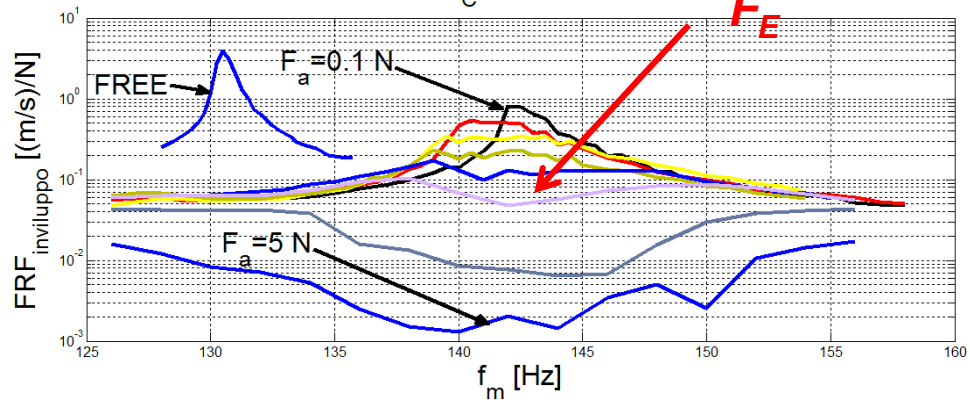
Envelope curve of the maximum amplitude

.....Let's take the envelope of the amplitudes

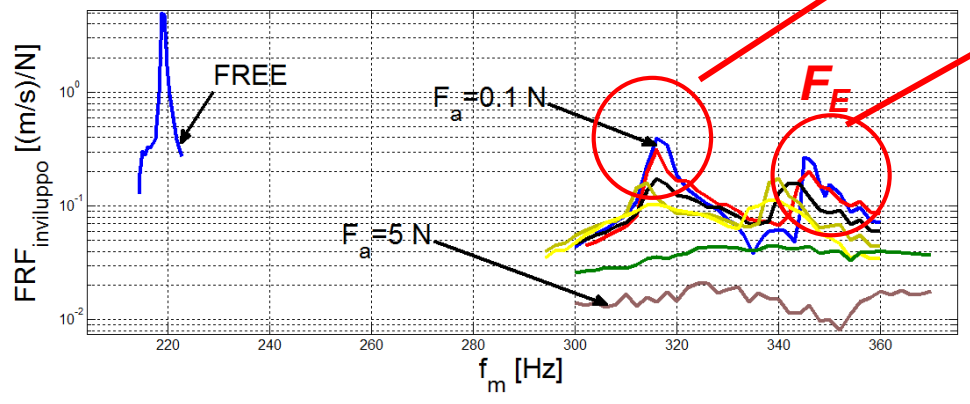


Response for different excitation force amplitudes

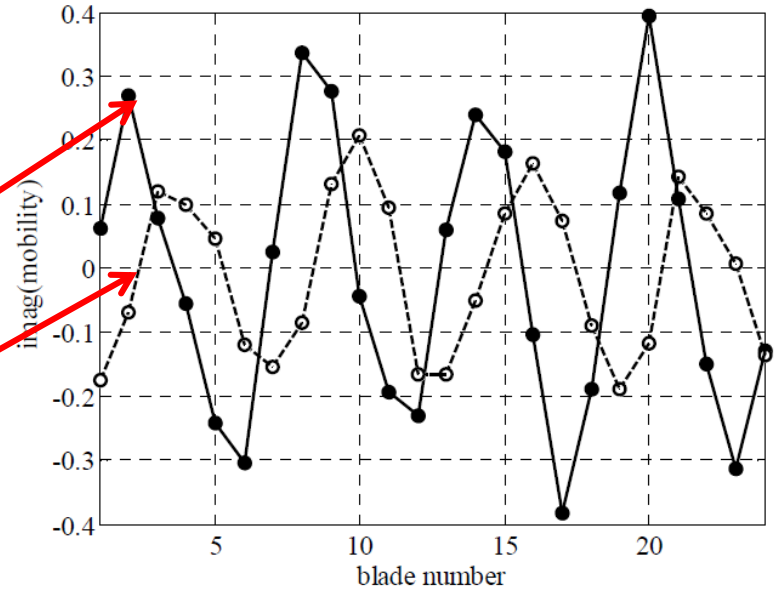
E.O.=2, $F_C=5$ Kg per piattello



E.O.=4, $F_C=5$ Kg per piattello



Operative deformed shapes of the two modes



Standing waves...no more rotating

Split of frequency due to mistuning

Forced response measurement on rotating bladed disks

Berruti T.M., Firrone C.M., Gola M.M., Calza P., "The effect of friction contacts on the dynamics of a rotating vane segments array : simulation and comparison with experimental result, World Tribology Congress, Torino 2013, pp1-4, ISBN 9788890818509.

Berruti T.M, Maschio V. –" Experimental investigation on the forced response of a dummy counter rotating turbine stage with friction damping", J of Eng. For gas turbines and power, vol. 134 n. 12. - ISSN 0742-4795 (2012) doi: 10.1115/1.40

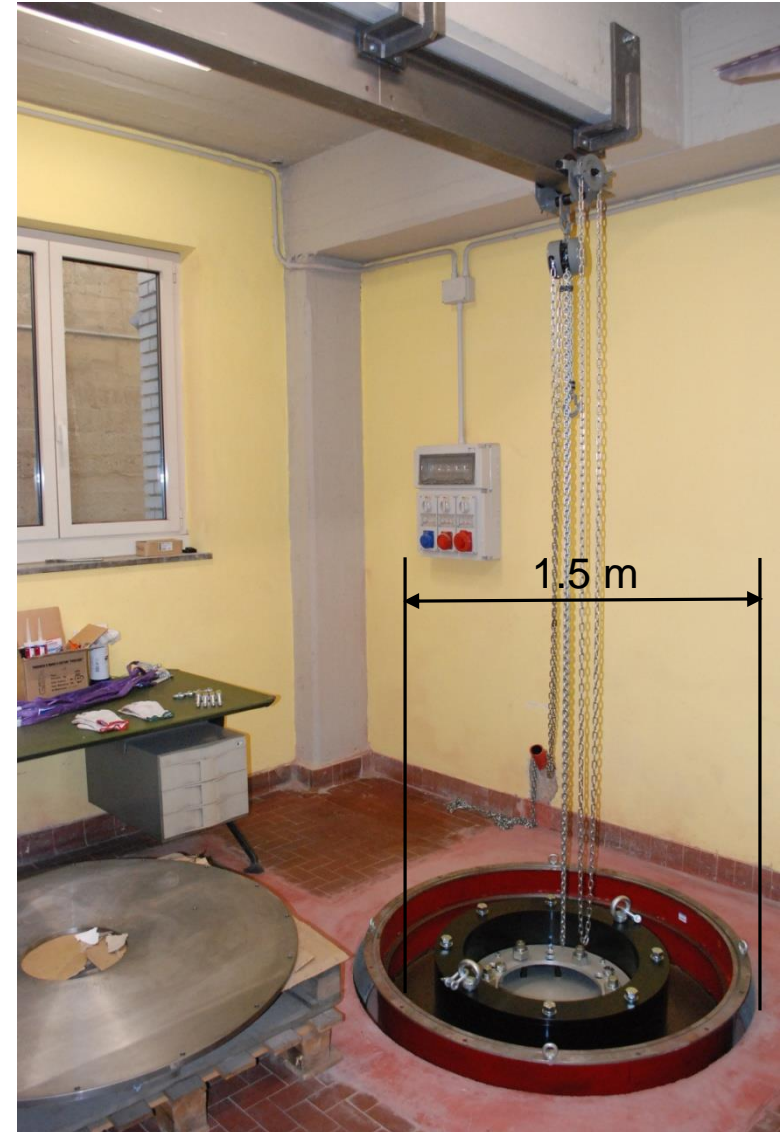
Battiato, G, Firrone, C.M.; Berruti, T. M. (2016) Forced response of rotating bladed disks: Blade Tip-Timing measurements, Mechanical Systems and Signal Processing vol. 85, pp. 912-926.

Rigosi G., Battiato G., Berruti T.M., (2017) Synchronous vibration parameters identification by tip timing measurements, Mechanics Research Communications, Volume 79,pp. 7-14.

SPINNING TEST RIG

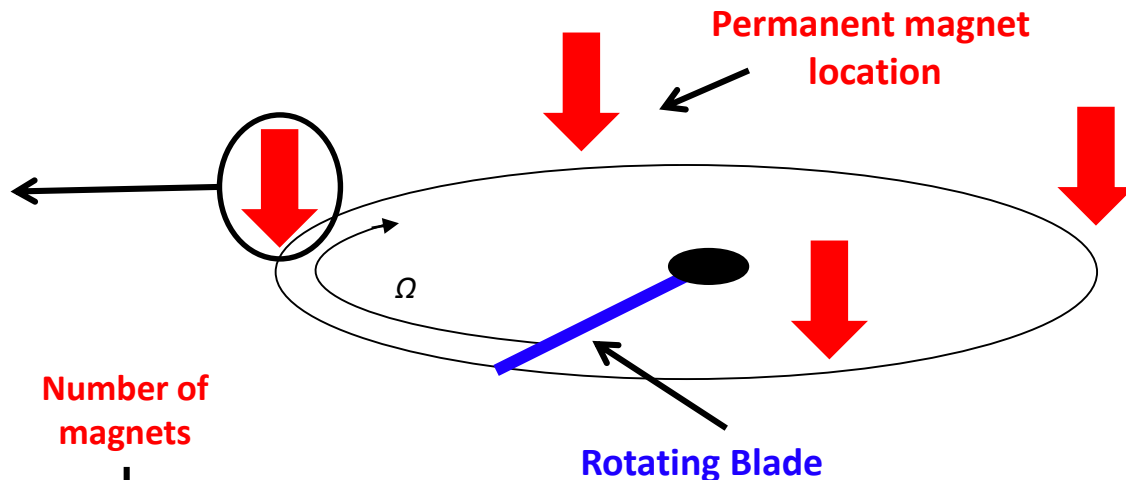
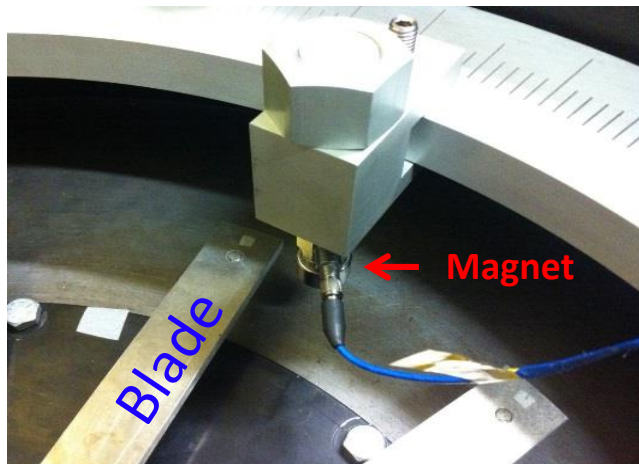
Main features

- rotation speed up to 4000 rpm (2500 rpm with this test article)
- test article diameter up to 650 mm
- 24 channel telemetry system
- permanent magnet excitation (1 to 24 magnets)
- 6 magnets with force transducers



The Excitation System: multiple EOs excitation

The excitation system uses cylindrical permanent magnets facing the rotating blades



During the rotation each blade is excited by a number of impulses equal to the number of permanent magnets

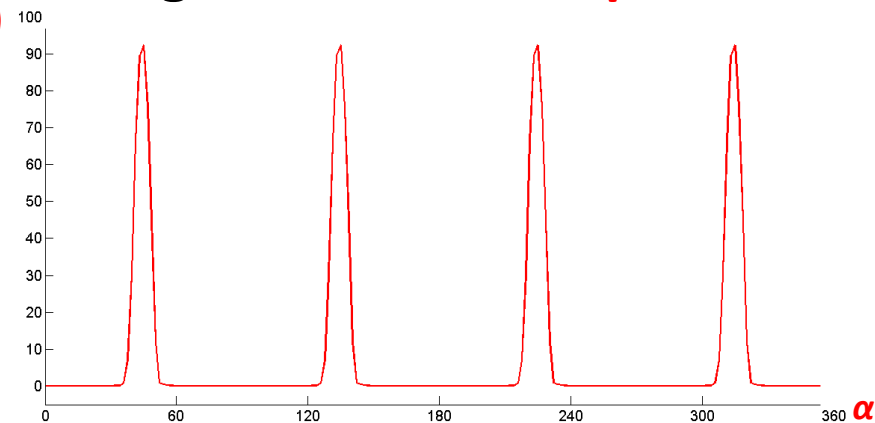
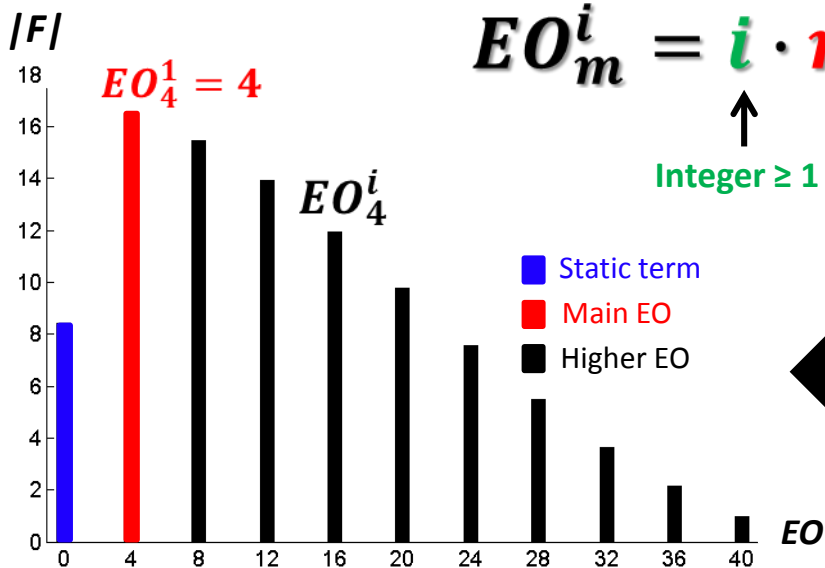
4 magnets \rightarrow 4 impulses

$$EO_m^i = i \cdot m$$

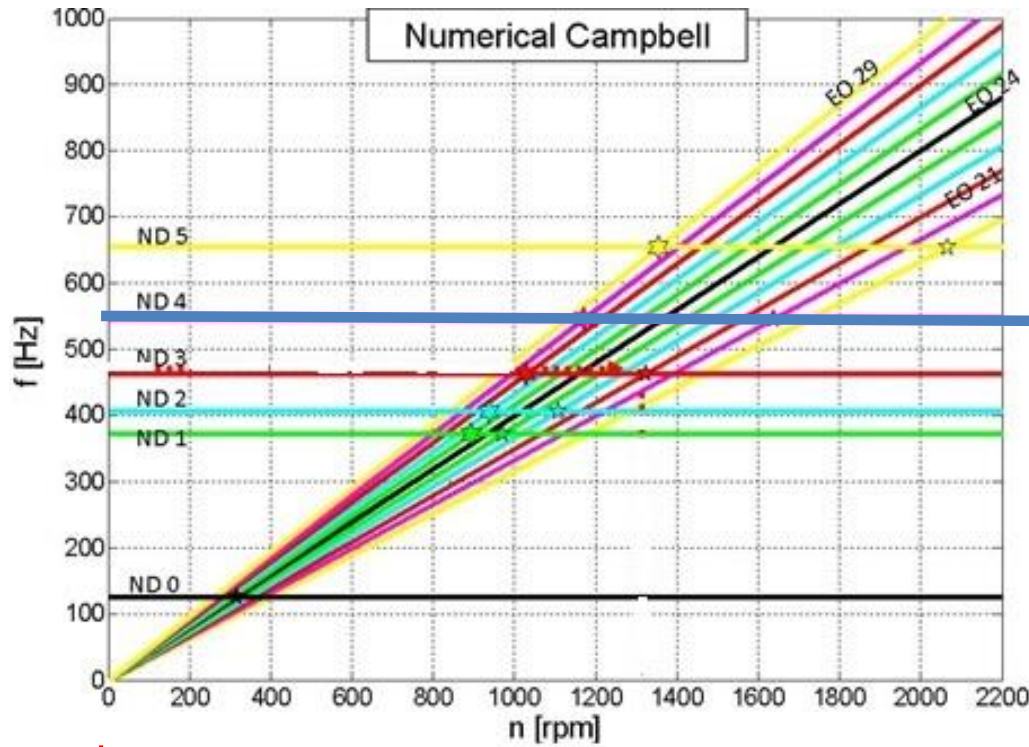
Integer ≥ 1

$F(\alpha)$

FFT



Choosing the mode to be excited

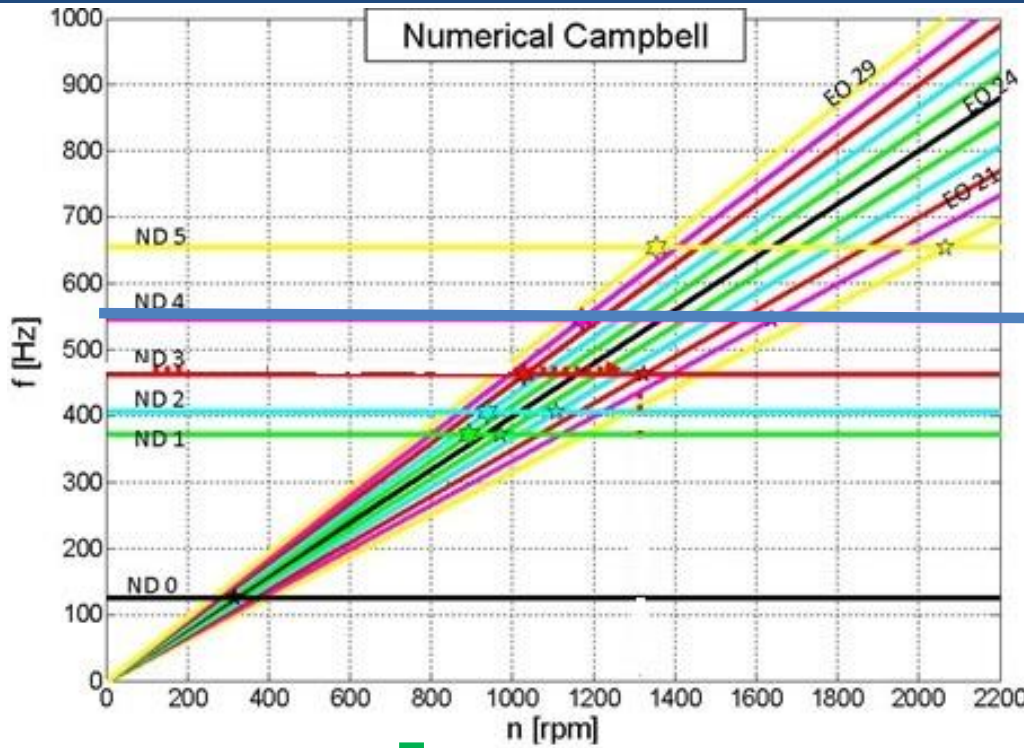


ND=4 $f_{res}=552$ Hz

$N_b=24$ number of blades

Speed range

Choosing the mode to be excited

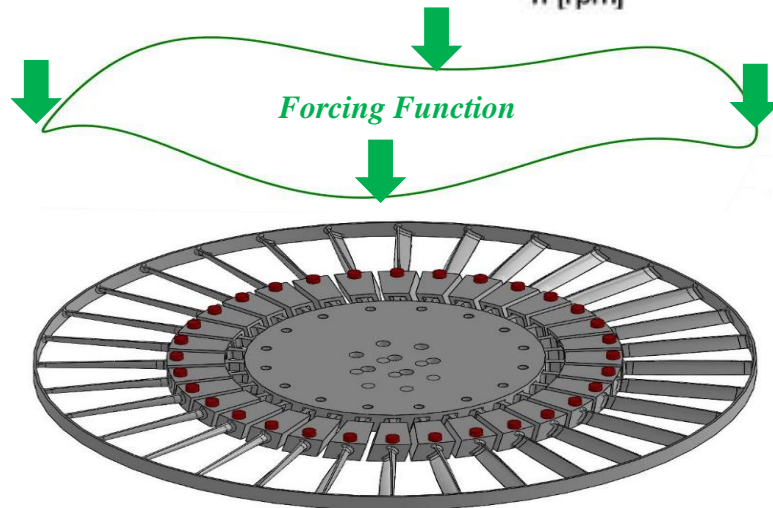


ND=4 $f_{res}=552$ Hz

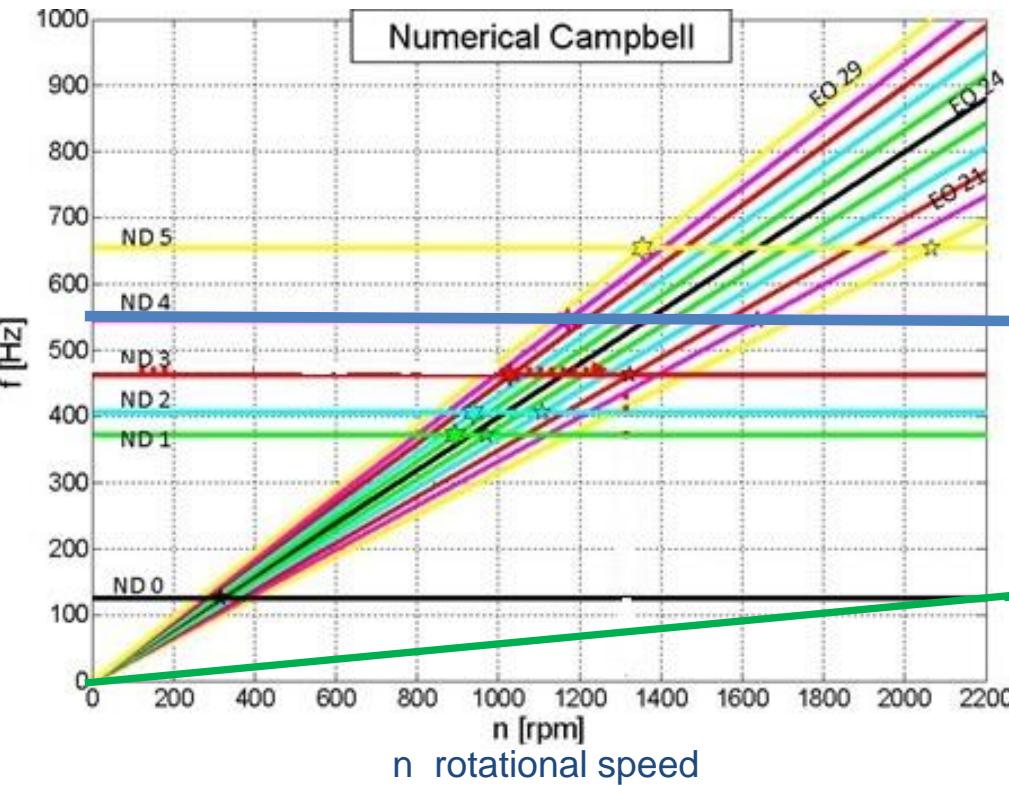
To excite the mode at ND=4...

...we want to meet the two conditions:

$$\left\{ \begin{array}{l} f_{exc} = f_{res} \\ EO = ND \end{array} \right.$$



Choosing the rotation speed



ND=4 $f_{res} = 552$ Hz

EO=4

8280 rpm

Speed too high for the test rig

$$EO \cdot n = f_{res}$$

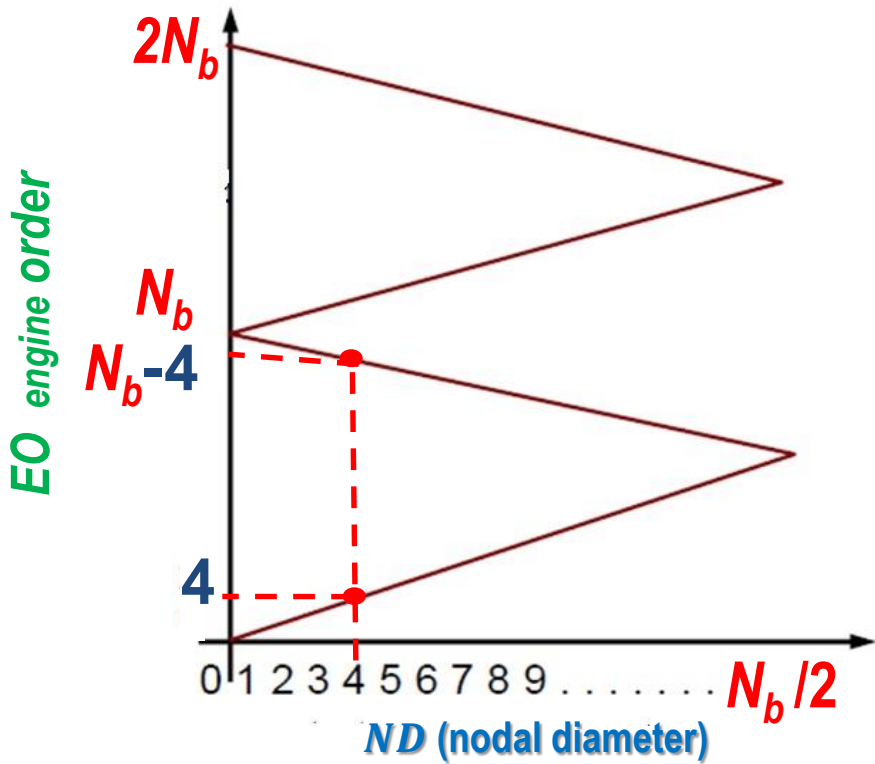
$$f_{res} = 552 \text{ Hz}$$

$$EO = 4 \text{ (magnets)}$$

$$n = \frac{60 \cdot f_{res}}{EO} = \frac{60 \cdot 552}{4} = 8280 \text{ rpm}$$

Choosing the Engine Order

Let's use the SAFE diagram...



In the spin rig EO=number of magnets

N=24 number of blades

To excite ND=4

EO=4 magnets

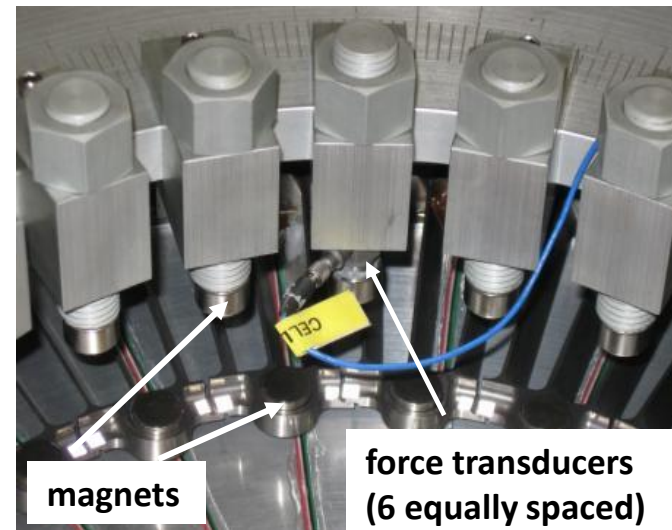
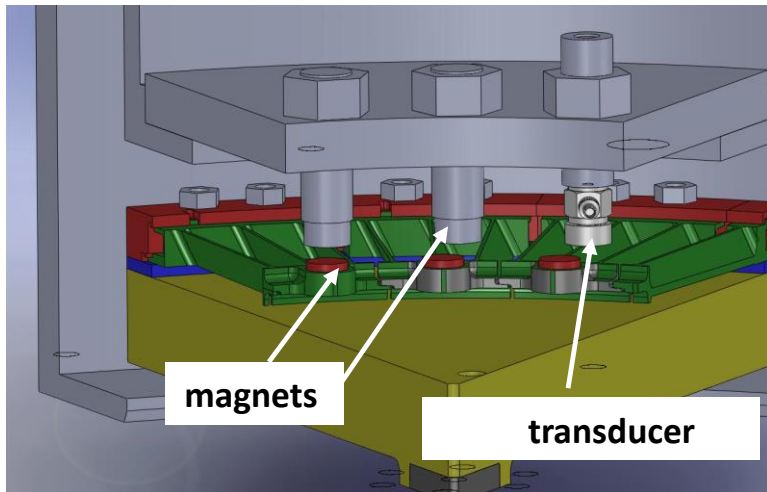
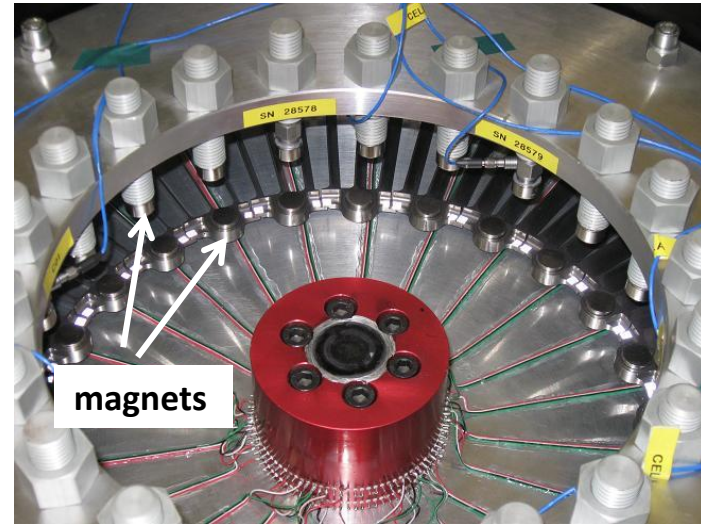
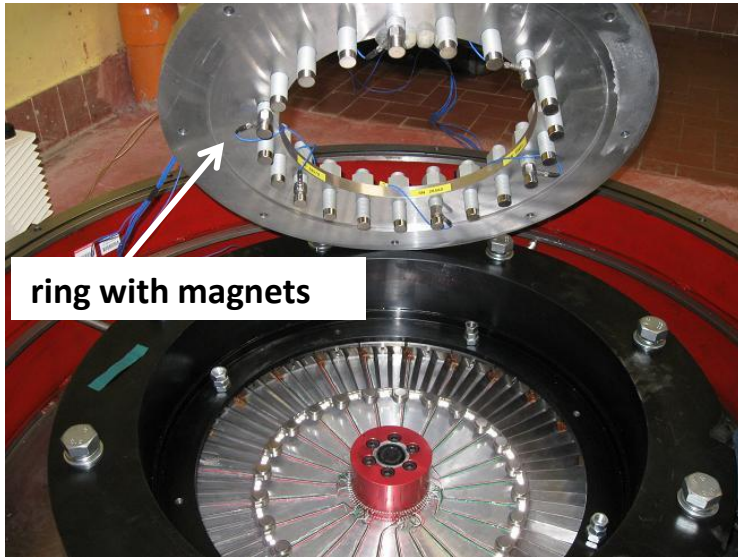
$$n = \frac{60 \cdot f_{exc}}{EO} = \frac{60 \cdot 552}{4} = 8280 \text{ rpm}$$

EO=24-4=20 magnets

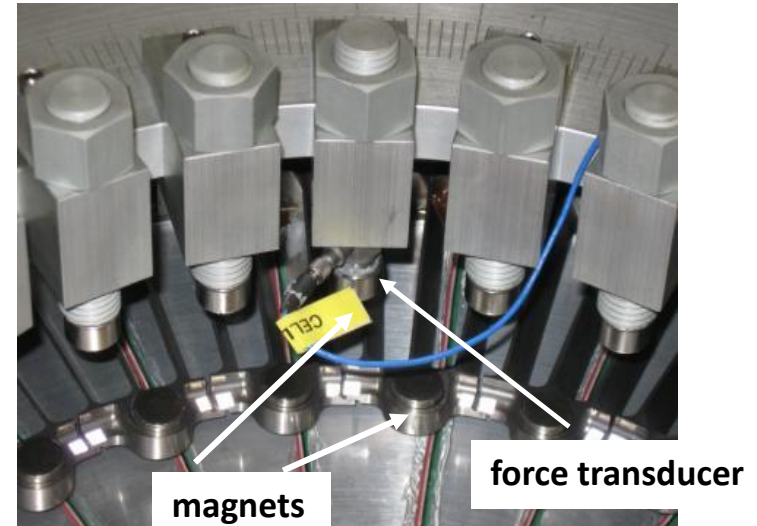
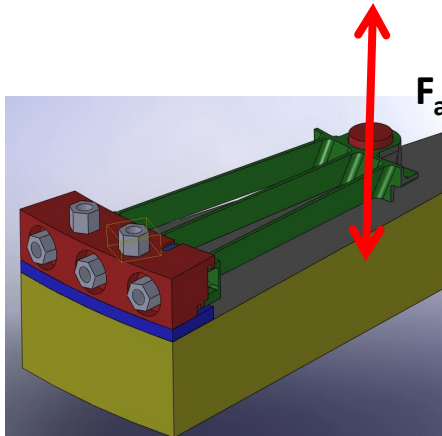
$$n = \frac{60 \cdot f_{exc}}{EO} = \frac{60 \cdot 552}{20} = 1656 \text{ rpm}$$

The excitation system: permanent magnet

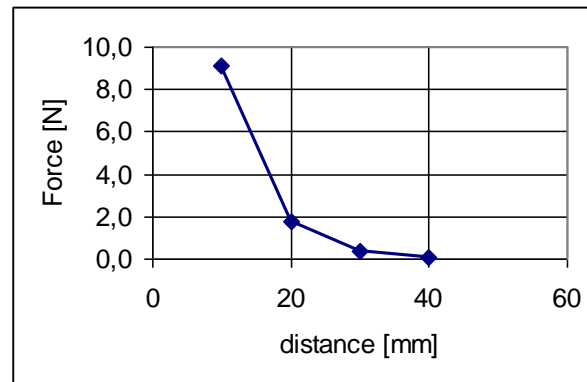
(example: magnets with diameter 18 mm, height 10 mm, magnetization N52).



Determination of the magnetic forces



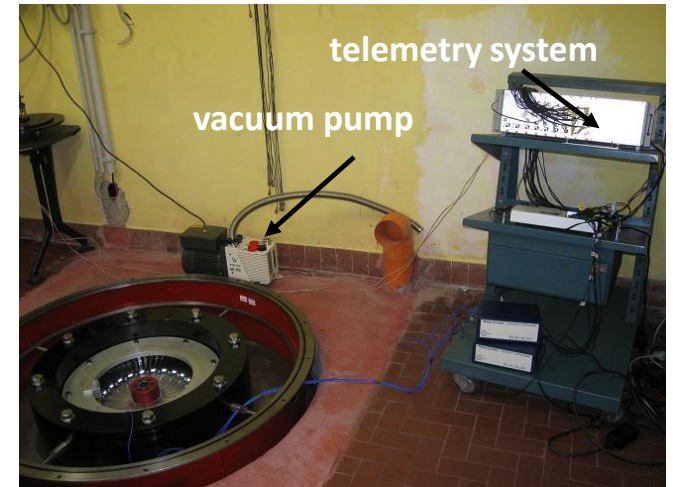
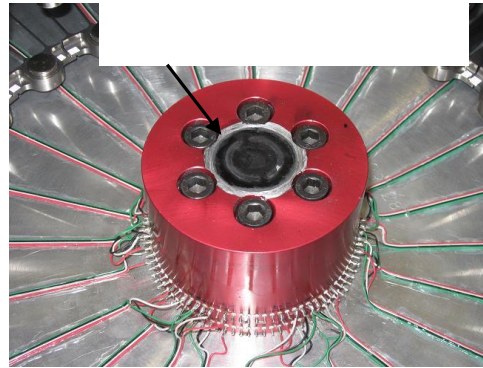
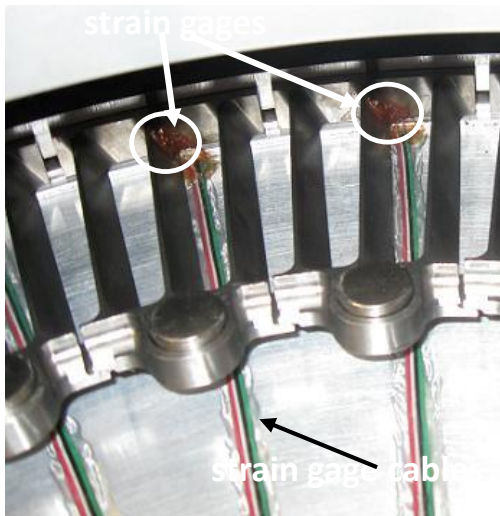
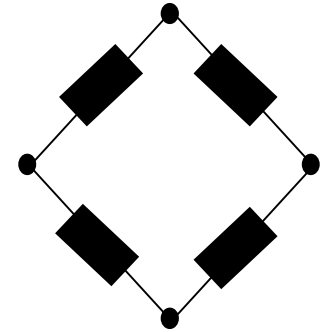
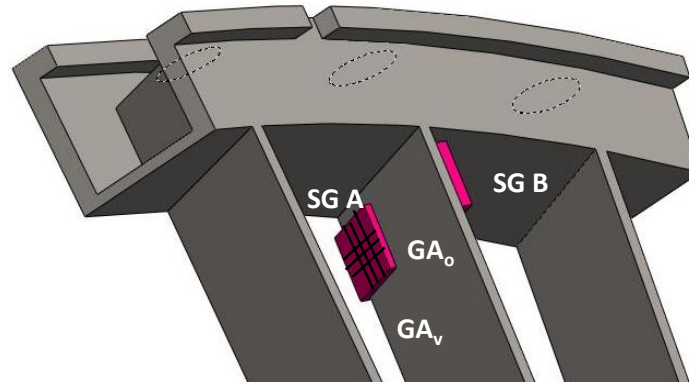
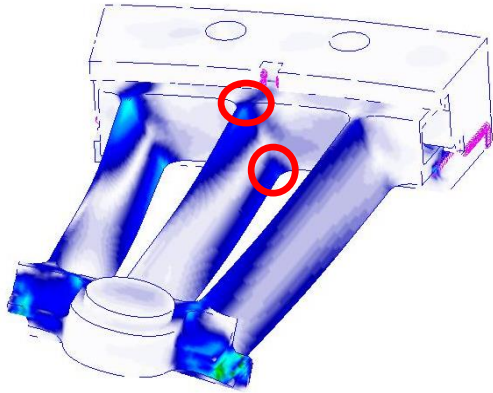
$-F_a$ from measurement of the force transducers.



gap [mm]	measured axial force amplitude F_a [N]
10	9.11
20	1.75
30	0.38
40	0.08

By increasing the gap of 4 times the force decreases of 100 times!

Strain gages and telemetry



Measurement example

Example

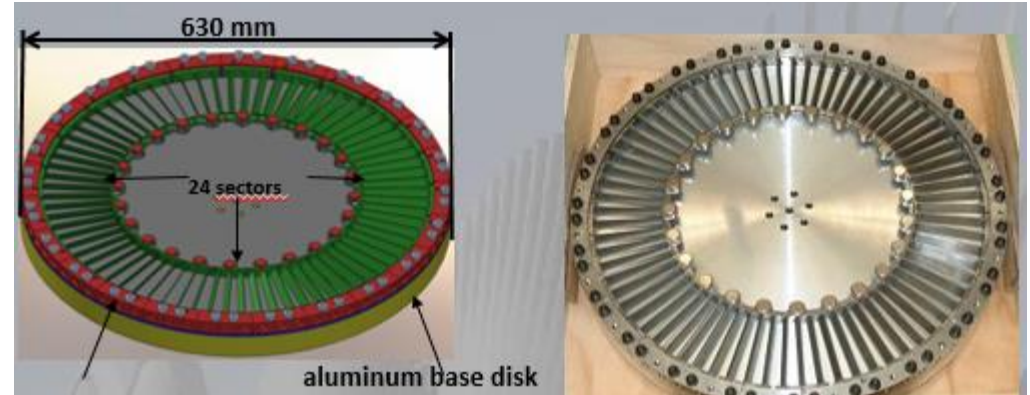
$n = 0 \div 1500 \text{ rpm}$ with $\Delta n = 2 \text{ rpm}$

$T = 4 \text{ s}$ time acquisition for each step of n

FFT of the signal from each strain gage and store of the amplitude corresponding to the excitation frequency

FFT of the signal from each force transducer and store of the amplitude corresponding to the excitation frequency

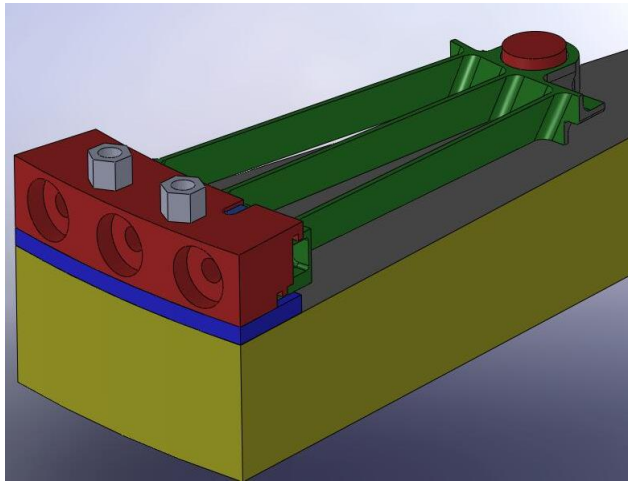
Calculation of the FRF for each sector;
ratio of the FFT from the strain gage and the FFT of the force (average of the FFTs of the six force transducers)



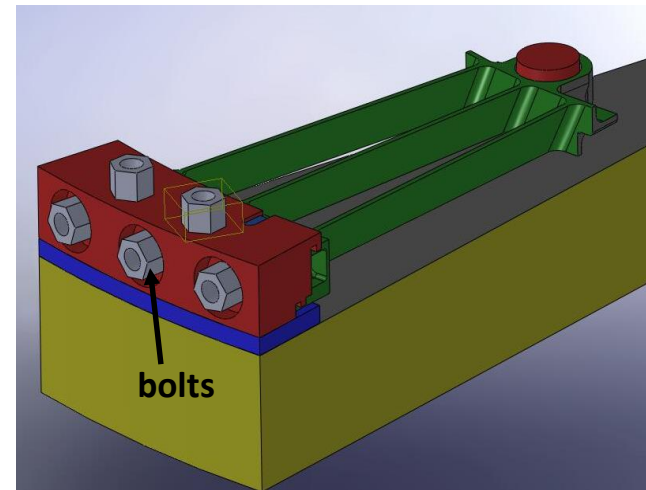
Test configurations

- A) sectors connected to the casing through the hooks as in the real case
- B) sectors rigidly connected to the casing through bolted joints

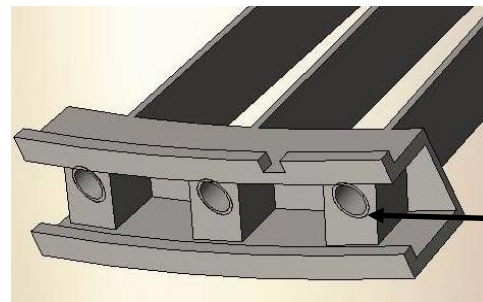
Configuration A
Free hooks



Configuration B
Tightened hooks



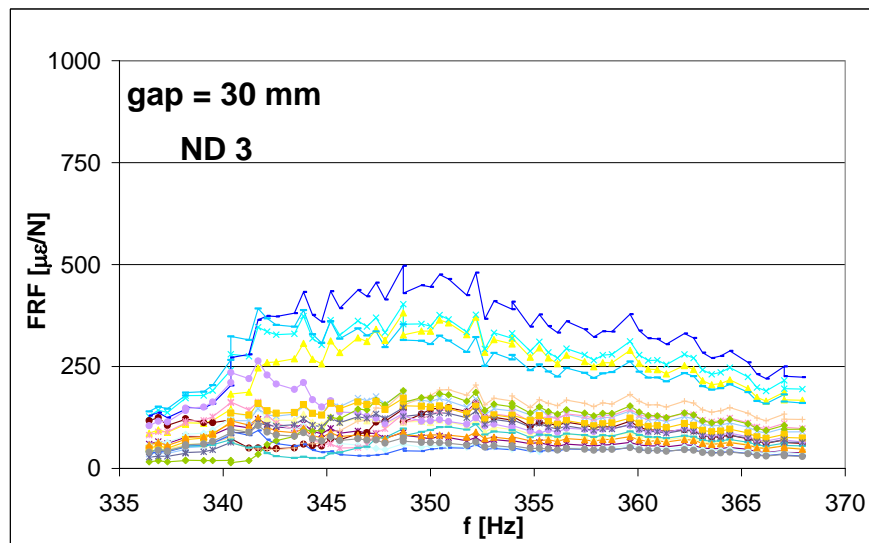
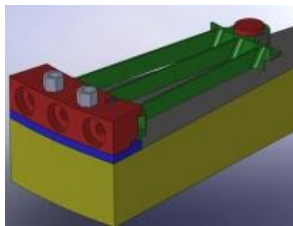
attachment detail



threaded holes

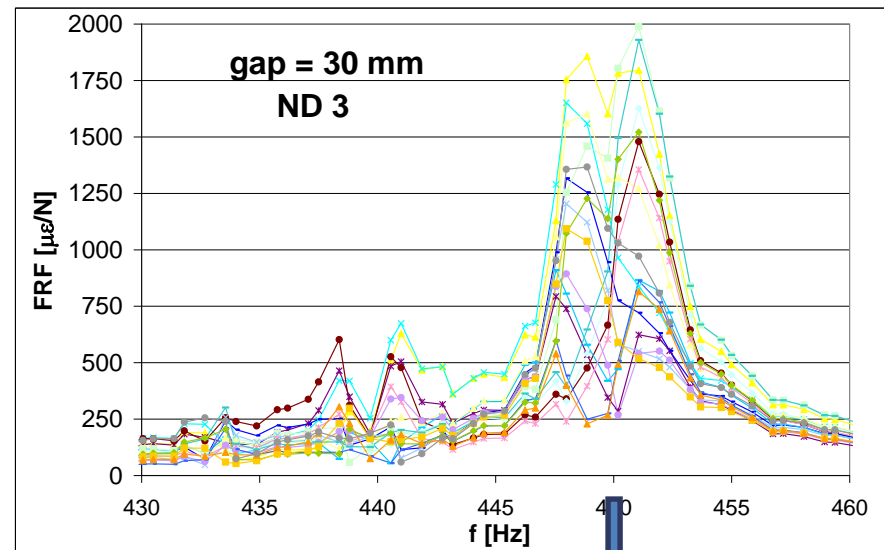
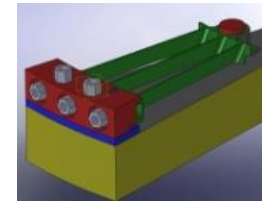
Example of test results

Configuration A - Free hooks



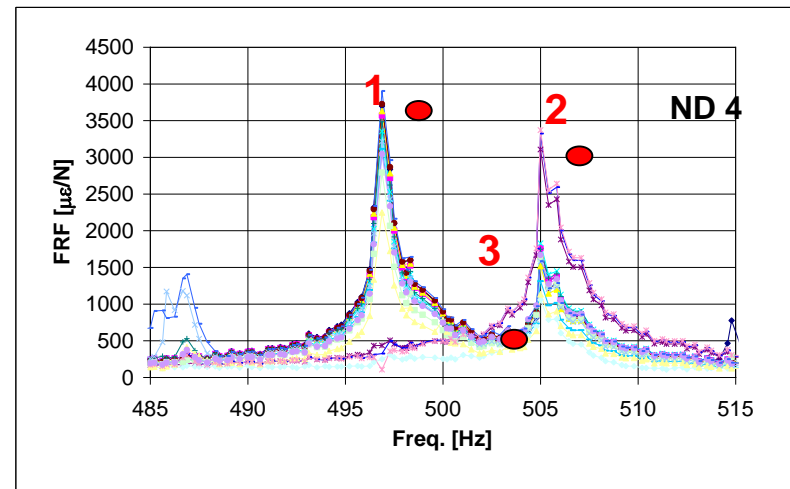
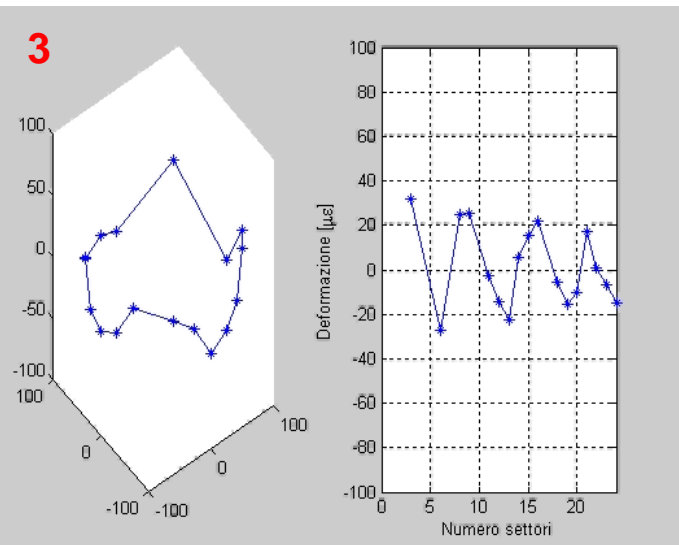
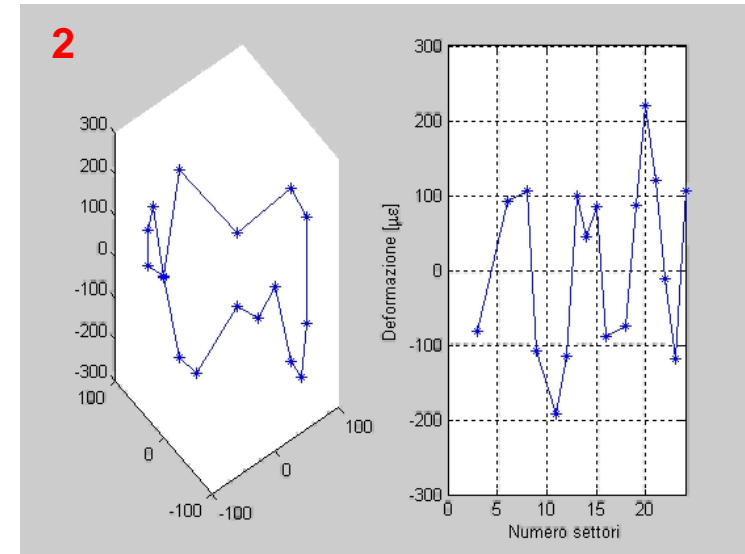
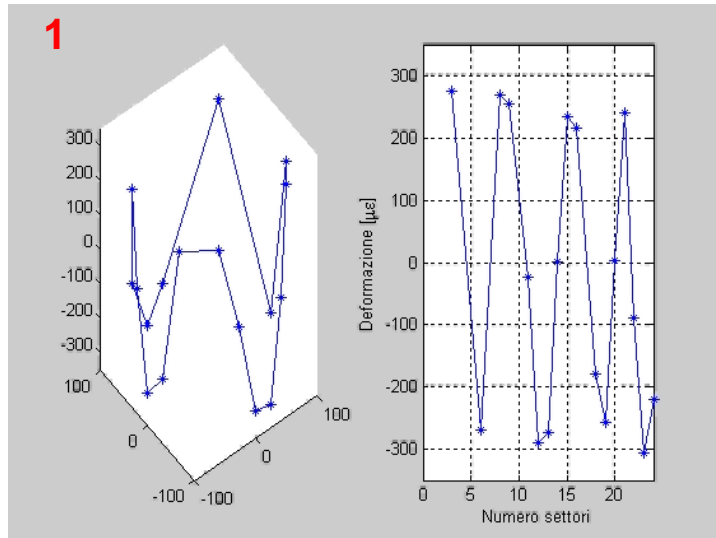
differences among the 24 sectors

Configuration B - Tightened hooks



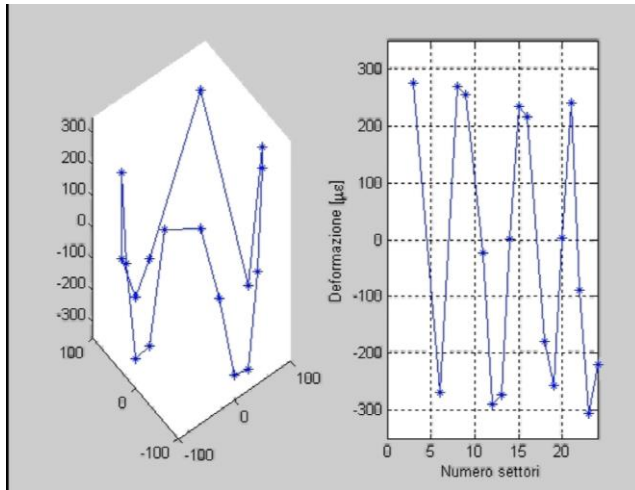
presence of two peaks at resonance

Spinning test results – standing and rotating waves

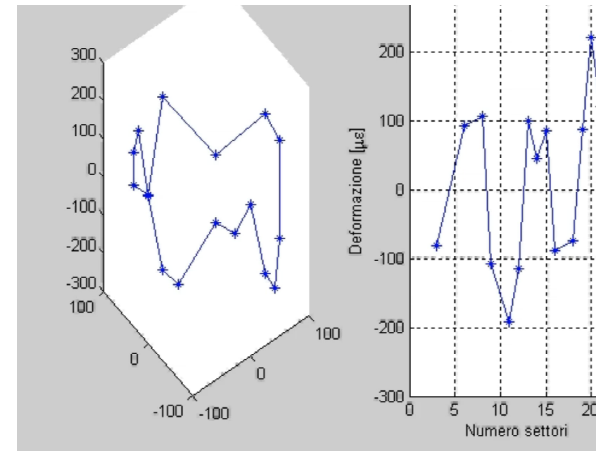


Spinning test results – standing and rotating waves

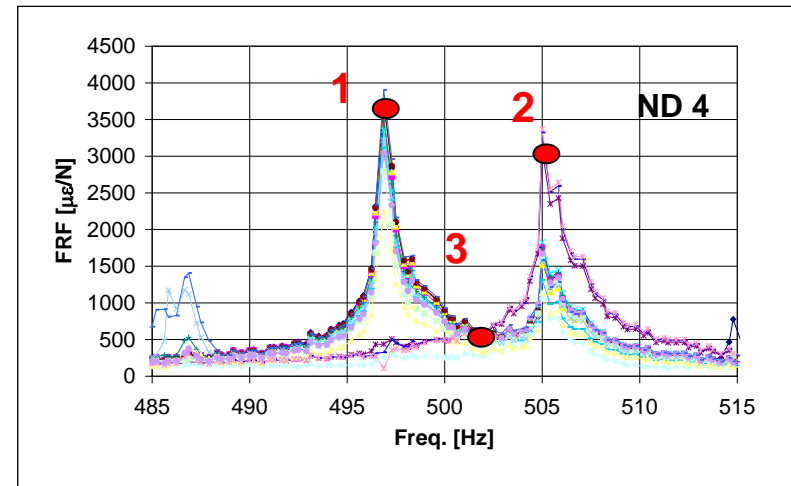
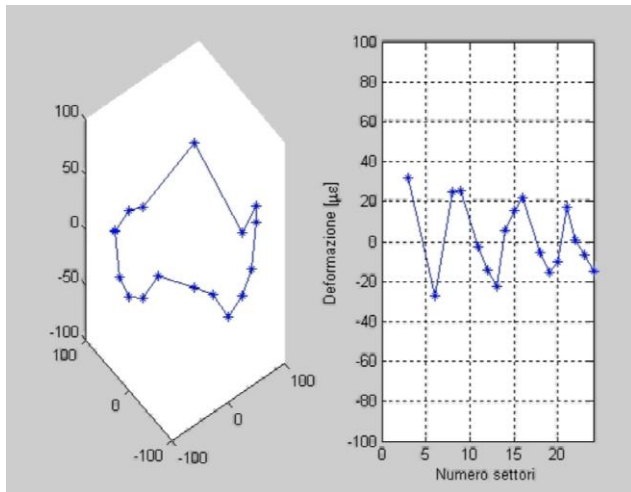
1



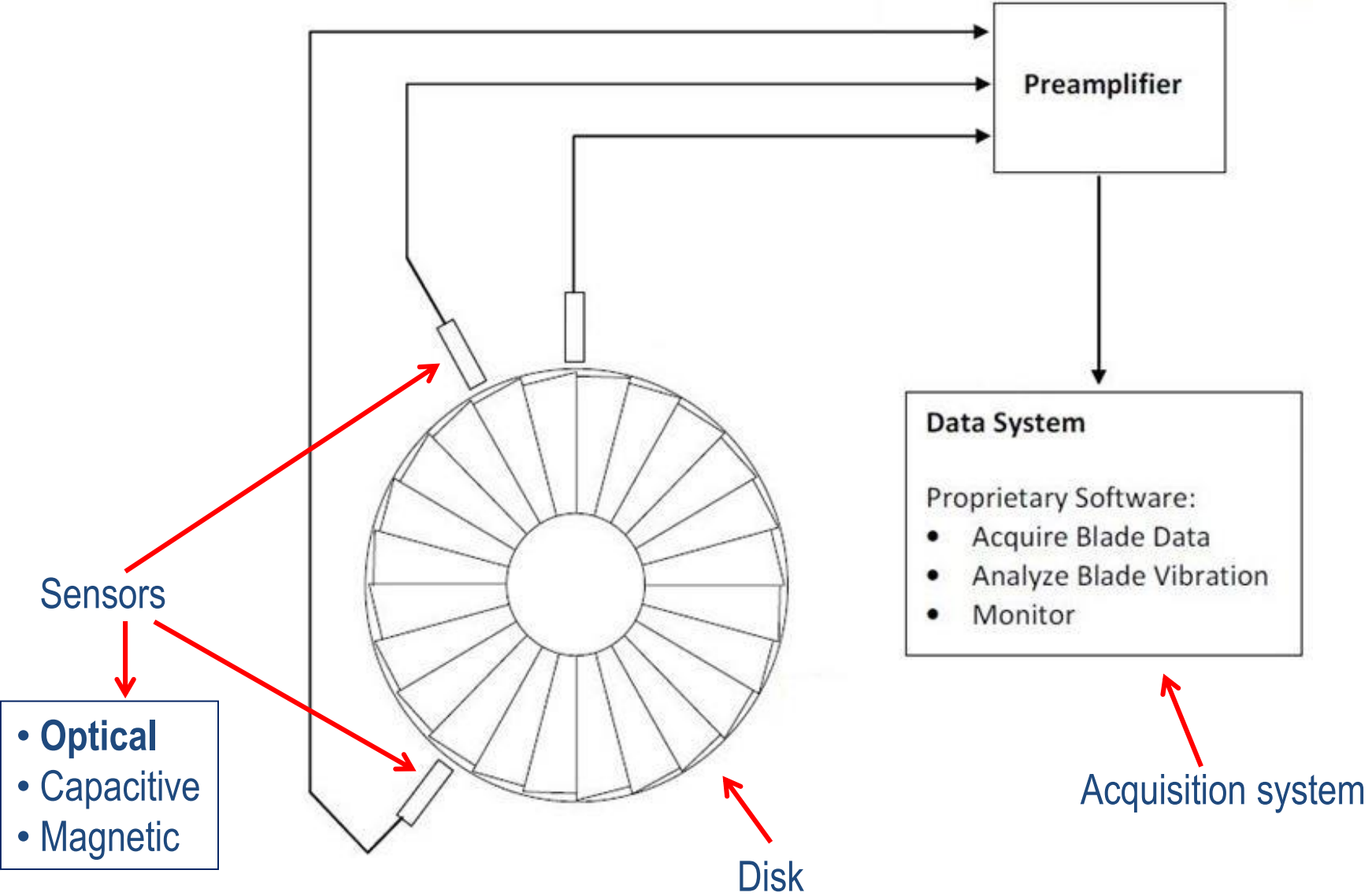
2



3



Blade Tip Timing Measurement System

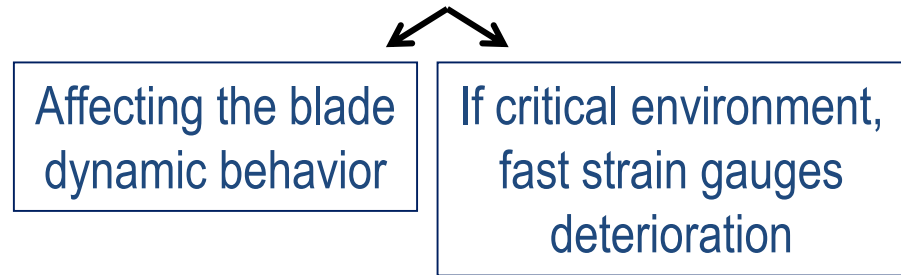


Blade Tip Timing Measurement System

BTT vs Strain Gauges

1) BTT is a Non-Intrusive Measurement system

- Strain gauges are attached on the blade



2) Each sensor detects the vibration of each blade

- Instead the strain gauges are attached only to few blades

BTT main outputs

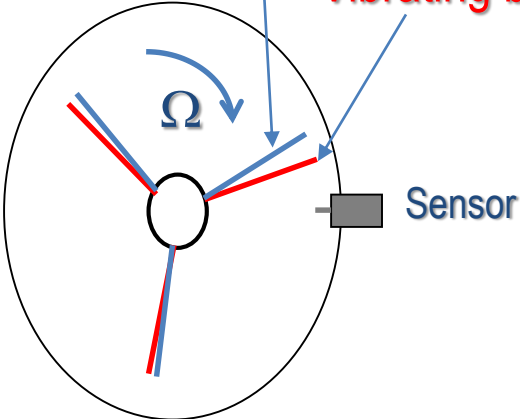
1. Blade resonance frequency
2. Blade maximum vibration amplitude

Blade Tip Timing Measurement System

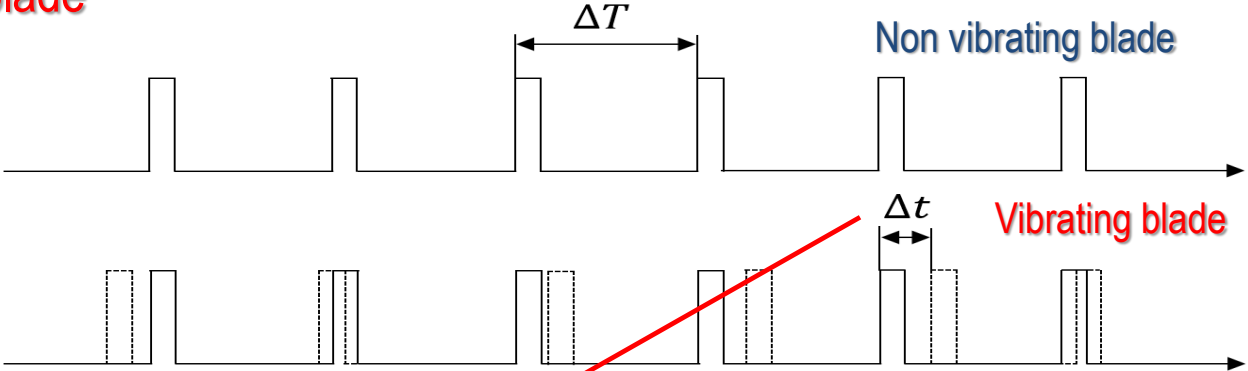
Basic principle

Non vibrating blade

Vibrating blade



ToA time of arrival



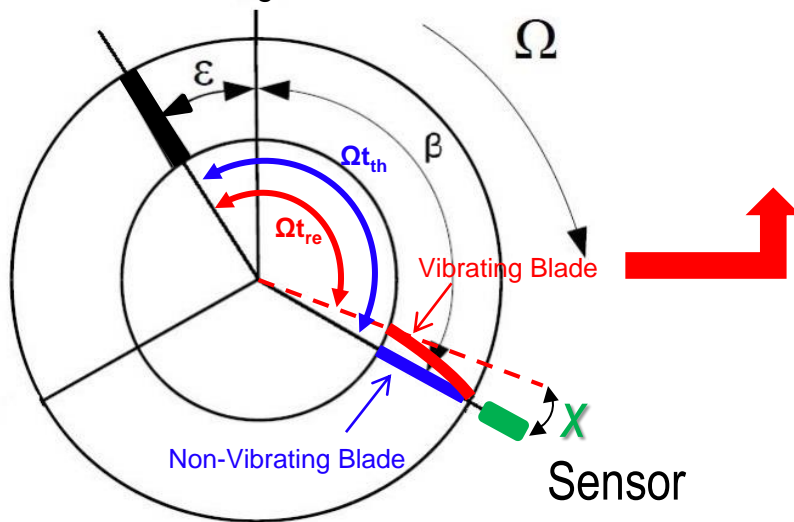
$$x(\Omega) = \Delta t \cdot \Omega$$

Vibration displacement at a given rotational speed Ω

Blade Tip Timing Measurement - Basic principle

In presence of vibration the **real** ToA (t_{re}) could be greater or less than the theoretical ToA (t_{th}).

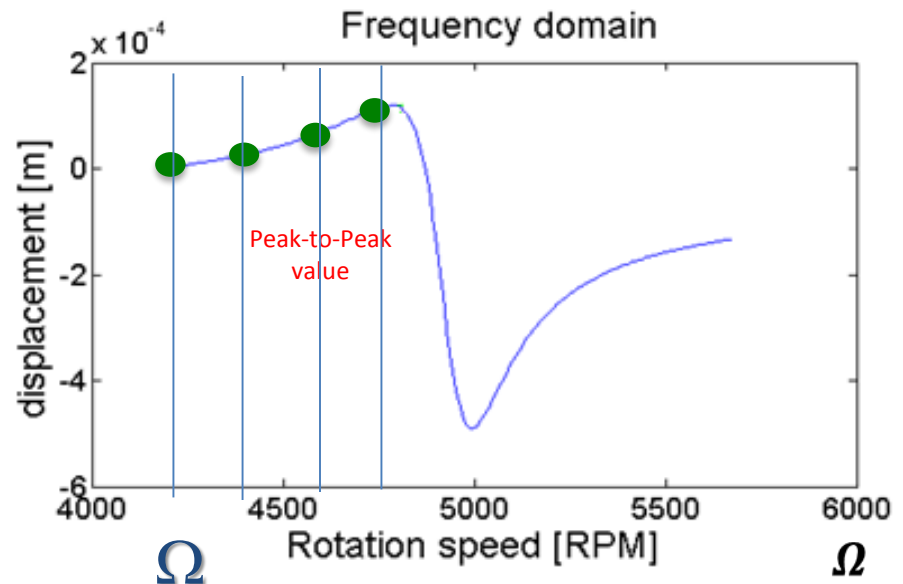
Blade at
time $t = 0$ Origin



The vibrating blade reaches the sensor in advance or in delay with respect to the non-vibrating reference $t_{re} > t_{th}$ or $t_{re} < t_{th}$

$$x(\Omega) = \Delta t \cdot \Omega = (t_{re} - t_{th}) \cdot \Omega$$

x



Blade Tip Timing Measurement - Basic principle - one sensor

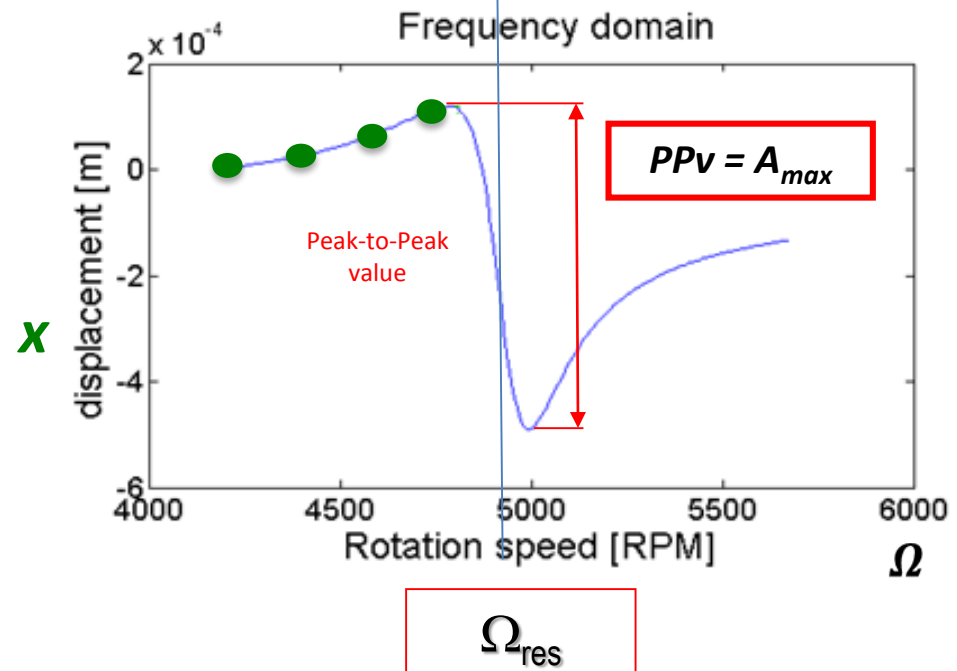
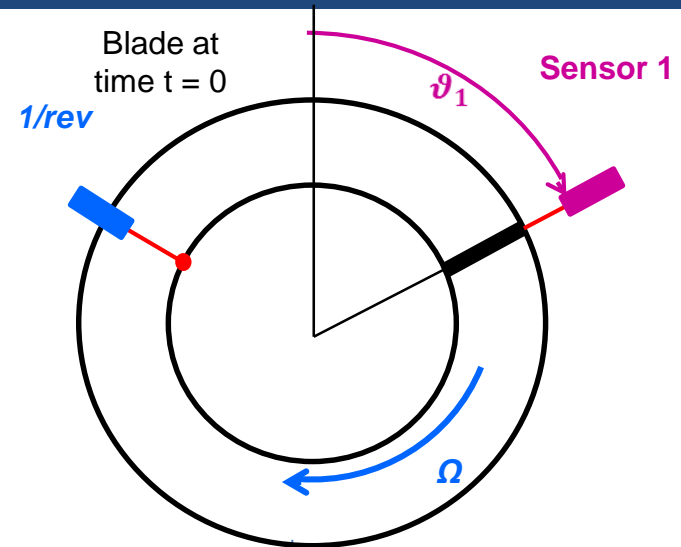
$$x(\omega) = A(\omega) \sin [EO \cdot \Omega t + \varphi(\omega)]$$

$$\omega = EO \cdot \Omega$$

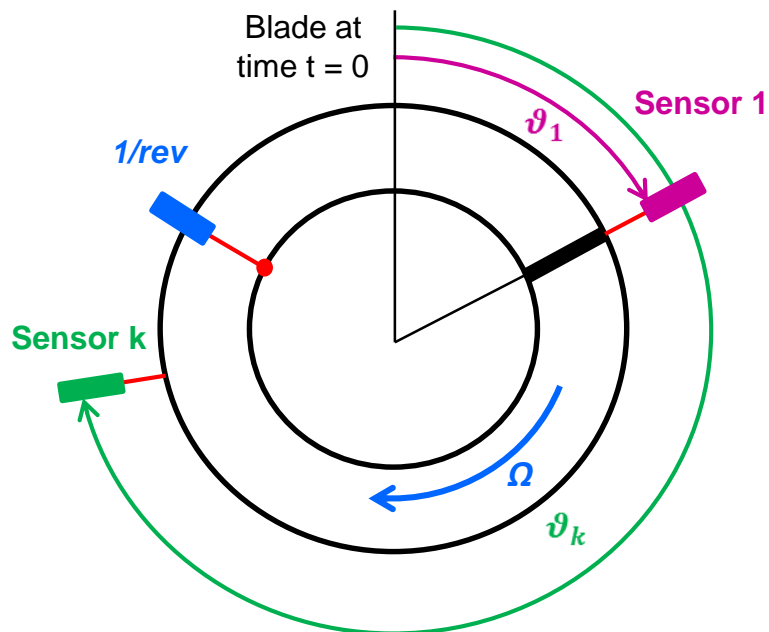
For a given probe 1

$\theta_1 = \Omega t_1$ Angular position of the sensor with respect to the blade

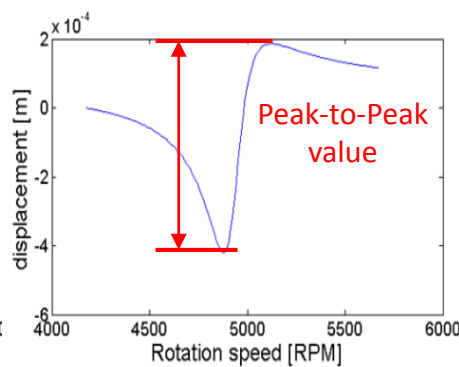
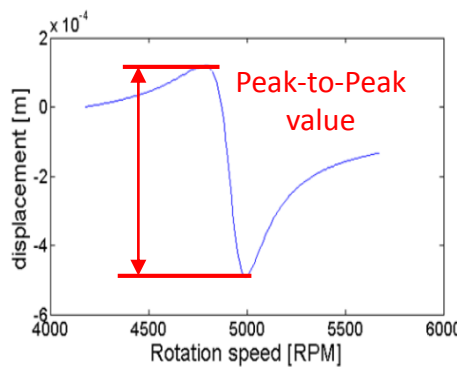
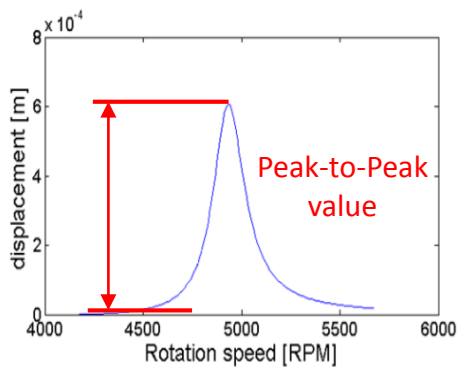
$$x(\omega) = A(\omega) \sin [EO \cdot \theta_1 + \varphi(\omega)] \quad \longrightarrow$$



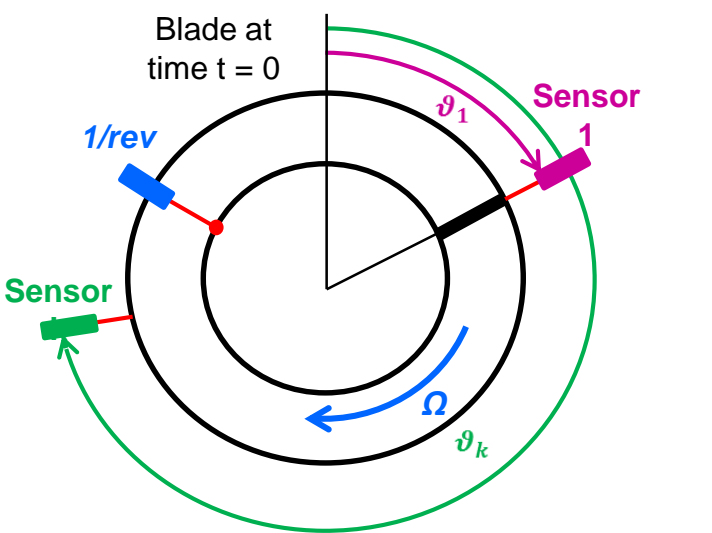
Blade Tip Timing Measurement System Basic principle - more sensors



Depending on the position of the blade θ_k with respect with the sensor.....

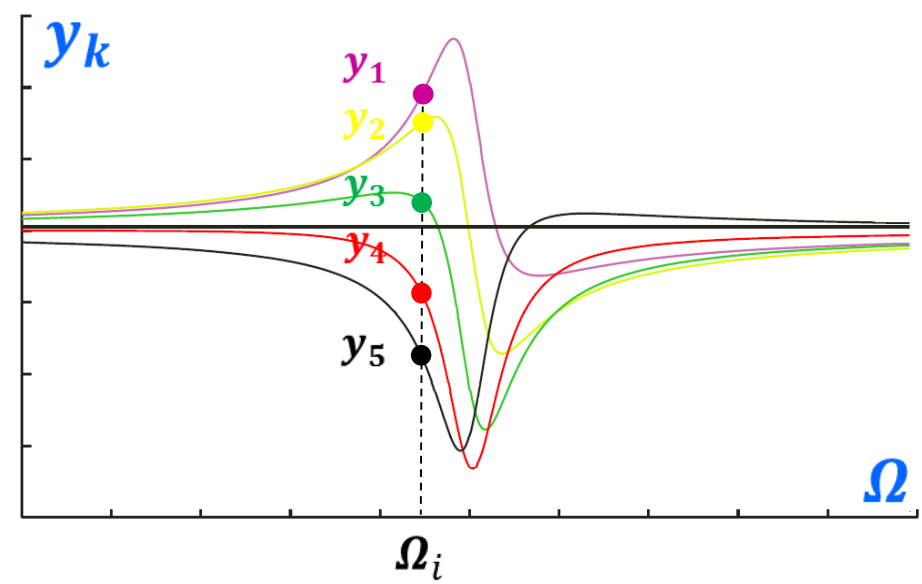


Blade Tip Timing Measurement System Basic principle - more sensors



$\theta_1 = \Omega t_1$ Angular position of the sensor 1 with respect to the blade

Blade response detected by each sensor

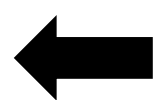


Forced response of the blade



$$y_k(\omega) = c(\omega) + A(\omega) \sin[E\Omega\vartheta_k + \varphi(\omega)]$$

$k > 3$ **Least Square Problem**
 $c(\omega_i), A(\omega_i), \varphi(\omega_i)$

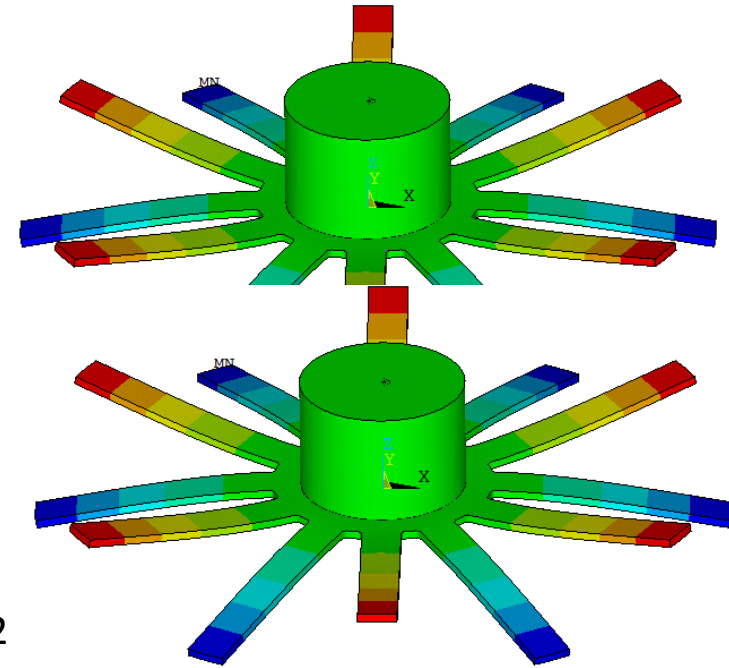


BTT – Measurement example



Disk

- Diameter: 440 mm
- Thickness: 5 mm
- Beam shaped beam
- Material: Aluminum
- Number of Blades: 12



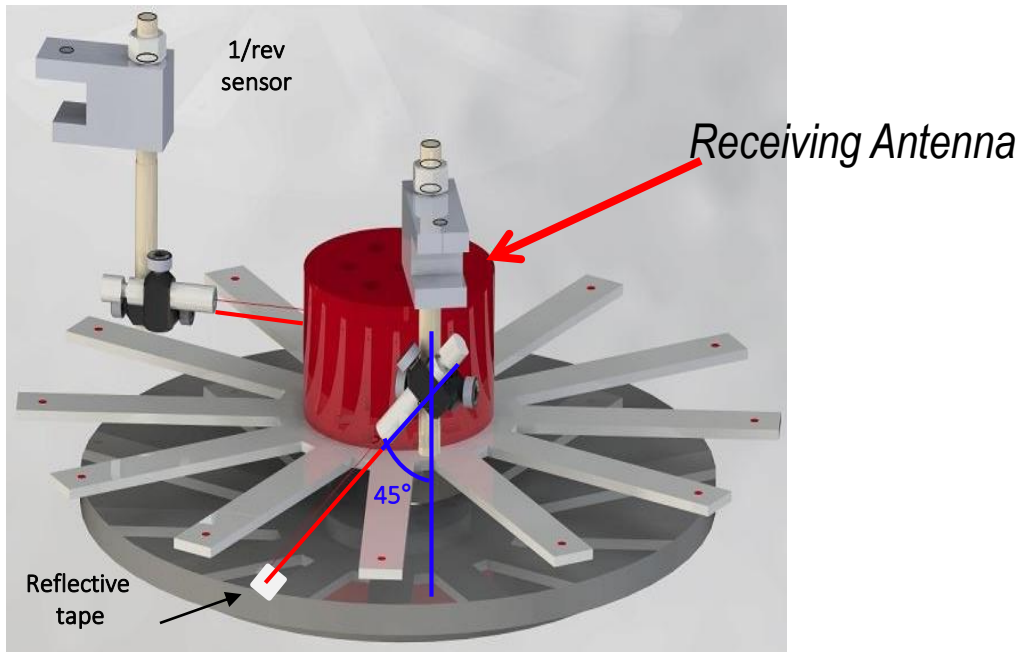
Bending out of plane
mode shapes

BTT – Measurement example - the spinning rig

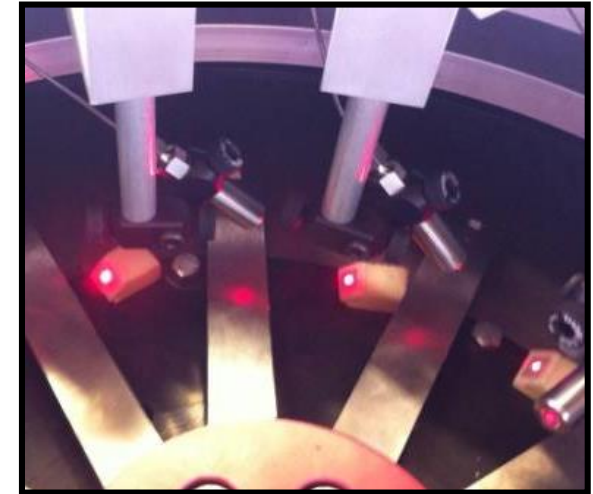


BTT – Measurement example – BTT vs. Strain gauges

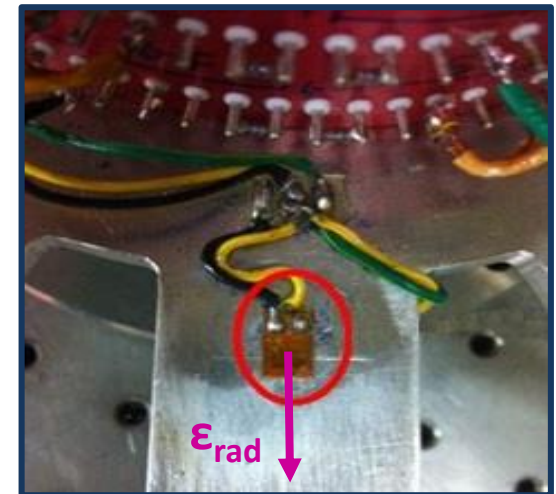
- Disk
- Excitation system: permanent magnets
- Blade Tip Timing measurement system (BTT)
- Strain gauges and telemetry system



BTT sensors

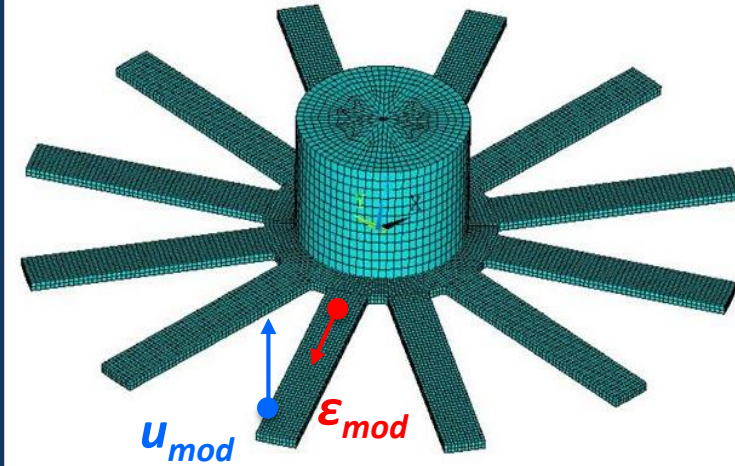
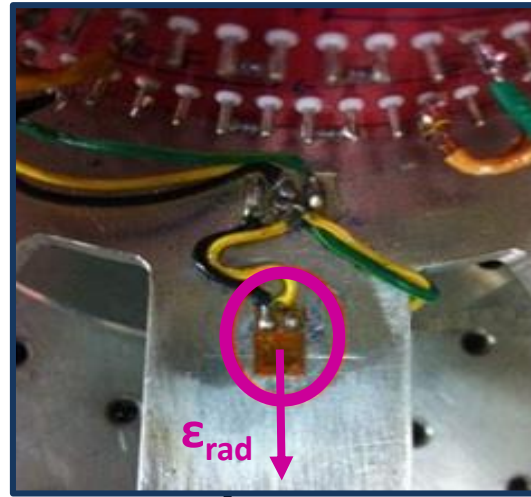
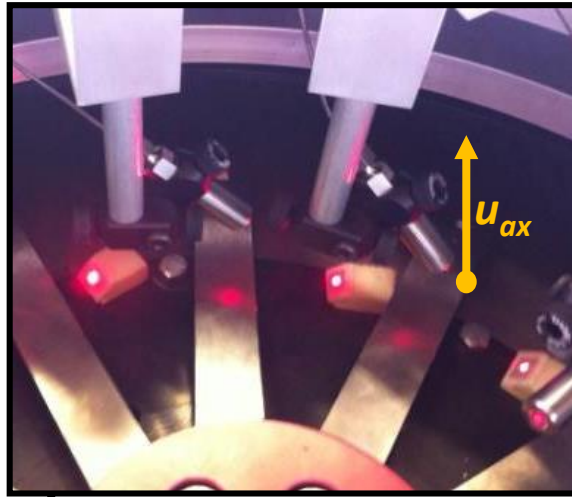


Strain Gauge



BTT vs. strain gauges

$A_{max} \approx 2000 \mu m$



$$u_{BTT} = u_{ax} \longleftrightarrow u_{SG} = K_{mod} \cdot \epsilon_{SG}$$

$$K_{mod} = \frac{u_{mod}}{\epsilon_{mod}}$$

$$e_f = \frac{|f_{SG} - f_{BTT}|}{f_{SG}} \cdot 100$$

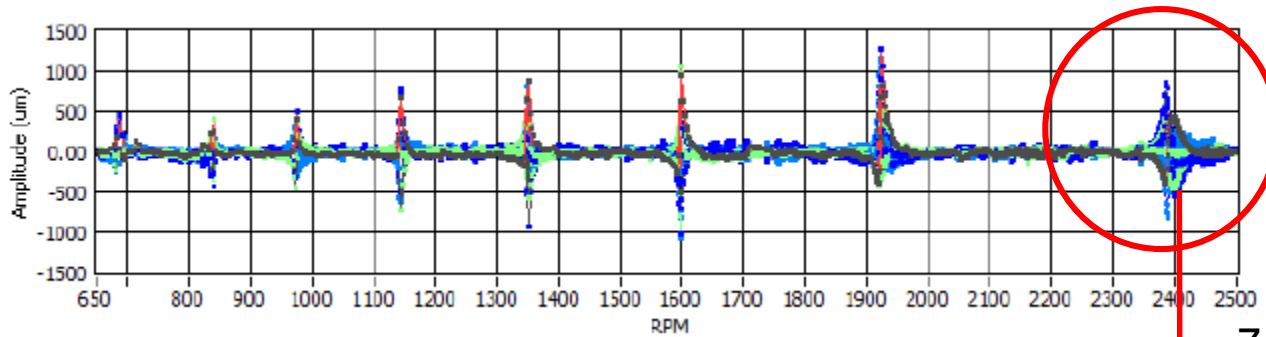
$$e_u = \frac{|u_{SG} - u_{BTT}|}{u_{SG}} \cdot 100$$

Strain Gauges Reference

ND	f_{SG}	f_{BTT}	e_f	u_{SG}	u_{BTT}	e_u
-	Hz	Hz	%	μm	μm	%
5	158,0	158,0	0	1662,23	1631,48	1,88
6	159,3	160,2	0,44	2298,75	2275,60	1,02

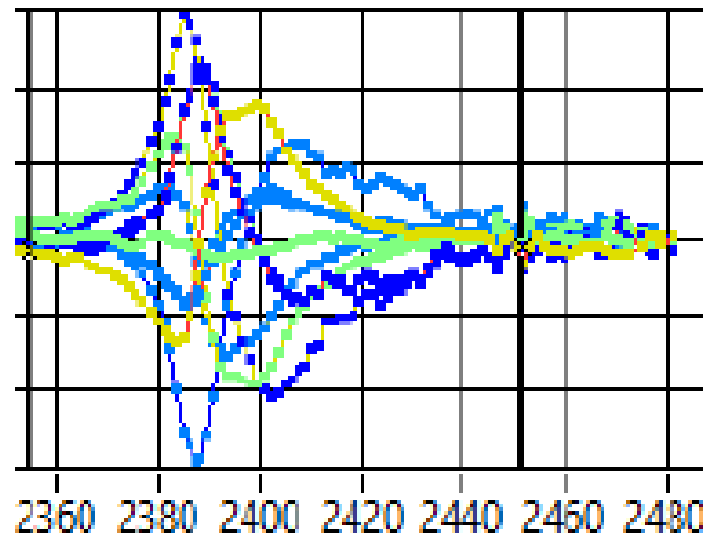
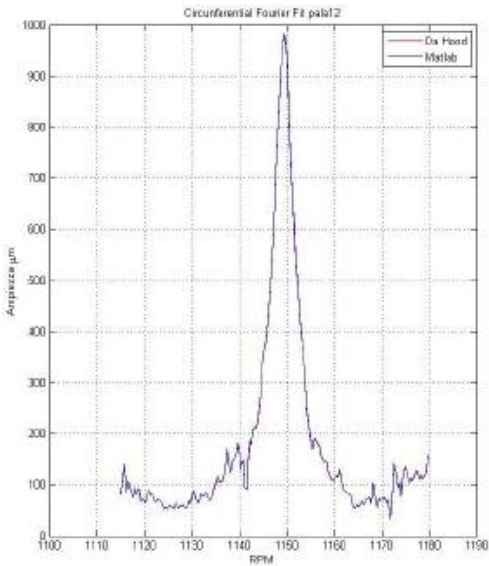
BTT – Measurement example – on a single blade

Signals for each blade



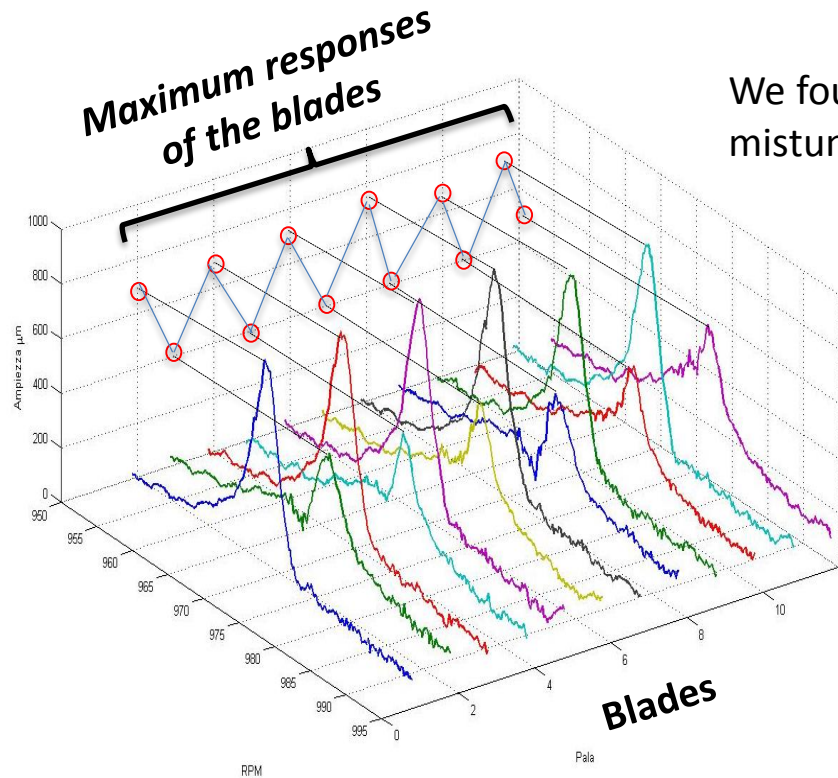
Zoom of the signals of the different sensors

Reconstruction of the forced response of the blade



BTT- ND observation through the disk mistuning

Forced responses of the 12 blades



We found again a modulation of the response due to small mistuning

$$6 = 2 \cdot 3 (=ND)$$

\downarrow
 $ND=3$

The presence of small mistuning here could be used to find the nodal diameter from the tip timing measurements

Battiato, G.; Firrone, C.M.; Berruti, T. M. (2016) [Forced response of rotating bladed disks: Blade Tip-Timing measurements](#). In: [MECHANICAL SYSTEMS AND SIGNAL PROCESSING](#), vol. 85, pp. 912-926.